Faculty of Sciences

Department of Bioscience Engineering

Interplay of bacterial endotoxins and transition metals in the inflammatory capacity of airborne particulate matter

Interactie tussen bacteriële endotoxines en transitiemetalen bij de ontstekingscapaciteit van fijn stof

Thesis submitted for the degree of doctor in bioscience engineering at the University of Antwerp to be defended by

Serena MORETTI

Supervisor: Prof. Dr. ir. Sarah Lebeer

Antwerpen, 2018

Doctoral Jury:

Prof. Dr. Silvia Lenaerts, University of Antwerp, Belgium

Prof. Dr. ir. Roeland Samson, University of Antwerp, Belgium

Prof. Apr. Paul Cos, University of Antwerp, Belgium

Prof. Dr. Els Van Damme, University of Ghent, Belgium

PD Dr. Andra Schromm, Research Center Borstel, Germany

ACKNOWLEDGEMENTS

A large part of succeeding in a PhD is the encouragement and support you get along the way, because beyond the fascinating lure of science is also its darker side. Facing the unknown with doubt, designing experiments with no ideal solution, dealing with equipment breakdowns, and of course, the numerous article and funding rejections. Through all the encouragement I've come out the other side – wiser (measured in grey hairs), humbled, and more resistant to failure!

Where better to start than the beginning. To my friends in South Africa who encouraged me to apply for a PhD abroad - Jan, Francois, Philippe, and Anita – thank you for treating me as an equal (despite my lack in years) and offering your wisdom, honesty and friendship beyond the distance. Leaving your home and the people you love is never easy, so I'd like to especially thank my family, including Suzaan for letting me go and at the same time I apologise for all the missed moments together. Mom and dad, thank you for all the love, support and sacrifices you made while I was growing up, always living by example, and teaching me to have pride and integrity in my work. You definitely got it right the fifth time round! For my siblings, Carla, Francesco, Marco, and Paolo, thank you for all the happy memories and toughening your little sister up for the real world.

Of course this thesis would not have been possible without all the financial opportunities I have received. So I would like to sincerely thank the EUROSA project for bridging the gap between South African and European universities such as Antwerp, truly a life-changing opportunity for young scientists, including myself. The FWO fellowship grant was also vital in the completion of this thesis, for which I gratefully thank them for their confidence in me as a researcher. The Rosa Blanckaert award also went to very good use in our young and developing laboratory.

Moving abroad, I knew exactly what I was giving up, but I had no idea what I would gain. It turns out I hit the jackpot! I found myself with a kind, encouraging, dedicated and passionate supervisor. Sarah, I am profoundly grateful for all your guidance and accepting me as a foreign student to be part of your lab – it has enormously enriched my life – and you have truly been an

inspiring supervisor to look up to. My initial work colleagues – Ashka, Wenke, Leen and Melanka – thank you for quickly becoming my friends, helping me get on my feet, and for continuing to keep my life exciting! The lab soon grew, with the very best colleagues and impressive scientists – Marianne, Eline, Ingmar, Sander, Camille, Ilke, Dieter, Stijn, Ines, Jennifer, Wannes, and Irina. Thank you all for the great lab atmosphere, your kindness, motivation, brainstorming, fun lab weekends, interesting chats, and of course, compliance for doing lab duties! A special thanks to Leen, with your boundless positive attitude you have always made my problems lighter, helped with a smile (even for the never ending vortexing of my samples) and kept the lab running safely and smoothly. Of course, as a new research group in the department, I am also very grateful for all the other departmental members who have always been so helpful and friendly. In the first year and a half of my PhD, the lab did not yet exist. So I absolutely need to thank all the laboratories which took me in and the people who guided me, including the help of Marijke at the CMPG lab (KU Leuven), Yannick and Magali at the LMPH lab of Prof. Paul Cos (UAntwerp), and Femke, Valentine and Karin at the SPHERE group of Ronny Blust (UAntwerp).

Apart from a great work environment, there are the people who made me feel happy and at home here in Belgium. From the tea club, the climbing group, and the Antwerp girls expats, you have filled my spare time with laughter, love, creativity and adventure! Maja, a big thank you for always bringing the group together and organising of special and memorable events. Mieke, I'm so glad you took a chance on a stranger and welcomed me into your home, it's a time I whole-heartedly cherish. Jaletta, we've managed to stick together all these years, thank you for all the advice and long skype conversations. Wenke, there is just too much to thank you for, I feel like the luckiest person in the world to have you as both my work colleague and friend, always there to offer sound advice and just a peer over my laptop away. Your enthusiasm, positivity, and encouragement have convinced me (a once cautious perfectionist) not to overthink everything, but to enjoy the rewarding benefit of an occasional risk, or to laugh and learn at any missed attempts. Lionel, meeting you has been the cherry on the top, and has convinced me that Belgium is a place I can call home.

Finally, to my amazing sister, Carla, I have always looked up to you and could count on you. You introduced me to philosophy many years ago and always encourage me to broaden my perspectives. Through the years I have found my passion in science and with this thesis receive my doctorate in philosophy, which I find very fitting to dedicate with all my love to you.

SUMMARY

Endotoxins or lipopolysaccharides (LPS) are constituents of the outer membrane of gram-negative bacteria and are well known for their high pro-inflammatory potency. As numerous as the bacteria from which they originate, endotoxins are ubiquitous in the environment because they are robust molecules resilient to degradation. As such, they are commonly found in a complex and heterogeneous mixture of airborne particles known as particulate matter (PM). This is the fraction of air pollution that is most reliably associated with severe inflammation and oxidative stress-related health effects (i.e. respiratory, cardiovascular and cerebrovascular diseases). Upon inhalation, the presence of endotoxins in PM may complicate the diseases in combination with other pollutants, however this is not yet well understood. In this PhD research, we therefore aimed to investigate the relative contribution of endotoxin – associated with other PM components - in inflammatory responses caused by PM.

First, we explored possible improvements for the current methods on collection and detection of ambient endotoxin concentration in an urban environment. With our more microbial-targeted approach using a Coriolis μ sampler, endotoxins were detected at approximately 10-fold higher concentrations in Antwerp (geometric mean 4.49 EU m^{-3}) compared to the urban air of other cities using filter-based samplers (average of 0.44. EU m^{-3}) for PM_{10} (particles sized between 2.5-10 μm and where endotoxins are predominantly found). These endotoxin concentrations were quantified with the recombinant Factor C (rFC) assay, which is a modern and more sustainable version of the gold standard limulus amebocyte lysate (LAL) assay. The rFC assay does not rely on the bleeding of the horseshoe crabs for their blood cells (amebocytes), but only uses the recombinantly expressed enzyme Factor C for endotoxin detection. This offers the rFC assay the advantage of less lot-to-lot variations, no false positives by fungal glucans, and reduced likelihood of interference compared to the LAL assay. Despite these advantages, the induction of inflammatory markers (IL-1β, IL-8, TNFα) by our air pollution samples, as measured in a human macrophage-like U937 cell line was not well correlated to the rFC-determined ambient endotoxin concentrations. Therefore, another bioassay for the detection of endotoxins was also applied. This assay was based on the human

recognition of endotoxin via the key innate immune receptor Toll-like receptor 4 (TLR4). As expected, we found endotoxin recognition via the HEK hTLR4 reporter cell line to be better correlated to the expression of interleukin-8 (IL-8), which is a key biomarker of inflammation-related diseases such asthma, and chronic obstructive pulmonary disease. However, samples from the traffic land-use class were found to significantly increase the activation of the TLR4 bioassay, compared to samples from the industrial and green locations, despite all areas having similar rFC-determined endotoxin concentrations.

Traffic is related to high emission of other PM components such as transition metals, which are well documented to also have a high oxidative and pro-inflammatory potential. Therefore, we explored how transition metals could affect the TLR4 bioassay and PM-related pro-inflammatory responses. Transition metals in our samples were carefully determined by ICP-MS and these concentrations were correlated to the TLR4 bioassay, rFC assay, inflammation and oxidative stress markers, and other PM-related parameters measured (e.g. particle count). Interestingly, especially iron, a well-known and abundant compound of traffic-related air pollution (e.g. by abrasion of road surfaces, brakes, tyres, and railway tracks), was found to enhance the TLR4 bioassay, in contrast to nickel and cobalt which was previously reported to directly activate TLR4. Moreover, because PM and air pollution samples are such complex mixtures, we subsequently showed that by dosing purified endotoxins (LPS) with Fe^{2+}, an increase up to 64% in bioactivity of the HEK hTLR4 cell line (EU ml^{-1}) could be found, while Fe^{2+} without LPS was unable to stimulate a response. Furthermore, exposure of human macrophage-like U937 cells to Fe^{2+} modulated the gene expression of pro-inflammatory and oxidative stress markers (TNFα, IL-1β, IL-8, HO-1) to LPS stimulation.

Thus, in this PhD thesis we could show that, although endotoxins are typically quantified in ambient air, their toxicity is significantly influenced by the associated particle composition. Especially iron, one of the most abundant transition metals occurring in urban PM, was found to modulate endotoxin activity.

SAMENVATTING

Endotoxines of Lipopolysachariden (LPS) zijn componenten van de buitenmembraan van gramnegatieve bacteriën. Ze zijn welgekend voor hun hoge pro-inflammatoire effect. Zoals de bacteriën zelf, komen ook endotoxines alomtegenwoordig voor, omdat de actieve component niet snel afbreken. Daarom worden ze vaak gevonden in het complexe en heterogene mengsel van luchtpartikels, beter gekend als fijnstof (PM, *particulate matter*). Dit is de fractie van luchtvervuiling die het meest geassocieerd wordt met een sterke immuunrespons en gezondheidseffecten die gerelateerd zijn met oxidatieve stress, zoals aandoeningen van de luchtwegen, cardiovasculaire en cerebrovasculaire ziektes. Bij het inademen, kan de aanwezigheid van endotoxines in fijnstof in combinatie met andere polluenten een belangrijke rol spelen in het ontstaan van deze ziekten of het verergeren van symptomen, maar deze interacties tussen fijn stof en andere polluenten zijn nog niet goed begrepen. Daarom richtte deze doctoraatsstudie zich op het onderzoeken van de relatieve bijdrage van endotoxines – geassocieerd met andere PM componenten – tot immuunresponsen veroorzaakt door PM in een stedelijke omgeving (Antwerpen).

Eerst hebben we bestaande verzamel- en meetmethoden voor stedelijke endotoxine-concentraties verbeterd en geoptimaliseerd. Met onze specifieke en doelgerichte aanpak voor bacteriën – die o.a. bestond uit het gebruik van een Coriolis µ staalname toestel, werden endotoxines gemeten aan 10 keer hogere concentraties in Antwerpen (geometrisch gemiddelde: 4.49 EU m^{-3}) in vergelijking met andere steden waar de stalen werden genomen met filters (gemiddelde van 0.44. EU m^{-3} in PM_{10}). Er werd voor het meten en kwantificeren van endotoxines ook gekozen voor een modernere en duurzamere methode, nl. de recombinant Factor C (rFC) test, in vergelijking met de klassieke gouden standaard, de limulus amebocyte lysaat (LAL) test welke afhangt van het bloed van degenkrabben voor bloedcellen (amebocyten). De rFC test maakt gebruik van het tot expressie gebracht gerecombineerde eiwit, factor C en heeft nog andere voordelen, zoals minder variatie tussen partijen van reagentia, het vermijden van valspositieve resultaten door schimmelglucanen en een verminderde kans op interferenties in vergelijking met de LAL assay.

Ondanks de voordelen van de rFC assay, was de correlatie tussen de gemeten endotoxineconcentratie en de inductie van ontstekingsmerkers (IL-1β, IL-8, TNFα) die gemeten werden in humane U937 macrofaagcellijn verrassend beperkt. Om dit verder uit te zoeken, werden de endotoxineconcentraties nog eens gemeten, maar dit keer met een test die de resultaten van de inductie van onstekingsmerkers en endotoxines beter zou correleren. Deze specifieke test is gebaseerd op de herkenning van endotoxines door het aangeboren menselijk immuunsysteem via de Toll-like receptor 4 (TLR4). Zoals verwacht was de endotoxines-herkenning via de HEK hTLR4 reportercellijn beter gecorreleerd met de expressie van interleukine-8 (IL-8). IL-8 is een van de belangrijkste bioindicatoren voor ontstekings-gerelateerde aandoeningen zoals asthma en chronische obstructieve longziekte. Bovendien verhoogden stalen genomen op plaatsen gekarakteriseerd door de aanwezigheid van stedelijk verkeer, de activatie van TLR4 significant, vergeleken met de stalen van de industriële en groene plaatsen. Desondanks werden op alle plaatsen gelijkaardige hoeveelheden endotoxineconcentraties gemeten met de rFC test.

Het verkeer is gerelateerd aan hoge uitstoot van andere fijnstofcomponenten zoals transitiemetalen, die een hoog oxidatief en pro-inflammatoire potentieel hebben. Daarom hebben we de invloed van transitiemetalen op TLR4 en PM-geassocieerde pro-inflammatoire respons verder onderzocht. Transitiemetalen werden nauwkeurig gemeten door gebruik te maken van ICP-MS, en deze resultaten werden dan verder gecorreleerd met de resultaten uit voorgaande experimenten (rFCtest, ontstekings- en oxidatieve stress indicatoren, en andere PM-geassocieerde parameters zoals de hoeveelheid fijnstofpartikels). In de literatuur werd reeds aangetoond dat nikkel en kobalt rechtstreeks TLR4 activeren, maar in onze experimenten was het vooral ijzer die een verhogend effect op de TLR4 heeft. Ijzer is een welgekende en veelvuldig voorkomende component van verkeersgeassocieerde luchtvervuiling (bijvoorbeeld door middel van het schuren van het wegdek, de remmen, de wielen en treinsporen). Bovendien, omdat PM en luchtvervuilingstalen een complex mengsel zijn, werden er experimenten ontworpen om op een gecontroleerde manier de interactie tussen LPS en Fe^{2+} aan te tonen. De combinatie van LPS en Fe^{2+} leidde tot een toename van de activiteit van de HEK hTLR4 cellijnen met 64%, terwijl Fe^{2+} alleen geen respons kon opwekken. Daar komt bij dat dezelfde soort blootstelling van Fe^{2+} en LPS op humane U937 macrofaagcellen de

genexpressie moduleren van pro-inflammatoire en oxidatieve stressmerkers (TNFα, IL-1β, IL-8, HO-1).

Samengevat werd in dit doctoraatsonderzoek aangetoond dat, hoewel endotoxines vaak worden gekwantificeerd voor de bepaling van de luchtkwaliteit, endotoxinetoxiciteit significant beïnvloed wordt door de compositie van de geassocieerde partikels. We stelden vast dat in het bijzonder ijzer, een van de meest abundante transitiemetalen in stedelijk PM, de endotoxineactiviteit moduleert.

CONTENTS

LIST OF ABBREVIATIONS

AED	Aerodynamic equivalent diameters
CFU	Colony forming unit
E. coli	*Escherichia coli*
EU	Endotoxin units
FBS	Fetal bovine serum
GM	Geometric mean
IL	Interleukin
LAL	Limulus amebocyte lysate
LBP	LPS binding protein
LPS	Lipopolysaccharide
MD-2	Myeloid differentiation factor 2
PAH	Polycyclic aromatic hydrocarbons
PAMPS	Pathogen-associated molecular patterns
PBS	Phosphate-buffered saline
PM	Particulate matter
PMA	Phorbol 12-myristate 13-acetate
pNPP	p-nitrophenyl phosphate
rFC	Recombinant Factor C
RT-qPCR	Reverse transcription quantitative PCR
TLR	Toll like receptor
TNFα	Tumor necrosis factor alpha
VMM	Flanders Environment Agency (translated)
WHO	World health organization

Chapter 1

Introduction and scope

"We live submerged at the bottom of an ocean of air"

-- Evangelista Torricelli 1644 quoted in Middleton 1963

1.1 Air pollution

As humans, we have an intimate relationship with the air around us. Although we breathe without much notice, we are vitally dependent on this exchange. Each day, we are exposed to more than 8 000 litres of inhaled air. This interaction goes far beyond the exchange of gases and extends to the diverse range of microscopic particles teeming in the air. The Industrial Revolution brought about dense clouds of smog, thereby visualizing air pollutants, and making us increasingly aware of the impact this dynamic interface between the human host and the external environment has on human health.

1.2 Particulate matter

Ambient particulate matter (PM) is known to affect more people than any other pollutant (WHO, 2006). PM is defined as a complex and heterogeneous mixture of liquid and solid particles (both organic and inorganic) suspended in the air. The World Health Organization (WHO) estimates that in 2012 around 3 million people died prematurely as a result of ambient air pollution exposure, not to mention years lived with disability. That is one in eight of total global deaths, making air pollution now the world's largest single environmental health risk. The health effects of air pollution are extensive, including stroke, heart disease, lung cancer, and both chronic and acute respiratory diseases, such as asthma, and recently Alzheimer's disease and dementia (EEA, 2017). Although the respiratory system constitutes the primary target of inhaled particles, there is also strong evidence implicated for adverse effects on the cardiovascular system, and to a lesser extent, the cerebrovascular system (Anderson *et al.*, 2012; Kelly, 2003; Valavanidis *et al.*, 2008).

1.2.1 Classification in size ranges

Regulatory agencies classify PM in relative size ranges known as "aerodynamic equivalent diameters" (AED) which influences the settling velocity, imply how the particles were generated, and importantly, where they may deposit in the respiratory system. Particle AEDs include coarse (PM_{10}: 2.5 – 10 μm), fine ($PM_{2.5}$: 0.1- 2.5 μm) and ultrafine ($PM_{0.1}$: ≤ 0.1 μm).

Particles larger than 10 μm have a relatively small suspension half-life and are largely filtered out by the nose and upper airway. The fine and ultrafine PM particles are capable of penetrating deeper into the respiratory tract, interfering with gas exchange and even translocating into systemic circulation (Geiser *et al.*, 2005; Nemmar *et al.*, 2002). Fine particles have subsequently received a lot of attention, however, the coarse PM fraction generally shows stronger pro-inflammatory effects *in vitro* (Huang *et al.*, 2002; Monn and Becker, 1999; Schins *et al.*, 2002). In fact, a study by Becker *et al.* (2005b) showed that the coarse fraction in PM_{10} accounted for 90-95% of the resulting inflammatory response in alveolar macrophages. Although recent research has focused mainly on the associated health effects of the fine and ultrafine fractions, the coarse PM fraction is recognized as having significant adverse effects on the bronchiolar region of conducting airways, which is the primary site of asthma and associated airway inflammation (Monn and Becker, 1999; Soukup and Becker, 2001).

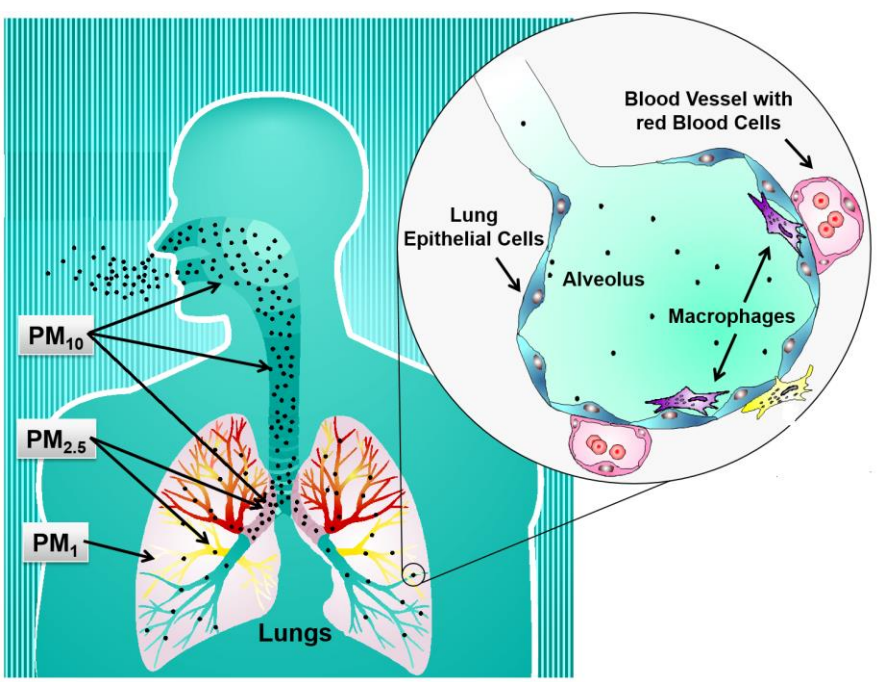

FIG 1.1: Deposition of various particle sizes in the different regions of the respiratory system. Adapted from Krug and Wick (2011)

1.2.2 Composition

Apart from these physical parameters, PM-induced toxicity is largely affected by chemical composition, which varies greatly with season and region of sampling, photochemical-meteorological conditions, and sources of emissions (Brüggemann *et al.*, 2009; Perrone *et al.*, 2010). A distinction may also be made regarding the particle's origin, i.e. primary or secondary. Primary particles are emitted directly in the air from both anthropogenic or natural sources, and are found in the atmosphere in the same chemical composition as they were emitted, whereas secondary particles are formed in the air by chemical reactions such as oxidation or transformation of precursor gases (e.g. SO_2, NO_x, NH_3) after their emission. Anthropogenic sources arise from human activities such as transport (fuel combustion, erosion of traffic infrastructure, abrasion of brakes and tyres), industry, power plants, agriculture, households and waste management (Srimuruganandam and Shiva Nagendra, 2012). Of note, diesel engines emit considerably more particulates per vehicle kilometre than gasoline engines (De Kok *et al.*, 2006). In contrast, particles may also originate from natural sources including dust storms, forest fires, living vegetation, sea spray and even volcanoes. Constituents commonly found in PM include inorganic ions (e.g. sulphates, nitrates, ammonium, salts), organic compounds (e.g. polycyclic aromatic hydrocarbons, quinones), minerals (quartz, asbestos, soil dust), transition metals, particle core of carbonaceous material (mainly from combustion processes and vehicular exhaust particles), and even biological material (e.g. pollen, fungal spores, and microbial products such as endotoxins) (Happo *et al.*, 2010; Vercauteren *et al.*, 2011).

Regarding the composition of particles in the various size ranges, ultrafine particles in an urban environment are typically generated directly by combustion and photochemical activity. The particles are unstable and persist briefly, aggregating to form larger particles (Valavanidis *et al.*, 2008). Fine and ultrafine particles are formed mostly by vehicular exhausts emissions, consisting mainly of organic and inorganic elements adsorbed onto the surface of a carbonaceous core (Brüggemann *et al.*, 2009). By contrast, part of coarse particles can be generated by combustion but mostly consist of mineral compounds, endotoxins and particles

arising from abrasive sources, such as brake wear, tyre wear and abrasion of road surfaces (Thorpe and Harrison, 2008). Most of the suspended PM consists of 90% to 95% of coarse particles, whereas smaller particles are only 1% to 8% of the total mass (Valavanidis *et al.*, 2008). However, ultrafine and fine particles are very high in numbers and have greater total surface area than larger particles.

While meteorological conditions such as temperature, solar radiation, and relative humidity may influence the formation of secondary particles (EEA, 2017), weather and season have also been shown to influence the concentration and composition of PM in many other ways. For instance, rainfall can have a strong influence on ambient PM concentrations, where particles are pulled down by precipitation, and air currents may transport particles over long distances (Johansson *et al.*, 2007). Furthermore, organic carbon concentrations from combustion sources are more prevalent in the winter, while emission from terrestrial vegetation will increase in spring and summer (Brüggemann *et al.*, 2009).

In Flanders, the first large-scale chemical characterization project of PM_{10} (Chemkar PM_{10}) was established to analyse the local differences in the chemical composition of six different sites in Flanders over a full year (Vercauteren *et al.*, 2011). Sampling sites were spread in location and ranged in the type of site: Houtum (rural background), Zelzate (industrial), Mechelen (suburban), Borgerhout (urban background), Aarschot (rural background) and Hasselt (suburban). Results showed that the most important fractions were 41% secondary inorganic ions (nitrate, sulphate and ammonium), 20% organic matter, 14% crustal matter, 8% sea salt and 4% elemental carbon. In figure 1.2, the concentration of sea salt logically decreased with distance from the North Sea. Furthermore, the average concentration for elemental carbon (EC) and crustal matter at the urban background site in Borgerhout was about 4 and 3 times higher (respectively) than at the rural site in Houtum, together with an average difference of 2.88 $\mu g\ m^{-3}$ for organic material. Copper (Cu), which was highly enriched in the urban Borgerhout site, is known to originate from the wearing of brake pads (Thorpe and Harrison, 2008). Additionally, the overall high correlations between Cu, EC and lighter PAHs likely suggest traffic as the main source of Cu in Flanders. These differences seem to indicate

that traffic is an important local source for PM pollution. As ammonium nitrate is the most significant contributor to PM mass, measures to reduce the precursor gases (NH_3 and NO_x) by targeting the agricultural (and traffic) emissions could have a relatively high effect in decreasing PM_{10} levels. However, whether this would also result in a corresponding reduction in the health effects of PM_{10} is unknown.

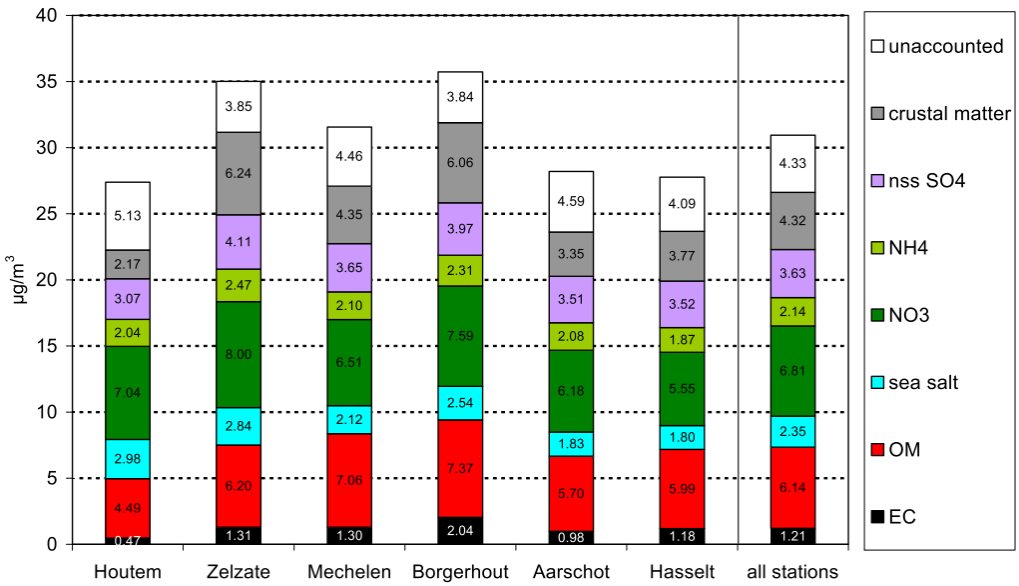

FIG 1.2: Averaged concentrations of the main fractions in PM_{10} over six sampling stations in Flanders, Belgium. Legend abbreviations: nss SO_4 (non-sea salt sulphate ion), NH_4 (ammonium ion), NO_3 (nitrate ion), OM (organic material), EC (elemental carbon). Vercauteren *et al.*, 2011

1.2.3 Regulations

Some air pollutants persist in the environment for long periods of time and they may accumulate in the environment and in the food chain, affecting humans and animals not only via air intake, but also via water and food intake. Overall, the small individual effects result in a large global public health burden. Furthermore, research has supplied mounting evidence for the adverse effects of air pollutants on human health, ecosystems, the built environment and the climate (EEA, 2017). This has caused governments globally to draft and implement laws

aiming to manage and reduce the emissions of primary and secondary PM sources. With the 2008/50/EC Air Quality Directive, the European Union (EU) extended its air pollution regulations, restricting the maximum allowed PM concentrations in the member countries (EU, 2008). These values and the stricter WHO Air Quality Guidelines (WHO AQG) (WHO, 2006) are listed in Table 1.1.

Table 1.1: The air quality standards and objectives as stipulated by the European Union and the WHO. These apply over differing periods of time because the observed health impacts associated with the various pollutants occur over different exposure times.

Pollutant	Averaging period	EU reference value	WHO air quality guideline	Unit
$PM_{2.5}$	Annual	25	10	$\mu g\ m^{-3}$
	Daily		25	$\mu g\ m^{-3}$
PM_{10}	Annual	40	20	$\mu g\ m^{-3}$
	Daily	50 (a)	50	$\mu g\ m^{-3}$
Lead (b)	Annual	0.5	0.5	$\mu g\ m^{-3}$
Arsenic (b)	Annual	6	6.6 (c)	$ng\ m^{-3}$
Cadmium (b)	Annual	5	5	$ng\ m^{-3}$
Nickel (b)	Annual	20	25 (c)	$ng\ m^{-3}$

(a) Not to be exceed more than 35 days per year
(b) Measured as content in PM_{10}
(c) AQG not set, reference level estimated assuming an acceptable risk of additional lifetime cancer risk of approximately 1 in 100 000

Furthermore, the EU has recently agreed on a revised National Emissions Ceilings (NEC) Directive (EU, 2016). It sets 2020 and 2030 emission reduction commitments for SO_2, NOx, non-methane volatile organic compounds, NH_3 and $PM_{2.5}$. Currently, air quality policies have delivered, and continue to deliver, many improvements. Reduced emissions have improved air quality in Europe, and, for a number of pollutants, exceedances of European standards are rare (Fig 1.3) (EEA, 2017). Nonetheless, long-term studies have shown correlations between morbidity and mortality with PM at concentrations well below the WHO recommended limit values (WHO, 2016). Although an overall reduction of ambient concentrations of PM is likely to result in reduction of PM-associated health risks, emission reduction strategies that take chemical and toxicological PM characteristics into account are probably more effective and

efficient. This highlights the need to gain more knowledge about the mechanisms underlying PM induced health problems, in order to shift to a more targeted approach.

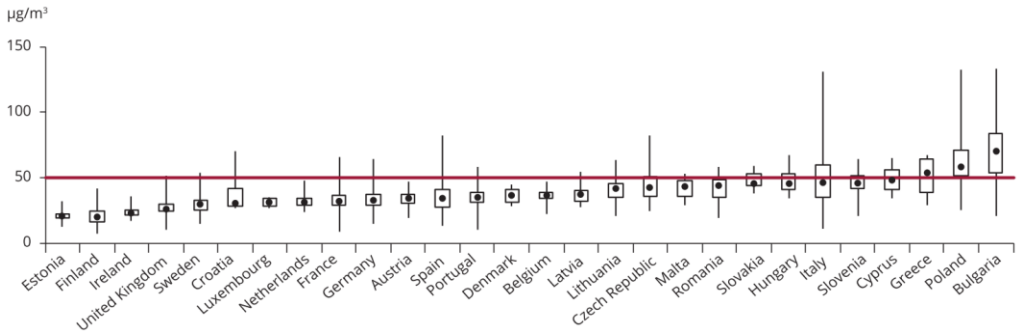

FIG 1.2: PM_{10} concentrations in relation to the daily limit value in 2015 in the EU-28
The graph is based on the 90.4 percentile of daily mean concentration values corresponding to the 36th highest daily mean. For each country, the lowest, highest and median 90.4 percentile values (µg m^{-3}) at the stations are given. The rectangles mark the 25th and 75th percentiles. The daily limit value set by EU legislation is marked by the red line (EEA, 2017).

1.2.4 Mechanisms of PM-induced toxicity

Numerous studies with varying populations, regions, and methodologies have associated an increase in respiratory and cardiovascular morbidity and mortality with a dose-dependent exposure to ambient PM (Analitis *et al.*, 2006; Baccini and Biggeri, 2012; Boldo *et al.*, 2006; Dominici *et al.*, 2003; Katsouyanni *et al.*, 2001; Stafoggia *et al.*, 2016). PM is thought to contribute to cardiovascular and cerebrovascular disease by the mechanisms of systemic inflammation, direct and indirect coagulation activation, and direct translocation into systemic circulation, while respiratory morbidity and mortality is caused by oxidative stress and inflammation that leads to pulmonary anatomic and physiologic remodelling (Anderson *et al.*, 2012; Kelly, 2003; Valavanidis *et al.*, 2008).

In the last years, numerous studies proposed the synergistic effects of oxidative stress and inflammation as the major biochemical pathways of PM-induced toxicity and health effects (Happo *et al.*, 2010; Michael *et al.*, 2013). A three-phase response model has been developed by Li *et al.* (2008) to explain the process (Fig 1.3). Cellular redox homeostasis is carefully maintained by an elaborate antioxidant defence system which is regulated by the glutathione/

glutathione disulphide (GSH/GSSH) ratio. Depending on the rate and level of change in this ratio, a cellular stress response is triggered that could be either protective or injurious in nature.

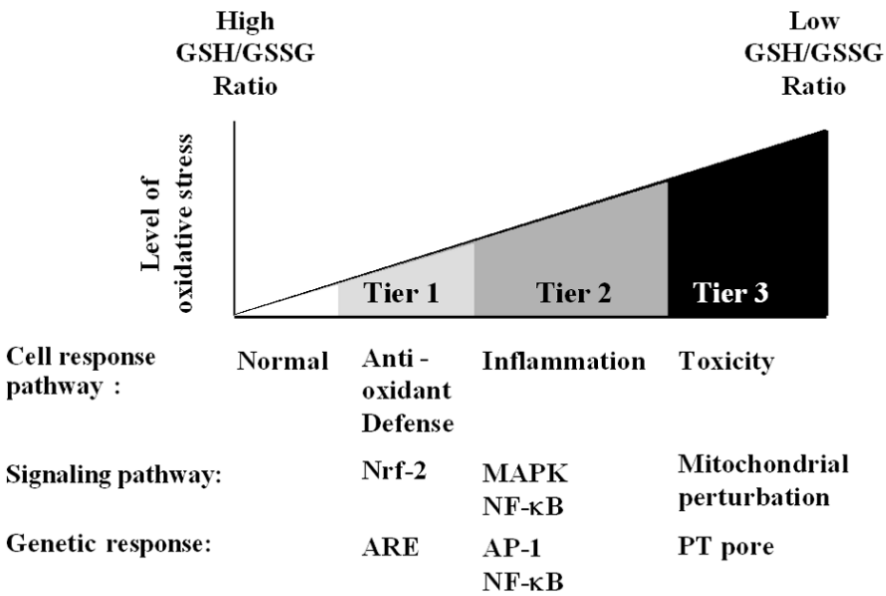

FIG 1.3: Hierarchical oxidative stress responses. At a low level of oxidative stress (Tier 1), antioxidant enzymes are induced to restore cellular redox homeostasis. At an intermediate level of oxidative stress (Tier 2), activation of MAPK and NF-κB cascades induces pro-inflammatory responses. At a high level of oxidative stress (Tier 3), perturbation of the mitochondrial permeability transition pore and disruption of electron transfer result in cellular apoptosis or necrosis (Li *et al.*, 2008)

In the first tier, oxidative stress is at a low level and the transcription factor Nrf2 (nuclear factor erythroid 2-related factor) leads to transcriptional activation of more than 200 antioxidant and detoxification enzymes to restore cellular redox homeostasis (Li *et al.*, 2008). Examples of these enzymes include NADPH quinone oxidoreductase, glutathione-S-transferase (GST), hemeoxygenase-1 (HO-1), catalase (CAT), and superoxide dismutase (SOD). With continued oxidative stress these enzymes become overwhelmed and can no longer neutralize the effects of reactive oxygen species (ROS). When this happens, (tier 2) activation of the redox-sensitive MAP kinase and NF-kB cascade induces pro-inflammatory responses, including cytokines and

chemokines. At higher levels of oxidative stress (tier 3), the permeability of the mitochondria is compromised and disruption of the electron transfer chain results in cellular apoptosis and necrosis (Li *et al.*, 2008).

Numerous studies have identified PM components capable of causing oxidative stress. These primarily include transition metals and organic molecules such as polycyclic aromatic hydrocarbons (PAHs) (Frampton *et al.*, 1999; Kelly *et al.*, 2007; Valko *et al.*, 2005). PAHs and nitro-PAHs are products of incomplete combustion processes and vehicular exhaust found in high concentrations in urban PM (Valavanidis *et al.*, 2006). They can induce oxidative stress indirectly, through biotransformation by cytochrome P450 and dihydrodiol dehydrogenase to generate redox active quinones that act as catalysts for free radical production. Transition metals, which are capable of forming cations, are well known for their substantial contribution to PM's oxidative capacity (Frampton *et al.*, 1999; Kelly *et al.*, 2007; Valko *et al.*, 2005). Two important variables influencing the oxidative burden posed by transition metals include their bioavailability and their redox activity (Costa and Dreher, 1997). The latter can be explained by the ability of redox active metals, such as iron, copper, manganese, vanadium, and nickel to participate in redox cycling reactions (Fig 1.4). Subsequently, reactive oxygen and nitrogen species are created, which can deplete intracellular antioxidants and cause cellular damage including lipid peroxidation, DNA adducts, and protein modifications (Valko *et al.*, 2005). Numerous sources contribute towards transition metals in PM, including the combustion of fuels, vehicular wear, industrial processes, and even the suspension of mineral dust (Thorpe and Harrison, 2008).

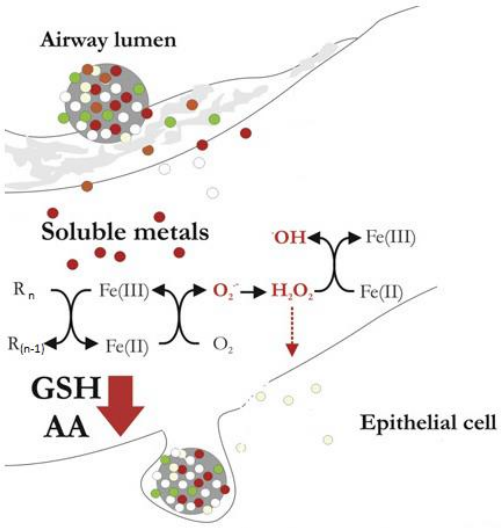

FIG 1.4: Mechanism for iron, a redox active metal, causing oxidative stress in the lung. Iron enters a redox cycle in the presence of biological reductants ($R_{(n=number\ of\ electrons)}$) and oxygen to generate the superoxide radical ($O_2^{\bullet -}$), hydrogen peroxide (H_2O_2), and the hydroxyl radical ($^{\bullet}OH$) in the Fenton reaction. This may result in the depletion of extra- and intra-cellular antioxidants such glutathione (GSH) and ascorbic acid (AA). Furthermore, the altered redox state may cause an upregulation of redox sensitive signalling pathways and transcription factors (NFκB and AP-1) leading to the increased production of cytokines and the development of airway inflammation. Adapted from Kelly *et al.* (2007)

Furthermore, the inflammatory response may also be directly activated by biological components of PM, such as pollen, fungi, and bacterial components. Macrophages and bronchial epithelial cells, which are the first line of defence for inhaled particles, contain pattern recognition receptors (such as Toll-like receptors) which recognize microbe-associated molecular patterns (MAMPs) present in the invading microbes (Table 1.2). As a result, intracellular signalling cascades are activated, leading to the induction of a pro-inflammatory response. This includes the release of i) antimicrobial mediators - which target the invading microbes, ii) chemokines - which recruit more immune cells to the site of infection, and iii) pro-inflammatory cytokines - which drive further inflammation. This innate inflammatory response will then induce the adaptive immune response, which is mediated by T and B (antibody-driven) cell lymphocytes and is more specific for the particular invading microbe (Kelly and O'Neill, 2015). Of the biological components of PM, endotoxins from gram-negative bacteria are ubiquitously present due to their resilience to degradation and are known

to be one of the strongest elicitors of the pro-inflammatory immune response, which is also why they are rigorously monitored in pharmaceutical products. In fact, the secretion of pro-inflammatory cytokines TNFα, IL-1β, IL-6 is greater in response to 1 μg/ml LPS than to 10 times more lipoteichoic acid (LTA) in gram-positive bacteria (Aulock *et al.*, 2006). Furthermore, larger pollen and fungal spores may be predominantly filtered out by nose cilia and mucus, while endotoxin remains active after being released from the membrane during death, lysis, or growth of bacteria and may thus accumulate in the coarse PM fraction. Endotoxins are also known to act as natural adjuvants, heightening the response of the stimulant, which may be significant for the various components of PM in the resulting inflammatory response. For these reasons, this PhD thesis focussed on endotoxin as a relevant biological component of PM.

Table 1.2: The human Toll-like receptors (TLRs) allow the detection of different types of infection (Parham, 2014)

Recognition of microbial products through Toll-like receptors				
Receptor	**Ligands**	**Microorganisms recognized**	**Cells carrying receptor**	**Cellular location of receptor**
TRL1:TLR2 heterodimer	Lipopeptides	Bacteria	Monocytes, dendritic cells, eosinophils, basophils, mast cells	Plasma membrane
	Glycosylphosphatidylinositol	Parasites		
TLR2:TLR6 Heterodimers	Lipoteichoic acid	Gram-positive bacteria		Plasma membrane
	Zymosan	Fungi		
TLR10 homodimer and heterodimers with TLR1 and 2	Unknown		Plasmacytoid dendritic cells, basophils, eosinophils, B cells	Unknown
TLR4 homodimer	Lipopolysaccharide (LPS)	Gram-negative bacteria	Macrophages, dendritic cells, mast cells, eosinophils	Plasma membrane
TLR7 homodimer	Single-stranded viral RNAs	RNA viruses	Plasmacytoid dendritic cells, basophils, eosinophils, B cells	Endosomes
TLR8 homodimer	Single-stranded viral RNAs	RNA viruses	NK cells	Endosomes
TLR9 homodimer	Unmethylated CpG-rich DNA	Bacteria, DNA viruses	Plasmacytoid dendritic cells, B cells, eosinophils, basophils	Endosomes
TLR3 homodimer	Double-stranded viral RNA	RNA viruses	NK cells	Endosomes
TLR5 homodimer	Flagellin, a protein	Bacteria	Intestinal epithelium	Plasma membrane

1.3 Endotoxin

Although the term endotoxin is occasionally used to refer to any cell wall-embedded microbial toxin, it is more commonly used (and within this thesis) to describe the biological activity of lipopolysaccharides (LPS) situated in the outer membrane of gram-negative bacteria. Endotoxin, or LPS, are amphipathic molecules comprised of a lipid A moiety anchored in the bacterial outer membrane, and with a core oligosaccharide and an O-specific chain orientated to the aqueous environment (Fig 1.5). LPS that comprise all three regions are known as smooth (S)-form LPS given their unwrinkled visible colony morphology, while LPS lacking the O-specific chain are named rough (R)-form LPS or lipooligosaccharide (LOS). While the O-specific chain is not necessary for *in vitro* survival, it has been shown to provide *in vivo* protection from phagocytosis and serum (complement)-mediated lysis for some gram-negative pathogens (Williams, 2007). The O-specific chain is a polymer of up to 50 repeating oligosaccharides (between 2-8 sugar monomers), and may exhibit enormous structural variability, differing between bacterial strains and functioning as an important surface antigen (thus also known as O-antigen). Serological identification of members of the family Enterobacteriaceae utilizes the variation inherent in this region of LPS and is the only means of identifying certain pathogenic strains of *E. coli* (Williams, 2007).

The O-antigen chain connects to the core oligosaccharide, which is made up of an outer and inner (proximal to lipid A) core. The outer core contains common sugars such as D-glucose (Glc), D-galactose (Gal), N-acetyl-D-glucosamine (GlcN)/galactosamine (GalN), while the inner core is more conserved and contains two uncommon sugars specific to LPS: Kdo (2-keto-3-deoxy-D-manno-octulosonic acid) and a seven-carbon heptose (Hep). The inner core residues are usually substituted by various charged phosphates groups, giving the LPS complex an overall negative charge that binds bivalent cations such as Ca^{2+} and Mg^{2+} for the structural and functional integrity of the outer membrane. The minimal bacterial LPS structure capable of sustaining bacterial growth and survival consists of one Kdo residue linked to lipid A (Rietschel *et al.*, 1994). Due to its importance, the structure of the lipid A is the most conserved moiety of LPS and consists of a phosphorylated disaccharide backbone substituted with fatty

acids (Steimle *et al.*, 2016). Lipid A is considered to be the bioactive center of the LPS, and is responsible for virtually all endotoxic activity by LPS in host cells as further discussed.

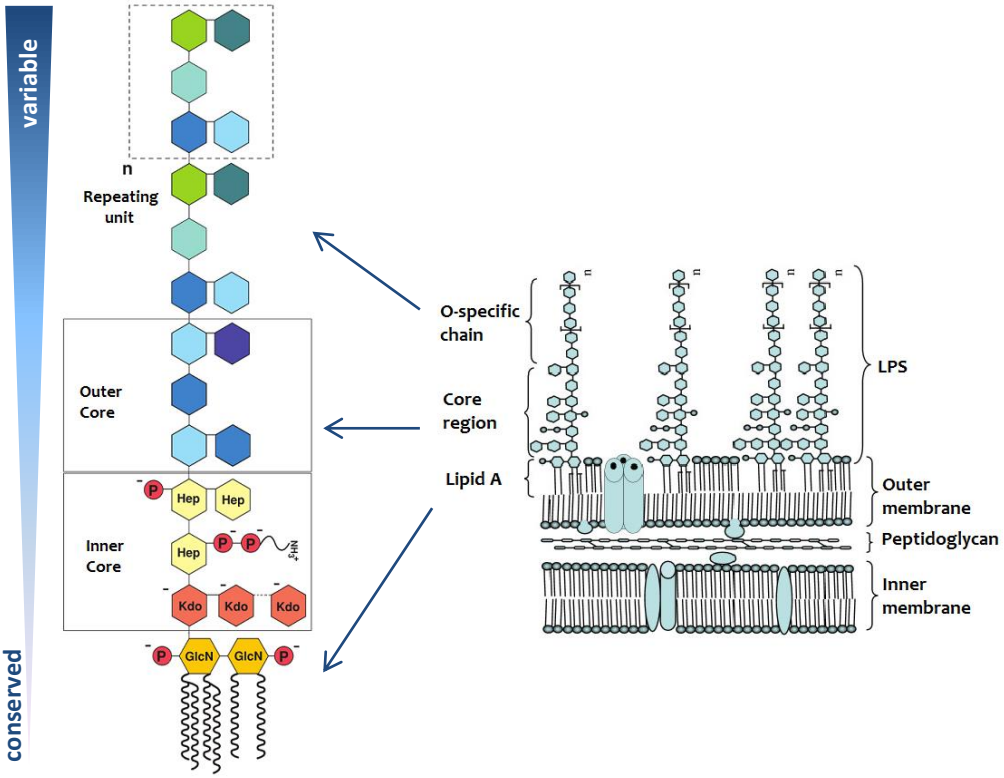

FIG 1.5: Scheme of the general chemical structure of LPS, which consists of a repetitive polysaccharide (O-specific chain) and the core oligosaccharide exposed to the extracellular environment, and the lipid A moiety embedded in the outer membrane (Cardoso *et al.*, 2006)

1.3.1 Biological recognition of LPS

Our innate immune system has been trained to detect endotoxin in picomolar concentrations (Gioannini *et al.*, 2004) as it represents a microbial-associated molecular pattern (MAMP), alerting the body to an invasion of gram-negative bacteria. The receptor responsible for recognizing endotoxin is Toll-like receptor 4 (TLR4), a member of the TLR family, found on the surface of many immune cells such as macrophages and epithelial cells (Lu *et al.*, 2008). Activation of TLR4 is an important step for the induction of inflammatory processes and

antibacterial defense mechanisms, but might also lead to multi-organ failure and shock upon excessive systemic LPS exposure (Lu *et al.*, 2008).

Extracellular LPS recognition is chaperoned by several proteins, including LBP (LPS binding protein), CD14, and MD-2 (myeloid differentiation factor 2). LBP is a soluble protein present in the fluid on the airways surface that directly binds to the lipid A component. The LBP-LPS complex is then transported to monocytes and macrophages where they facilitate the association between LPS and the cell surface protein CD14. In turn, CD14 assists the transfer of LPS to the TLR4/MD-2 receptor complex and modulates LPS recognition. Upon stimulation, a complex signal transduction cascade is initiated as summarized in Figure 1.6. A signal complex containing the three adaptor proteins: MyD88 (myeloid differentiation factor), TIRAP (Toll/IL-2-receptor-domain-containing-adaptor protein) and TOLLIP (Toll-Interacting protein) is formed. This complex stimulates a phosphorylation cascade which activates IRAK (interleukin-receptor-associated kinase), TRAF6 (TNF-receptor-associated factor), and eventually IKK (IκB kinase) and MAPK (mitogen-activated protein kinase) pathways. IKKa, IKKb and IKKc form a complex which phosphorylates and subsequently degrades IκB (inhibitor of κ light chain gene enhancer in B cells) proteins. This leads to the activation of nuclear factor-κB (NF-κB) which may now translocate into the nucleus and induce the expression and release of numerous inflammatory mediators such as interleukins IL-1β, IL-6, IL-8 and tumor necrosis factor alpha (TNFα) (Liebers *et al.*, 2008; Lu *et al.*, 2008)

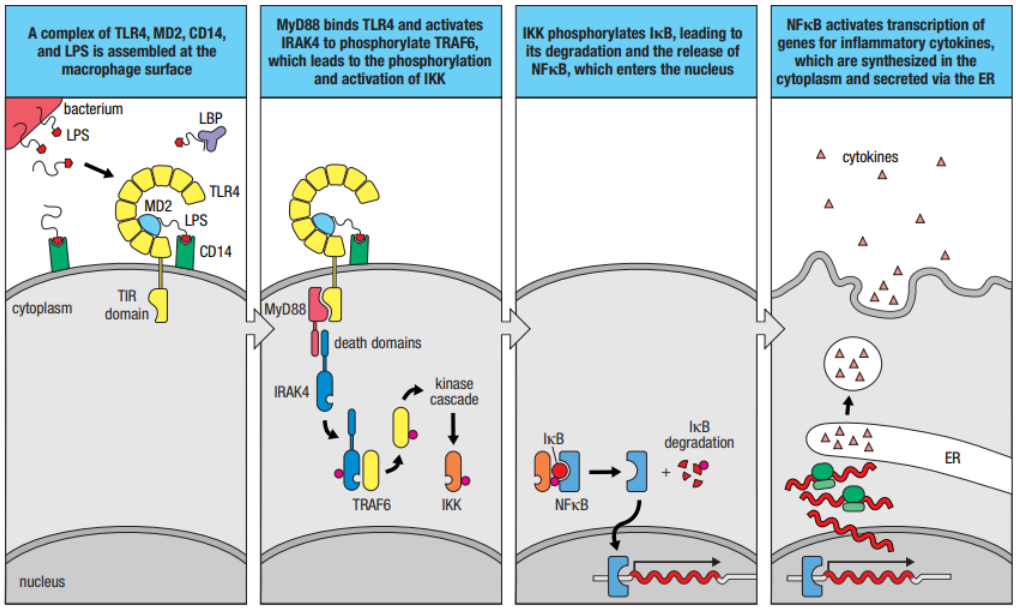

FIG 1.6: Stimulation of TLR4 by LPS on macrophages leads to the activation of the transcription factor NFκB and the production of inflammatory cytokines (Parham, 2014)

Furthermore, a MyD88-independent pathway was later discovered when studies using MyD88 knockout mice found that stimulation of TLR4 still lead to the activation of NF-κB (although delayed), yet without the production of pro-inflammatory cytokines. This MyD88-independent pathway was shown to be responsible for induction of Type I interferons and interferon-inducible genes. The differences between the pathways are briefly summarized in Figure 1.7 (Kawai *et al.*, 1999; Lu *et al.*, 2008).

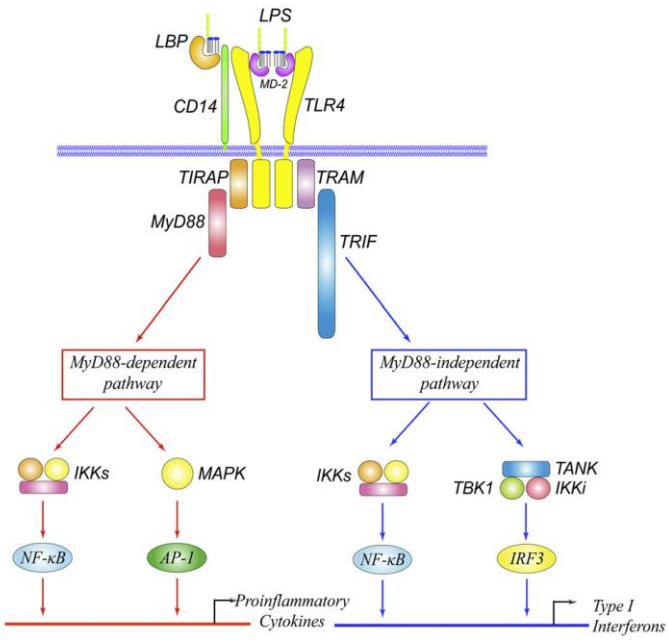

FIG 1.7: Schematic representation of LPS recognition and intracellular TLR4 signalling pathways, with major components indicated. Components previously not introduced include TRIF (TIR-domain-containing adapter-inducing interferon-β), TRAM (TRIF-related adaptor molecule), TANK (TRAF associated NFκB activator), TBK1 (TANK binding kinase 1), AP-1 (activator protein 1) and IRF3 (Interferon regulatory factor 3). Adapted from Lu *et al.* (2008)

1.3.2 Endotoxin detection methods

There have been many efforts to establish rapid and reliable detection methods for LPS, most of which are aimed at clinical samples and for testing pharmacological products, but have also been applied for the detection of airborne endotoxins. The first method approved by the US Food and Drug Administration for LPS detection in the 1940s was called the rabbit pyrogen test, which simply measures the ability of an endotoxin to induce fever in an animal (Stromberg *et al.*, 2017). In 1956, Bang discovered that amoebocytes from the horseshoe crab (*Limulus Polyphemus)* agglutinate upon addition of endotoxin. Bang and Levin subsequently used this concept to devise a method for endotoxin detection. Since the lysates of amoebocytes were required, it was called the limulus amoebocyte lysate (LAL) assay, and has been the gold standard for the endotoxin detection over the last 30 years. In the main pathway, Factor C is

triggered by extremely low levels of endotoxin, which activates intermediate serine proteases in the coagulation event to cause gelation or cleaves chromogenic substrates (Fig 1.8). Despite its sensitivity, several of the following drawbacks of the LAL assay have become apparent over the years: i) lack of specificity owing to LAL-reactive materials and fungal contaminant β-D-glucan; ii) batch-to-batch fluctuation in the sensitivity of commercial lysate to endotoxin; iii) presence of various interfering components from different sample types, and iv) a dwindling population of horseshoe crabs (Stromberg *et al.*, 2017). This prompted the urgent need for an alternate source of LAL, which was met with the technological advances in genetic engineering. The recombinant Factor C (rFC) assay was developed by a genetically engineered recombinant Factor C produced from the cDNA of the Mangrove horseshoe crab (*Cacinoscorpius rotundicauda*) and expressed in insect cell lines using a baculoviral expression system (Ding and Ho, 2001). Upon stimulation by trace levels of LPS, the proenzyme rFC gains full enzymatic activity to hydrolyze a synthetic fluorogenic substrate, as illustrated in figure 1.8.

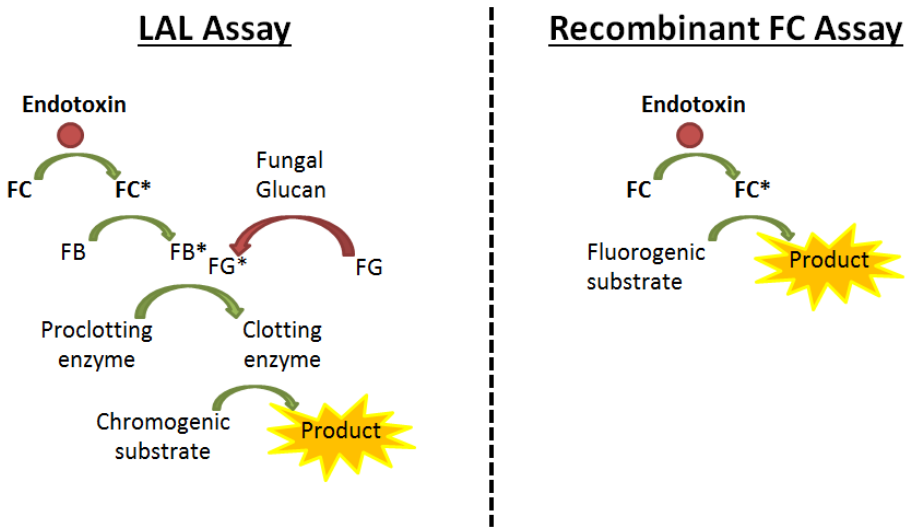

FIG 1.8: Enzymatic pathways of the LAL and rFC assays
The kinetic LAL assay relies on an endotoxin-activated enzymatic cascade from the Atlantic horseshoe crab (*Limulus Polyphemus*) to cleave a colorimetric substrate (p-nitroaniline), however, this assay may also be activated by fungal (1→3)-β-D-glucans. The rFC assay uses a genetically engineered recombinant Factor C which can directly hydrolyses a fluorogenic substrate.

The structural motif necessary for activation of Factor C depends, in part, on the acylated (β1-6)-D-glucosamine disaccharide phosphate molecule of lipid A (Fig.1.9) (Gutsmann *et al.*, 2010). For different bacterial species, deviations in the acylation pattern or the phosphorylation state (at position: 1 or/and 4') influence the activation of Factor C and cytokine production in monocytes or macrophages differently. For instance, it was found that underacylated lipid A (tetra- and penta-acyl) exhibited high LAL activity, whereas they are inactive or only weakly active in the production of cytokines (Schromm *et al.*, 2000). Furthermore, about 1000-fold more LPS from *P. aeruginosa* was necessary to induce TNFα of comparable amounts to *E. coli* LPS, while no significant release of IL-10 or IFN-γ could be induced (Dehus *et al.*, 2006).

In solution, LPS molecules will tend to aggregate to form supramolecular structures due to their amphipathic nature. This aggregation is essential for the activation of both Factor C and cytokine production since activity in the monomeric state is either strongly reduced or absent. While the type of aggregate structure is not as important for the activation of Factor C, only LPS adopting inverted conical structures (which expose the hydrophobic acyl group) are biologically highly active (Schromm *et al*, 2000). Furthermore, endotoxin may exist free or still membrane bound. Older studies on pure bacterial cultures suggest that LPS still embedded in the cell membrane is not as capable of activating the LAL assay as free LPS (Jorgensen and Smith, 1974; Mattsby-Baltzer *et al.*, 1991). In contrast, the biological activity of inhaled endotoxins appears high when still bound (Rylander *et al.*, 1989).

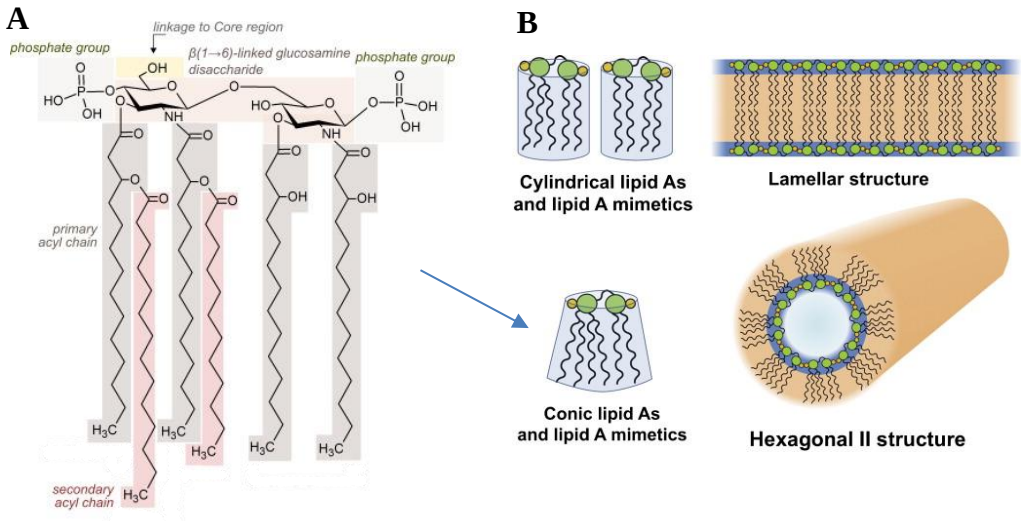

FIG 1.9: A) Chemical structure of *E. coli* lipid A, B) structural aggregates of lipid A
The LPS structure of *E.coli* is considered to be close to that optimally recognised by human cellular LPS receptors by forming conical structures. Deviations from this bisphosphorylated diglucosamine backbone with six acyl chains are typically seen to result in molecules of lower biological activity and forming lamellar structures. Adapted from A) Steimle *et al.* (2016) and B) Calabrese *et al.* (2015)

1.3.3 Bacterial sources of airborne endotoxins

Endotoxin is as abundant in our environment as the bacteria from which they originate. Subsequently, by better understanding the changes in airborne bacteria and their sources, we may in turn understand the fluctuations in ambient endotoxin concentrations. Bacteria enter the near-surface atmosphere by aerosolization from various surfaces exposed to air currents. Besides soil and vegetation, oceans and seas are also known to contribute to the bacterial content of the atmosphere by ejection of aerosol droplets into the air (Aller *et al.*, 2005). Other potential sources of airborne bacteria have been identified, as illustrated in Figure 1.10. The relative contribution of these sources varies greatly and dominant sources tend to change with time and space. One area of expanding research is source-tracking, which allows an estimation of the relative contribution of the sources of airborne bacteria at a particular location. Hereby, the taxonomic identifications of airborne organisms are used to determine contribution of the putative source environments, in which these taxonomic units are typically found (Bowers *et*

al., 2011a; Bowers *et al.*, 2011b; Cao *et al.*, 2014). For example, source tracking allowed Bowers and colleagues (2011b) to discover that dog faeces was likely the dominant source of bacteria in outdoor air during winter periods in Cleveland and Detroit.

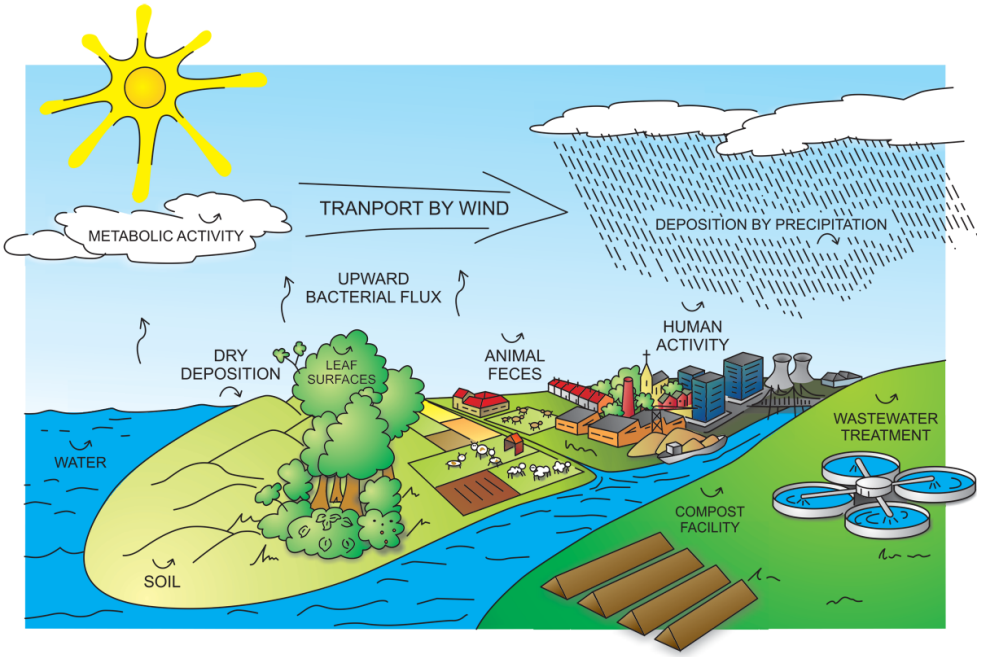

FIG 1.10: Scheme of typical processes that determine the composition of local airborne bacterial communities. Abundant sources of aerosolized bacteria are marked with an upward arrow. Soil and leaf surfaces are often considered the main contributors of airborne bacteria (Bowers *et al.*, 2011c). Other sources of airborne bacteria include water bodies (Blanchard, 1989; De Leeuw *et al.*, 2011), humans and animals (Fujimura *et al.*, 2010; Pan *et al.*, 2007; Sciple *et al.*, 1967; Zhao *et al.*, 2014), faecal material (Bowers *et al.*, 2011c), wastewater treatment (Han *et al.*, 2012), and composting facilities (Albrecht *et al.*, 2007). In case airborne bacteria are transported upwards, indicated as upward flux, they can be transported over medium or long distances and may occur in cloud droplets. Mechanisms leading to deposition are indicated with a downward arrow. Published in co-authored review of Smets *et al.* (2016)

As also shown for air pollution composition (section 1.2.2), a general trend can be observed in different studies correlating the composition of the bacterial communities and the environmental factors. Of these factors, seasonality, meteorological conditions, anthropogenic influences, and variability in bacterial sources play an influential role in shaping the abundance and composition of airborne bacterial communities across time and space. How and to what extent these factors affect the bacterial communities is, however, very context dependent. In

Milan (Italy), summer communities differed less from each other than the communities sampled during the other seasons, possibly owing to the stability of the air and particulate matter levels in summer (Bertolini *et al.*, 2013). It may be possible that, in addition, the stressors in summer, such as ozone, drought and solar radiation all together induce a constant selective pressure, which leads consistently to the survival of adapted species. In relation to this, there are two general speculations for the correlation of meteorological factors with community composition: the shifts in atmospheric stressors select for different adaptations of bacteria (e.g. spore formation, pigmentation), or the wind, temperature, precipitation and season affect the contribution of different source environments for the airborne bacteria at a set location (e.g. more leaf-associated bacteria in summer) (Bowers *et al.*, 2013; Huffman *et al.*, 2013; Jones and Harrison, 2004). In the case of the latter, source contribution is playing the leading role in the abundance of the different bacteria in the atmosphere. This implies that airborne bacteria are no more than a collection of organisms dispersed from different sources, and therefore less likely to be part of an atmospheric ecosystem. However, airborne bacterial communities are distinctly different from their source environments, possibly because many of the bacteria do not survive in the atmospheric environment (Bowers *et al.*, 2011a). The specific selection pressure in the atmosphere may, additionally, be caused by other ecological factors, such as availability of certain substrate. This ecological point of view rather fits into the "atmosphere biome" hypothesis of Morris *et al.* (2011), whereby the airborne microbes actively interact with each other and with the environment. This hypothesis is supported by the studies on adaptations and metabolic activity of airborne bacteria. It is likely these two explanations co-exist, as also stated by Womack *et al.* (2010). This means that only a certain fraction of bacteria in the atmosphere would be metabolically active. Further information can be found in our review (Smets, Moretti *et al.*, 2016) (shared first authorship).

1.3.4 Endotoxin as a component of PM

Owing to the wide abundance of bacteria, LPS are ubiquitously present in the atmosphere, either still associated with or released from bacteria following cell lysis or growth. Furthermore, because of their extreme resiliency, thermostability and relatively low sensitivity

towards pH changes, these molecules are able to persist in the environment for long periods of time and remain biologically active (Ding and Ho, 2010).

Inhalatory endotoxin exposure has been associated with a range of respiratory health effects, including both acute and chronic airway inflammation (Liebers *et al.*, 2008; Rylander, 2006). Research on airborne endotoxins has mainly focused on occupational exposure where exceptionally high concentrations are related to prominent gram-negative bacterial reservoirs, e.g. agriculture and waste management (Rylander, 2006; Spaan *et al.*, 2008b). Although an international exposure limit has not yet been established – mainly due to the absence of an international standard protocol for sampling and analysis of airborne endotoxins – the Dutch Expert Committee on Occupational Safety (DECOS, Netherlands) published a report proposing an occupational exposure limit of 90 EU m^{-3} (DECOS, 2010). An important note to consider, as suggested by Nilsson *et al.* (2011), is that an occupational exposure limit is intended for the working population, i.e. people between 20-65 years of age, who are healthy and only exposed during a limited period of time. An exposure limit for the general population is generally considerably lower, also taking children, elderly, sick and other susceptible individuals into consideration, as well as the much longer exposure time.

Subsequently, the lower endotoxin concentrations found in an urban environment may also be highly relevant. Moreover, when endotoxins are associated with pollutants such as PM, co-stimulation may result in a more complex and heightened immune response (Degobbi *et al.*, 2011; Imrich *et al.*, 1999; Ryan *et al.*, 2009). Most studies have shown that endotoxin is predominantly found in the coarse, PM_{10} fraction (Allen *et al.*, 2011; Heinrich *et al.*, 2003; Schins *et al.*, 2004). Also, the highest concentrations in outdoor air may be associated with warmer seasons, although this is highly dependent on the bacterial sources (Degobbi *et al.*, 2011). The subsequent chapters will further focus on endotoxin as a component of PM, together with better understanding the immunological response and synergistic effects.

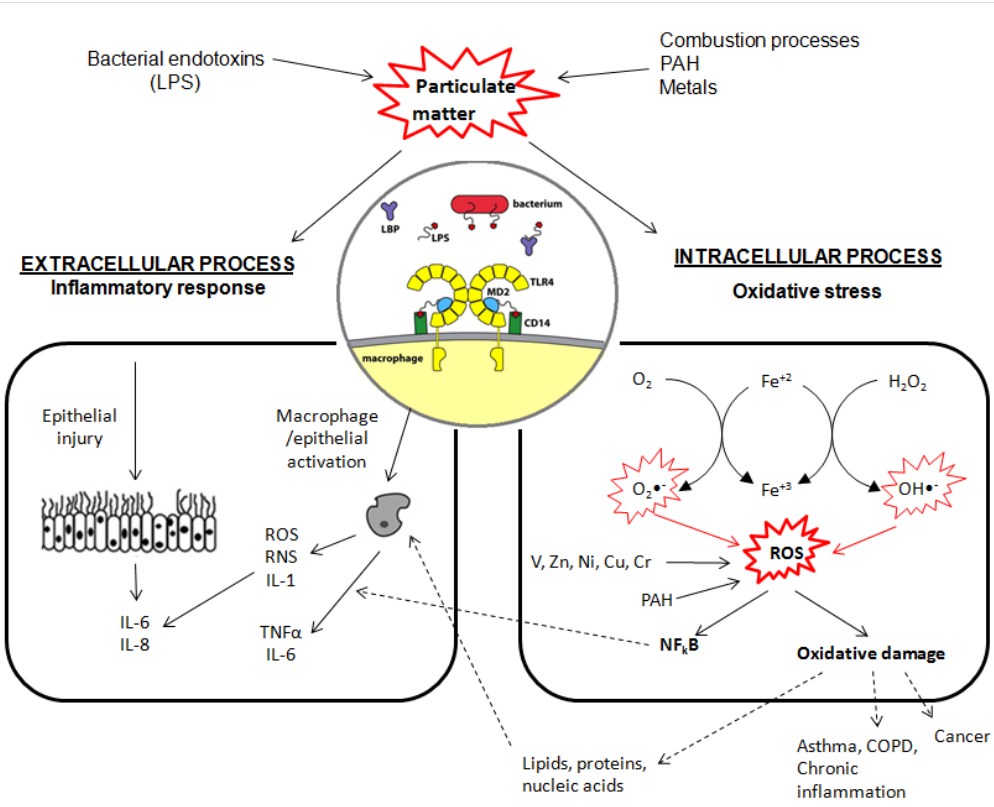

FIG 1.11: Illustration of cellular oxidative stress and the pro-inflammatory response induced by PM particles in the lung. Adapted from (Michael *et al.*, 2013)

1.4 Objectives and thesis structure

The common research theme of the Bioscience Engineering Department at the University of Antwerp is air pollution, given its high relevance in Flanders. The topic is addressed by the four major research lines within the department, namely: the photocatalytic degradation of air pollution, the biomonitoring of air pollution using urban plants, computational fluid dynamics and modeling, and recently the (micro) biological and immunological studies of air pollution. As the first PhD student in the newly established laboratory, we set out to investigate the role of bacterial endotoxins in the inflammatory response of ambient urban PM. Although not always explicitly mentioned, an important objective of this PhD was also to explore possible analyses, method developments and validate assays for further projects. To highlight key steps

for these developments and optimizations, they are therefore indicated with this sign in the following chapters.

To understand the role of ambient endotoxin in PM associated inflammation, we first needed to know the abundance of endotoxin in an urban environment. In chapter 2, we assessed the current literature and methodology for endotoxin monitoring. Subsequently, we decided to apply a more microbial approach to collect air samples in order to increase the recovery of endotoxins. Here, we collected air samples in the city of Antwerp over two different sampling campaigns. In the first campaign in 2014, we collected samples from numerous locations within Antwerp to better understand the widespread concentrations of ambient urban endotoxins. Furthermore, many optimizations were performed during this campaign. The second sampling period in 2015 focussed on two sampling sites for each representative land-use class (urban traffic, green, and industrial). The 2015 samples were further analysed in the following chapters.

Once we had quantified endotoxin, we subsequently asked the question of whether assays such as the LAL or rFC assay where sufficiently predictive/accurate for the bio-activity of endotoxins in these complex environmental samples. For this reason, in chapter 3, we used the HEK hTLR4 cell line to monitor the human host immune recognition of endotoxin through TLR4 and investigated the transcriptional regulation of pro-inflammatory genes (IL-1β, IL-8, TNFα) in the macrophage-like U937 cells. We compared endotoxin quantification (measured with the rFC assay) with the stimulation of TLR4 in the HEK cell line over the different urban land-use classes. Furthermore, we established which assay was better correlated to the pro-inflammatory markers.

In chapter 4 we turned our focus to the particle count and composition of the PM from the different urban land-use classes. Here, transition metals were quantified in the collected air samples due to their importance as atmospheric contaminants and their key association with oxidative stress responses. We investigated the correlation of these metals to the each other, the

particle count, and the inflammatory response. Furthermore, since nickel and cobalt are known to directly activate TLR4, we investigated the potential involvement of transition metals with TLR4 stimulation to help explain the disparities between endotoxin quantification (rFC assay) and TLR4 stimulation in the HEK cell line. Additionally, we also confirmed whether the transition metals collected with the impinger sampler were recovered in similar and relevant concentrations to those typically measured and reported by the Flemish Environmental Agency (VMM).

From chapter 4, we found iron concentrations to be well correlated with the stimulation of the HEK hTLR4 cell line. Therefore, in chapter 5 we further investigated the validity of the HEK hTLR4 cell line to report TLR4 stimulation, and explored whether the correlation of iron may be linked to causative and synergistic effects between LPS and iron. Once we confirmed the synergistic effect between iron and LPS, we investigated the transcriptional regulation in the macrophage-like U937 cell line during co-exposure to better understand the mechanism behind this effect. Here we monitored the mRNA expression of biomarkers for the resulting pro-inflammatory and oxidative stress responses, and TLR4, TLR2 and MD-2 expression. To further evaluate the regulation of these genes, the samples collected in 2015 were screened for their relative expression.

Finally, in chapter 6 we summarize the main findings of the thesis and briefly discuss an ongoing project aimed at integrating these results with a larger PM fingerprinting campaign at the department.

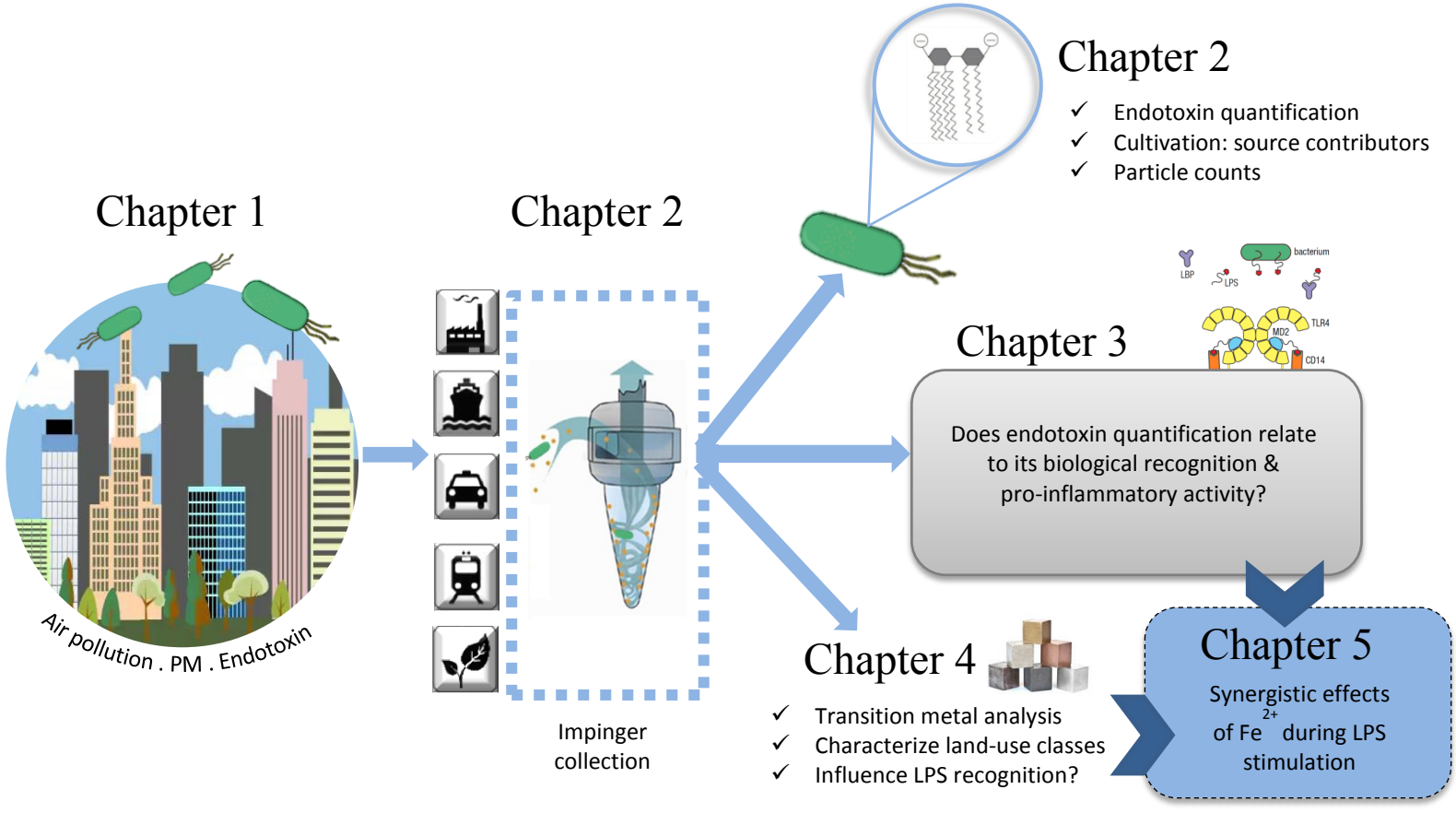

FIG 1.12: Graphical overview of the chapters of this PhD thesis

Chapter 2

Ambient endotoxin concentrations in an urban environment

"Measurement is the first step that leads to control and eventually to improvement"

-- H. James Harrington

Adapted from Moretti S, Smets W, Oerlemans E, Blust R, Lebeer S (2018). The abundance of urban endotoxins as measured with an impinger-based sampling strategy. Accepted in *Aerobiologia*

2.1 Introduction

Studies have monitored and sampled ambient, outdoor endotoxin concentrations in urban environments mainly using filter-based methods (Table 2.1). These filter-based methods have typically been used for the collection of PM, being advantageous for their strict cut-off limits on particle size. This has provided us with insights on composition and quantity of the different particle ranges. i.e. endotoxin predominately found in the coarse PM fraction (Allen *et al.*, 2011; Heinrich *et al.*, 2003; Schins *et al.*, 2004). However, concerns exist over the large amount of problems and variation resulting from the endotoxin extraction process from the filters (Duchaine *et al.*, 2001; Gordon *et al.*, 1992; Heinrich *et al.*, 2003; Mueller-Anneling *et al.*, 2004; Spaan *et al.*, 2008a).

TABLE 2.1: Comparison of ambient endotoxin concentrations in PM_{10} from previous urban studies using filter-based samplers and the LAL assay for endotoxin quantification.

Location	**Samples**	**EU m^{-3}**			**Reference**
		Mean	**Min**	**Max**	
Southern California	104	0.44	0.03	5.44	Mueller-Anneling *et al.* (2004)
Munich, Germany	48	0.081	0.041	0.141	(Morgenstern *et al.*, 2005)
Stockholm, Sweden	18	0.05	0.02	0.107	Nilsson *et al.* (2011)
Torino, Italy	18	0.512	Not reported		Traversi *et al.* (2011)
Turin, Italy	47	0.42	0.09	0.94	Traversi *et al.* (2010)
Guangzhou	34	0.386	0.106	1.017	Cheng *et al.* (2012)
Hong Kong, China	32	0.350	0.080	1.245	
Regina, Canada	100	1.57 (summer)	0.15	6.41	Wheeler *et al.* (2011)
	79	0.12 (winter)	0.02	0.58	

Impingement, whereby airborne particles are directly collected in liquid, is already known as a useful alternative for microbial air sampling and bypasses the lengthily and problematic filter-extraction procedures. In terms of physical efficiency, certain impingers appear at least as

useful as dry air filters for the collection of coarse airborne particles. Their added advantage lies in their increased biological efficiency, whereby microbial stress is limited (e.g. shear forces and desiccation) and cell viability is preserved (Dybwad *et al.*, 2014; Griffin *et al.*, 2011).

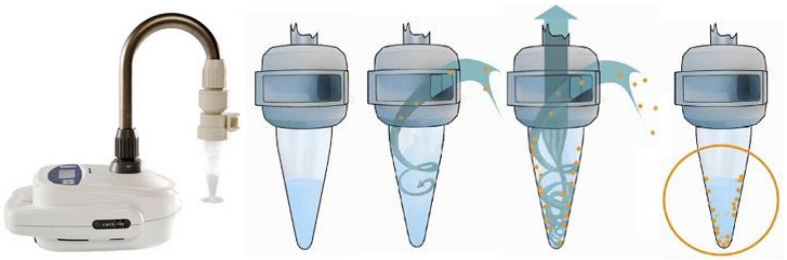

FIG 2.1: The illustrated principle of the Coriolis®µ air sampler

2.2 Aim

Despite the potential of an impinger-based collection strategy, this microbial-targeted approach has not yet been applied for the monitoring and collection of ambient urban endotoxins. This chapter therefore explored the application of a cyclonic impinger sampler (Coriolis®µ air sampler, Bertin Technologies) for the quantification of airborne endotoxin concentrations in an urban environment (i.e. Antwerp, Belgium) measured over urban traffic, urban green, and industrial land-use classes. Since particles were directly collected in liquid, an alternative measure to PM_{10} (expressed as µg m^{-3}) was investigated by counting particles per m^3 air with a Coulter counter. Furthermore, a link between airborne endotoxins and their cultivable bacterial source was investigated.

2.3 Materials & Methods

2.3.1 Air sampling

In total, 87 samples were collected from 11 monitoring locations within Antwerp (Belgium), a city of just over half a million inhabitants and accommodating the second largest harbour in

Europe. Antwerp provides an excellent European urban model due to its diverse environmental elements, such as heavily trafficked roads in densely-built locations, tram and train lines, urban green elements such as parks and tree linings, and an industrial harbour region. The city, including the harbour region, is also well monitored for its air quality by the Flanders Environment Agency (VMM).

Samples were collected at a median sampler height of 1.6 m using the Coriolis® µ air sampler (Bertin Technologies, France), a swirling aerosol collector, where air was drawn in a pyrogen-free, polycarbonate cone containing 15 ml of ultra-pure water (which was chosen for its applicability for the various downstream analyses). The air drawn in at a flow rate of 300 L min^{-1} (for 40 min; 12 m^3 air per sample) creates a vortex in the cone and airborne particles are deposited in the water by centrifugal force.

The flow rate and sampling time were optimized to ensure sufficient concentrations over the different sampling locations for each downstream analysis

The Coriolis sampler technology has been validated by the Health Protection Agency (HPA; Porton Down, UK) and ISO 14698-1 certified for biological/physical efficiency with a d50 < 0.5µm (i.e. at a particle diameter of 0.5 µm and above, the sampler efficiency is 50% or more). To test for contaminants, both the sampling water and filled cones were regularly tested in all analyses. All sampling sites were distributed spatially within and around Antwerp and representative of various levels of pollutants and microbial exposure (Fig 2.2): urban traffic (B, C, D, E, F), urban green (G, H, I, K), industrial (A, J) with J being the harbour and A being an urban industrial metal recycling plant. These land-use classes were adapted from the "continuous urban fabric (S.L. > 80%)", "green urban areas", and "port areas" respectively defined by Urban Atlas, which was developed by the EU's Copernicus Land Monitoring Service based on satellite image interpretation for the reference year 2012 (freely accessible at http://land.copernicus.eu/).

A minimum of three samples were taken from each location. Typically, three samples were collected per day and representative of the three different land-use classes (traffic, green and industrial) to account for confounding day-to-day variation. Sampling occurred during the day (10:00 to 16:00) over two sampling periods, namely August to December 2014 (n=42) and July until September 2015 (n=45), during which temperature and humidity were measured on site (Appendix A1) and meteorological events such as fog were also recorded. While the first sampling period included numerous locations within the city for a broader overview of endotoxin concentrations, the second sampling period focussed on two sampling sites for each representative land-use class, i.e. urban traffic (B, C), urban green (G, I), and industrial (A, J).

	Name	Description
A	Harbour	Industrial harbour area
B	Traffic 1	Street canyon with high-traffic
C	Traffic 2 (trams)	Street canyon with high city traffic opposite tram lines
D	Traffic 3 (train)	Open traffic road near train and harbour
E	Traffic 4 (Ring)	Open major ring junction of motorway (Ring)
F	City campus	City centre of Antwerp
G	Park	Park located near Ring and bordered by trees
H	Campus G	University campus site in green area, but near tunnel ventilators of bypassing motorway.
I	Campus DE	Greener campus in suburbs
J	Metal plant	Green residential area across a metal recycling factory
K	Pasture	Cow pasture across light-traffic road in suburbs

FIG 2.2: The eleven sampling locations in Antwerp
Sites marked with a star are indicative of the main (more frequently sampled) sites which included VMM stations. More information of the sampling sites is provided in chapter 3. Google maps (2014)

A subset of sampling sites in both sampling campaigns (A, B, D, J) was chosen based on their close location near (within five meters distance from) existing monitoring stations of the VMM to obtain additional information such as PM_{10}. These PM_{10} values are determined using automated monitors (ESM FH 62 I-R and series 8500 FDMS system) to provide real-time measurements (reported every half-hour). These results are also validated with the reference Leckel SEQ 47/50 sequential gravimetric sampler (VMM 2011).

After collection, samples were transported on ice back to the laboratory. The volume of every sample was normalized to 15 ml with ultra-pure water to compensate for evaporation losses of the collection liquid during sampling. The samples were briefly vortexed, aliquoted accordingly for the various assays, and stored in glass vials at -20°C (typically within 12 hrs) until analysed.

2.3.2 Quantification of ambient endotoxins

All samples were thawed only once and endotoxin quantification (EU ml^{-1}) was determined in triplicate using the recombinant Factor C (rFC)-assay according to manufacturer's instructions (Lonza Walkersville Inc., MD, USA; lot 0000 416 097). For rFC assay analysis, a blank and a five-point standard curve (10, 5, 1, 0.1, 0.02 EU ml^{-1}) was set up in glass vials using endotoxin standards (Escherichia coli O55:B5 lot 0000 396 350; Lonza Walkersville Inc., MD, USA). The samples (neat or diluted) were vortexed and added to a 96-well plate heated to 37°C before the 100 µl mixture of enzyme, buffer, and fluorogenic substrate was added with a multichannel pipette. The plates were incubated at 37°C for 1 h and read (t=0 and t=60 min) in a fluorogenic microplate reader (MX Synergy, BioTek; Gen5 software) at excitation and emission wavelengths of 380 and 440 nm, respectively. Background fluorescence was subtracted, and log change in fluorescence was plotted against log endotoxin concentration over the range of 0.02 to 10 EU ml^{-1} (R^2>0.98). The endotoxin concentration for a sample was calculated from the arithmetic mean of those dilutions that fell within range of the standard curve and expressed as endotoxin unit (EU) per m^3 of air based on the sampling conditions. The majority of the samples were analysed at a 1:2 dilution, whereas a few high outliers were diluted either 1:10 or 1:100. A single lot (0000 416 097) of rFC was used for all analyses. Endotoxin

distribution plots were constructed in GraphPad Prism v6.05 for Windows (GraphPad Software, La Jolla California USA, www.graphpad.com). Endotoxin concentrations were log-transformed to obtain normal distribution for the mean to be indicated.

Endotoxins are fastidious to work with and several points are good to keep in mind:

- ✓ Endotoxins are adherent. Plastics (e.g. polypropylene) are avoided and glass is preferably used.
- ✓ Due to the ubiquitous and durable nature of endotoxins, all reagents and consumables must be endotoxin-free. Glassware was heat sterilized at 250°C for 3 hrs, while sampling cones were first cleaned in the dishwasher, then with 0.5M NaOH for 24 hrs to degrade endotoxins (higher concentrations of NaOH weaken the polycarbonate cones and cause them to crack), then rinsed thoroughly three times with ultrapure water.
- ✓ Vigorous vortexing is often required to avoid micelle formation and endotoxin adsorption on the glassware walls.
- ✓ Endotoxins are stored in aliquots and should only be thawed once, since freeze-thaw cycles can significantly decrease concentrations, as also shown by Duquenne *et al.* (2013).

2.3.3 Determination of cultivable bacteria

Between 15 and 150 µl of sample was plated out in triplicate onto Reasoner's 2A (R2A) agar (Carl Roth GmbH & Co. KG, Germany), which was previously found to be the most suitable medium for the culture of many airborne bacteria (Hyvärinen *et al.*, 1991) supplemented with 100 mg l^{-1} cycloheximide to prevent overgrowth with fungi, and incubated at room temperature for 7 days. The colony forming unit (CFU) concentrations were determined and plates out of the range of 30-200 CFU or contaminated with cycloheximide-resistant fungi were discarded. Predominant colonies were identified using colony PCR and Sanger sequencing the 16S rRNA gene region with universal 27F (Lane, 1991) and 1492R primers (Turner *et al.*, 1999) ordered from Integrated DNA technologies (IDT) (Heverlee, Belgium).

2.3.4 Particle distribution (Coulter counter)

In addition to the PM_{10} mass per m^3 air concentrations determined by the VMM monitoring stations, particle distribution and count were determined by Coulter counter analysis (Beckman Coulter Inc.) from the impinger-samples taken within five meters of the VMM stations (locations A, B, D, J). Samples were diluted 1:4 in Isoton solution and 500 µl of sample analyte was analysed in duplicate using the Coulter Counter containing a 50-µm aperture. Using the Multisizer 3 software, particles representing the coarse PM fraction (ranging between 2.5 µm - 10 µm) were counted and expressed as particles m^{-3}.

2.3.5 Statistical analyses

Data was analysed using R, version 3.1.2 for Windows (R core team, 2013). The Shapiro-Wilk test was used to confirm the data or their logarithm transformation were normally distributed before further analyses. Linear regression analysis was done for the logarithmic transformed data of the CFU concentrations, particle counts, PM_{10} measurements and endotoxin concentrations of all samples.

2.4 Results

2.4.1 Substantial variation in urban endotoxin concentrations

During the first sampling period in 2014, endotoxin concentrations distributed over 11 sampling sites within Antwerp (not more than 15 km apart) exhibited substantial variations, ranging from 0.45 to 93.71 EU m^{-3}, with a geometric mean of 7.43 EU m^{-3} (95% confidence interval: 5.03-10.96) (Fig 2.3). In the second sampling period in 2015, sampling focussed on six of the 11 sites and showed significantly lower endotoxin concentrations and lower variation than in 2014 ($p<0.0001$, unpaired t test with Welch's correction), ranging from 0.65 – 11.72 EU m^{-3} with a geometric mean of 2.80 EU m^{-3} (95% confidence interval: 2.23- 3.53).

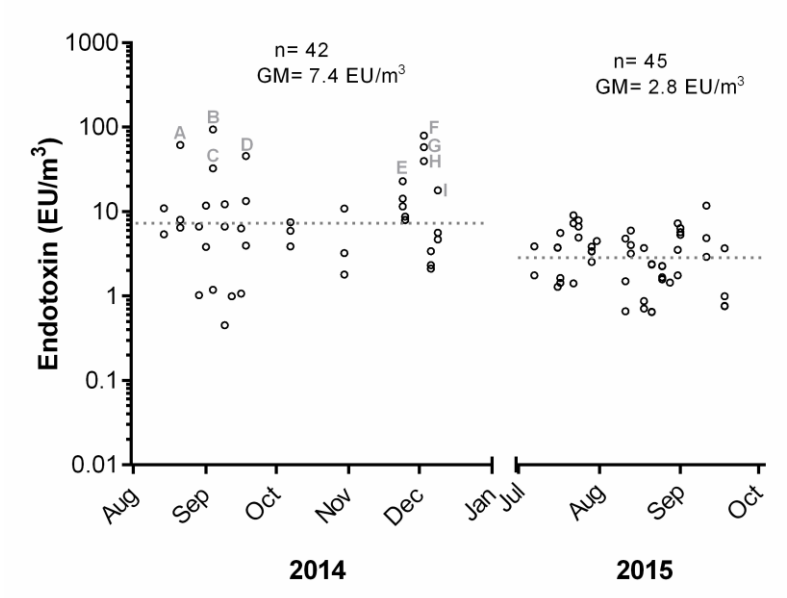

FIG 2.3: Temporal monitoring of ambient endotoxin concentrations
Endotoxin concentrations from the first (Aug to Dec 2014) and second sampling period (July-Sep 2015) in Antwerp. Geometric means of the periods are indicated individually with the dotted lines, while very high peaks in endotoxin levels in 2014 (labelled A-I) were investigated by identifying the culturable bacterial fraction (see Table 2.2). Logged endotoxin concentrations from 2014 and 2015 were both found to be normally distributed (Shapiro-Wilk test).

To investigate potential spatial patterns and source contributors, the locations were grouped into three land-use classes: traffic, industrial, and urban green based on the proximity to busy traffic roads, emitting industries, and green areas. Although greener urban areas have many microbial sources (from plants, soils, and animals), the urban traffic and urban green groups did not differ significantly from each other in terms of endotoxin concentrations (Fig 2.4). Moreover, the industrial group showed significantly lower levels than both the urban traffic (one-tailed, parametric, unpaired t-test, $p<0.0001$) and green areas ($p=0.0004$).

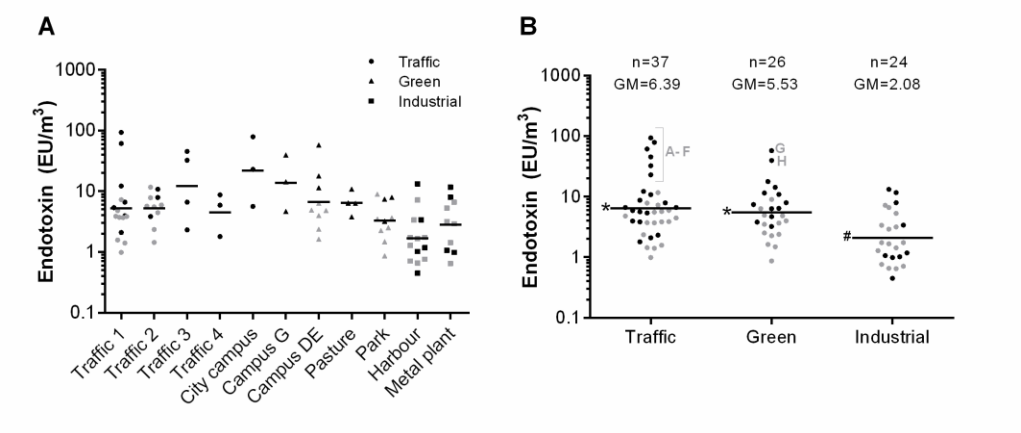

FIG 2.4: Spatial monitoring of ambient endotoxin levels within Antwerp
A) Airborne endotoxin concentrations from 11 locations within Antwerp, with the geomean indicated for each location. B) Locations grouped together into three land-use classes: urban traffic, urban green, and industrial, with the geomeans and sample size indicated. The second sampling period (2015) is illustrated in grey points and focuses on six of the sampling sites, divided equally over the categories. Several very high data points from the urban traffic and green areas are labelled A-H. Normal distribution was confirmed by the Shapiro-Wilk test or the Central Limit Theorem ($n \geq 30$) applied. Statistical significance (p value < 0.05), as determined by t-tests are indicated by different symbols (*, #)

2.4.2 Cultivable bacterial sources of endotoxins

In order to gain a perspective on the cultivable bacterial source and how they affect the quantified endotoxins, samples were cultured on R2A media. Herein, we investigated i) the relationship between airborne endotoxins and CFU m^{-3}, and ii) identified dominant colony morphologies from plate samples. Linear regression analysis (Fig 2.5) shows that 57% of the variation of airborne endotoxin concentrations could be explained by these CFU determinations (R^2= 0.57; p=<0.0001; n=58), which was independent of sampling period and land-use class.

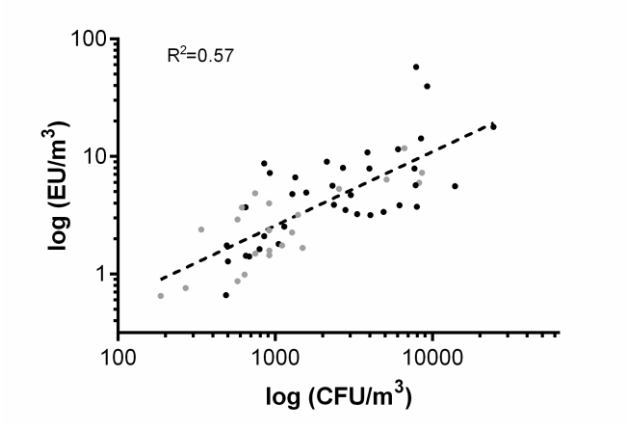

FIG 2.5: Correlation between endotoxin concentration and CFU counts
Log-transformed data of both endotoxin concentration (EU m^{-3}) from all 11 locations within Antwerp and the colony counts (CFU m^{-3}) detected on R2A plates (R^2= 0.57; n=58). The second sampling period (2015) is illustrated in grey points

Furthermore, the samples showing very high endotoxin concentrations, labelled A-I (Fig 2.4) appeared to be mostly dominated (70-100%) by particular gram-negative species for that location in time (Table 2.2). This suggests the aerosolization of a particular dominating species from single point sources, thereby resulting in high fluctuations of urban airborne endotoxin concentrations. Alternatively, a subset of the samples (E, I) contained multiple equally dominant gram-negative species, suggesting numerous source contributors. For instance, sample "E" from the city campus included bacteria commonly associated with human skin and soil, as well as *Pseudomonas tolaasii* known for causing brown rot of mushrooms. Furthermore, *P. tolaasii* was isolated as dominant colonies from additional locations (Campus DE, Campus G, Park, Traffic 4) within this two-day sampling period, suggesting its wide-spread proliferation during this time in the Antwerp urban air.

TABLE 2.2: Identification of dominant plate isolates
The full 16S rRNA gene of selected colonies from the R2A plates of samples showing very high endotoxin concentrations were sequenced and the putative species identification is provided based on BLAST (more than 97% similarity). Each sample was mostly dominated by a single gram-negative species, or equally shared multiple species

	Location	Date	Putative species	Commonly found
A	Traffic 1	21/08/14	*Pseudomonas oryzihabitans*	Human pathogen/soil/ moist environments
B	Traffic 1	04/09/14	*Pseudomonas cedrina*	Plant
C	Traffic 3	04/09/14	*Pseudomonas marginalis/ cedrina/ azotoformans*	Soil/plant
D	Traffic 3	18/09/14	*Rhizobium huautlense*	Plant
E	City campus	24/11/14	*Acinetobacter iwoffii* *Massilia* *Pseudomonas tolaasii*	Human skin Soil/water Soil/mushroom
F	City campus	03/12/14	*Pseudomonas marginalis/ azotoformans/cedrina*	Soil/plant
G	Campus DE	03/12/14	*Methylobacterium radiotolerans*	Soil/plants
H	Campus G	03/12/14	*Ralstonia pickettii*	Moist environments such as soils, water
I	Campus DE	09/12/14	*Sphingomonas melonis* *Methylobacterium radiotolerans* *Ralstonia pickettii*	Plants Soil/plants Moist environments

Although no clear correlations of endotoxin concentrations were apparent for temperature or humidity, other meteorological conditions such as fog are known to provide a more favourable environment for airborne bacteria (Vaïtilingom *et al.*, 2010). Not only does the moisture protect airborne bacteria from desiccation (listed as an important stressor in section 1.3.3), but it also contains organic compounds available for metabolization (Vaïtilingom *et al.*, 2010). In this study, indeed the samples collected throughout an extremely foggy period (F-H) measured substantially higher endotoxin concentrations than on average for the specific locations.

2.4.3 Correlations of endotoxin concentration, PM_{10}, & coarse particle count

As also mentioned in chapter 1, previous studies have shown endotoxins to be most commonly associated with the coarse PM fraction, i.e. PM 2.5-10 μm (Allen *et al.*, 2011; Heinrich *et al.*, 2003; Schins *et al.*, 2004). Figure 2.7 presents the correlations between the log-transformed data of PM_{10} (μg m^{-3}) obtained from the VMM, 2.5-10 μm particle count measured by the

Coulter counter and illustrated in Fig 2.6 (particles m^{-3}), and the airborne endotoxin concentrations (EU m^{-3}). For our samples, PM_{10} showed no significant correlation to the endotoxin concentrations measured in the impinger samples (R^2=0.07; p= 0.079; n=47) (Fig 2.7A), while the particle count (2.5-10 µm m^{-3}) determined in these impinger samples with the Coulter counter provided a weak but significant correlation to endotoxin (R^2=0.24; p<0.0001; n=64) (Fig 2.7B). Both methods are an indicator of particle concentrations, with PM_{10} values being indicative of the mass measurement of airborne particles (µg m^{-3}), while the Coulter counter measurement represents the particle number actively collected by our impinger sampler (Fig 2.7). Of note, the Coulter counting also depends on the stability of the particles in the liquid phase (agglomeration or dissolving). Nevertheless, these two methods showed a moderate and significant correlation to each other for the samples studied here (R^2=0.47; p<0.0001; n=47) (Fig 2.7C).

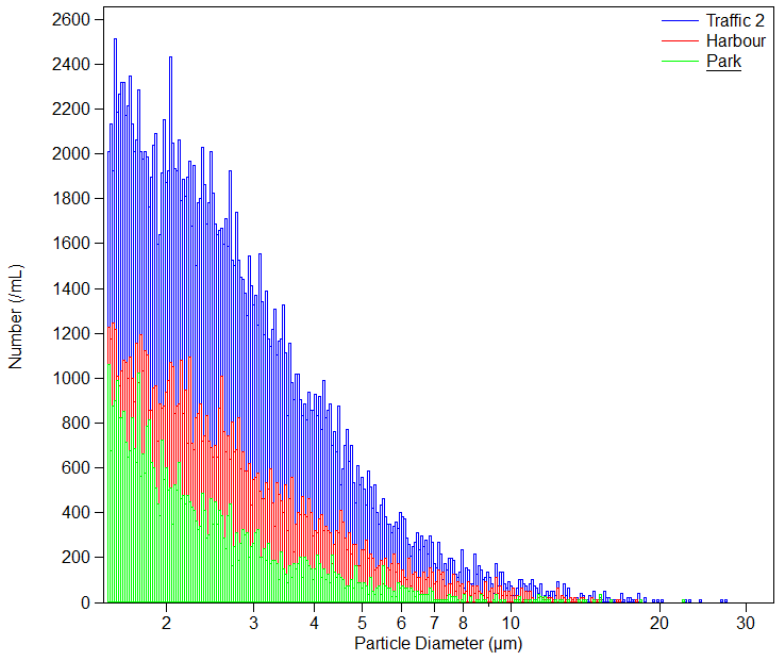

FIG 2.6: Typical pattern of the particle distribution from Coulter counter
An overlay of the distribution of the number of particles (per ml) ranging from 0.5-30 µm, measured by the Coulter counter, for three of the locations, i.e. traffic 2 (blue), harbour (red), and park (green). Although the Coriolis sampler does not have a strict cut-off limit, not many particles exceeded the 10 µm diameter.

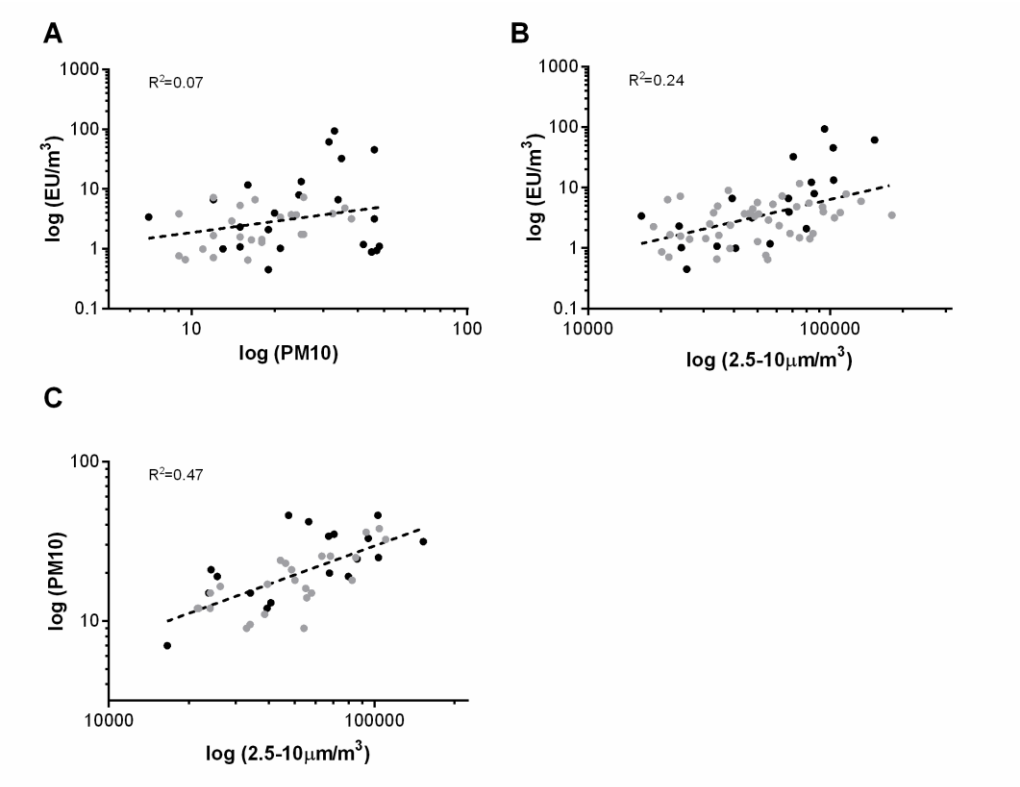

FIG 2.7: Correlations between PM_{10}, particle count, and endotoxin concentration
Log-transformed data of PM_{10} (μg m^{-3}), 2.5-10 μm particle count using the Coulter counter (particles m^{-3}) and the airborne endotoxin concentrations (EU m^{-3}). The second sampling period (2015) is represented in grey points

2.5 Discussion

The aim of this chapter was to gain insights into the abundances and potential bacterial sources of ambient urban endotoxins in Antwerp by applying a microbial-targeted collection strategy. Furthermore, endotoxins were quantified with the more recently validated rFC assay (Alwis and Milton, 2006; Thorne *et al.*, 2010) (also introduced in chapter 1, section 1.3.2). In comparison with previous studies which used the traditional LAL assay, the rFC assay offers several advantages, including no interference from fungal glucans (reduces false positives), reduced likelihood of interference from other PM components due to a more simplified

reaction pathway, less inter-lot variation, and its supply does depend on the lysate of the endangered horse-shoe crab (see figure 1.8 in Chapter 1).

One of the first intriguing findings presented in this chapter was that we detected endotoxins at quite high concentrations (geometric mean of 4.49 EU m^{-3}) compared to the urban air of other cities (Table 2.1). There are no indications that Antwerp would contain more sources of bacterial endotoxins than these other cities, given its high urbanization and industrialization level, limited green and agriculture areas, and measured bacterial CFU m^{-3} in a magnitude of 10^2-10^4 on par with previous urban airborne microbial studies (Bowers *et al.*, 2012; Maron *et al.*, 2006). Therefore, we believe that these differences may have arisen from the microbial-targeted collection strategy employed here, compared to filter-based sampling in most other studies.

As previously mentioned, there are several problems associated with the recovery of endotoxin from filters, especially with the relatively lower endotoxins concentrations found in an urban environment. Endotoxins are adherent molecules, difficult to extract from the filters (Duchaine *et al.*, 2001). Therefore, the use of detergents (e.g. Tween 20, 0.01% triethylamine), which in turn interfere with endotoxin quantification (Spaan *et al.*, 2007), is often needed. Moreover, the extraction procedure from filters include several steps, increasing the chances of contamination and endotoxin loss, which are all important factors resulting in inter-laboratory variation (Spaan *et al.*, 2007; Thorne *et al.*, 2003).

In contrast, the impinger sampler used here (Coriolis® µ) increases the biological efficiency, also allowing samples to be cultivated. Indeed, we found a significant correlation between cultivable bacteria (CFU m^{-3}) and endotoxin concentration, with CFU count explaining up to 57% of the variation of airborne endotoxins. This is quite surprising, since biologically active endotoxin does not rely on viable or cultivable bacteria, and colony counts on R2A medium cannot discriminate between endotoxin LPS-containing gram-negative and non-LPS containing gram-positive isolates, which also reside in urban air. Nonetheless, we found airborne endotoxin concentrations to depend on viable gram-negative bacterial sources. No doubt the survival rate of the collected bacteria may have been increased with the use of phosphate-

buffered saline (PBS) solution as the collection liquid, however PBS would have interfered with the downstream analysis.

Furthermore, sequencing of the 16S rRNA gene of selected isolates suggest that large airborne endotoxin fluctuations may be linked to the proliferation of certain dominant gram-negative species originating from specific source contributors and promoted by meteorological conditions such as fog. For example, bacteria commonly associated with humans, soil, plants (including plant pathogens) and water (including moisture) were often detected, together with bacterial species known for their bioremediation potential. Nonetheless, due to the bias associated with culture-based methods, these data allow only a limited insight in what is driving the fluctuations of the endotoxin concentrations. Culture-independent-based methods may allow even better insight in airborne microbial communities and their sources (Bowers *et al.*, 2011a; Bowers *et al.*, 2011c). Fellow PhD student Wenke Smets also tried to implement 16S rRNA amplicon gene sequencing-analysis on outdoor air samples collected with the Coriolis sampler (Smets, 2018), but this turned out to be very difficult to implement because of the technical difficulties caused by the low biomass of air samples.

In contrast to these specific gram-negative bacterial sources for the urban air determined by culture, we could not find the greener urban areas to be (in general) higher in airborne endotoxin concentrations than the urban traffic locations. Although urban green vegetative areas are often associated with microbial sources (plants, soil, etc.) (see also figure 1.10 in chapter 1), airborne endotoxin requires both a source and resuspension (Jones and Harrison, 2004). High traffic movement and street canal effects provide indeed considerable aerosolization in urban traffic areas. Moreover, a substantial source of bacterial reservoirs, such as domestic animals, cigarette smoking, organic waste, and kitchen emissions also exists in urban areas (Cheng *et al.*, 2012).

Finally, we also determined the correlation between endotoxin concentrations and airborne particles, since particles are important ‘vectors’ to which endotoxins may associate and promote their persistence in the air. Indeed, the 2.5 -10 µm particle count concentrations

determined here with a Coulter counter showed a weak, but significant correlation to airborne endotoxin concentrations (R^2=0.24, p<0.0001; n=64). The correlation coefficient (Pearson r = 0.49) lies within the correlation of endotoxin with PM_{10} reported by Mueller-Anneling *et al.* (2004) for the winter (r = 0.33) and summer (r = 0.72) sampling periods. However, PM_{10} mass concentrations could not be significantly correlated with the sampled endotoxin concentrations for our samples. This is likely due to the independent collection of PM_{10} mass concentrations by the VMM monitoring stations, albeit in parallel with the impinger samples.

2.6 Conclusion

In conclusion, we believe this chapter shows a promising alternative approach for the monitoring of ambient urban endotoxins, which potentially offers a more accurate and time-dependent view of endotoxin concentrations. Understanding the short-term fluctuations of airborne endotoxin may prove to have additional biological relevance, complementing the average daily concentrations offered by filters, which often function at a much lower collection rate. However, no collection strategy is without its drawbacks and several hurdles will still need to be overcome. Although the impinger used here collects airborne particles (efficiency with a d50 < 0.5µm), it does not offer the strict size cut-off limits as with the filter-based samplers, which complicate comparisons with current air pollution standards. Thus, further technological improvements and more detailed measurements will be important. Nevertheless, the relatively quick collection of concentrated air samples in ultrapure water is well suited for immunological testing, and the increased recovery of endotoxin allowed us to explore the relative contribution of endotoxins in PM-induced inflammatory responses, as shown in the next chapters.

Chapter 3

Host reception &

pro-inflammatory response

"Between stimulus and response is the freedom to choose"

-- Viktor E. Frankl

3.1 Introduction

Once ambient endotoxins have been quantified, they are often correlated to inflammatory biomarkers (Heinrich *et al.*, 2003; Tager *et al.*, 2010; Traversi *et al.*, 2011). Although higher levels of urban endotoxins have been related to higher levels of immune biomarkers, such as IL-6 and TNFα, direct proportionality is not often observed (Hetland *et al.*, 2005; Steerenberg *et al.*, 2004). What is currently lacking, is the link between quantified endotoxin – as a constituent of urban PM - and the host immune recognition through toll-like receptor 4 (TLR4), which is the key human immune receptor for endotoxin detection as introduced in chapter 1. This relationship may vary depending on i) the different assays and their specificity of endotoxin recognition (Gutsmann *et al.*, 2010), ii) interfering or synergistic PM components or iii) different LPS potencies from gram-negative bacterial populations (Dehus *et al.*, 2006; Erridge *et al.*, 2002).

In chapter 2 we made use of the more recent rFC assay, which is essentially a fluorometric assay from the purified and cloned first component (Factor C) in the enzymatic cascade of the LAL reaction. The LAL and rFC assays are reported to correlate well from livestock environments and house dust samples, although the LAL assay typically leads to higher values (Alwis and Milton, 2006; Thorne *et al.*, 2010). The rFC assay was chosen to reduce false positives from fungal glucans and the likelihood of interferences from other PM components.

Alternatively, the HEK-Blue TLR4 bioassay is designed for studying the stimulation of human TLR4 by monitoring the activation of an NF-κβ-inducible secreted embryonic alkaline phosphatase (SEAP) reporter gene (Fig 3.1). This bioassay was created by co-transfecting the HEK293 cell line with genes from the hTLR4 pathway (including co-receptors MD-2 and CD14) and a SEAP reporter gene. Levels of SEAP secreted into the culture medium upon TLR4 stimulation can be easily determined by measuring the absorbance (405nm) from the hydrolysis of p-nitrophenyl phosphate (pNPP) by the alkaline phosphatase. Since the

absorbance is in direct proportion to the amount of endotoxin present, the concentration of endotoxin can be calculated from a standard curve. Compounds known to activate NF-κβ may interfere with the assay in a TLR4-independent manner. These include cytokines such as TNFα and IL-1β, and ligands of TLR3 (poly I:C), TLR5 (flagellin) or NOD1 (C12-iE-DAP) which are endogenously expressed in the HEK293 cells (as reported by the manufacturers, InvivoGen).

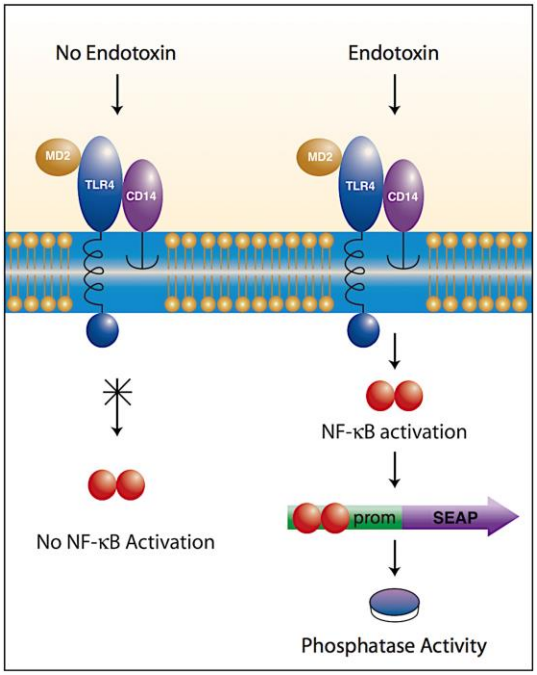

FIG 3.1: HEK-Blue hTLR4 assay mechanism used in this chapter to monitor TLR4 stimulation. This simplified scheme is not taking into account other components that can directly/indirectly activate NF-kB and interfere with endotoxin detection. As illustrated by the manufacturer, InvivoGen.

3.2 Aim

This chapter aimed to bridge the gap between endotoxin quantification and the inflammatory response by investigating the biological recognition of endotoxin via the human Toll-like receptor (TLR4/MD-2) complex. Endotoxin concentrations were quantified from a diverse

representation of outdoor urban PM samples to determine whether their associations with different sources - and possibly other PM components - are relevant for their biological recognition by the TLR4/MD-2 complex and subsequent inflammatory response. This is knowledge currently lacking in literature.

3.3 Materials & Methods

3.3.1 Samples

Samples of the second collection period from July until September 2015 (n=50) described in chapter 2 were used since this campaign focussed on equal sampling sites for each representative land-use class, i.e. urban traffic (B, C), urban green (G, I), and industrial (A, J). Furthermore, three samples were collected per day and representative of the three different land-use classes to account for confounding day-to-day variation.

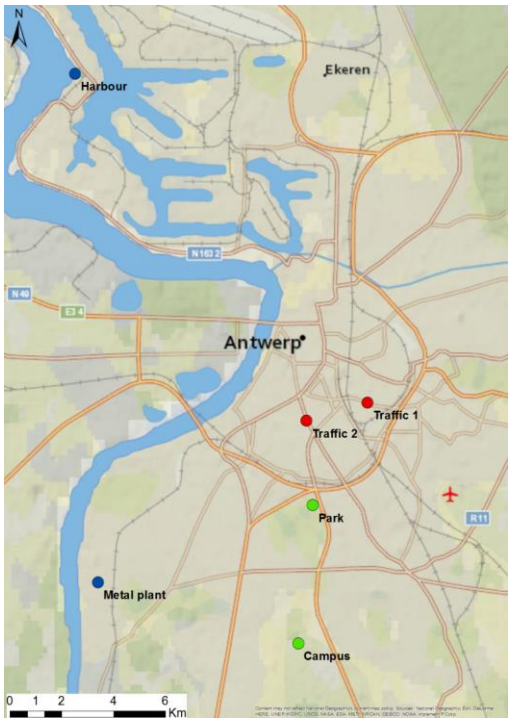

FIG 3.2: Geographical representation of the six sampling sites, grouped into urban traffic (red), urban green (green), and industrial (blue). Google maps (2015).

FIG 3.3: Traffic 1. Situated within the city ring, on the Plantin en Moretuslei (51°12'33.6"N, 4°25'54.9"E), a four-lane road with high traffic intensity (29500 vehicles/day: VMM 2014). This sampling site was next to the VMM "Borgerhout: roadside" monitoring site which reported a 2015 yearly average of 45 µg m^{-3} NO_2, 29 µg m^{-3} NO, 24 µg m^{-3} PM_{10}, 15 µg m^{-3} $PM_{2.5}$, 2.67 µg m^{-3} black carbon.

FIG 3.4: Traffic 2. Situated within the city ring, on the street canyon of Mechelsesteenweg (51°12'19.5"N, 4°24'37.2"E). This is a major road into the city centre with both vehicle and tram traffic.

FIG 3.5: Campus. Situated 3.7 km from the city ring, this university campus (Drie Eiken) is representative of a greener urban area (51°09'23.7"N, 4°24'25.7"E).

FIG 3.6: Park. Situated with in the Nachtegalen Park, just 700 m from the ring of Antwerp, and 200 m from the major E19 highway entering the city (51°11'13.9"N, 4°24'44.0"E).

FIG 3.7: Harbour (51°16'51.3"N, 4°19'47.8"E). This sampling site was a central site within the harbour and next to the VMM "Boudewijnsluis" monitoring site which reported a 2015 yearly average of 22 µg m^{-3} PM_{10}, 13 µg m^{-3} $PM_{2.5}$, 1.4 µg m^{-3} black carbon, 0.17 ng m^{-3} PAH.

FIG 3.8: Metal-recycling plant (51°10'12.6", 4°20'27.4"E). This sampling site was located next to a major precious metal recycling plant and also closely monitored by the VMM "Hoboken" which reported a 2015 yearly average of 27 µg m^{-3} NO_2, 10 µg m^{-3} NO, 25 µg m^{-3} PM_{10}, 15 µg m^{-3} $PM_{2.5}$. This site is well known to be in exceedances of lead, arsenic, nickel.

3.3.2 TLR4 stimulation in HEK293 cells

HEK-Blue™ hTLR4 cells are stably transfected with human TLR4/CD14/MD2 (Invivogen). The cells were cultured in DMEM (Gibco, Life Technologies), supplemented with 10% (v/v) heat-inactivated fetal bovine serum (FBS), normocin (100 µg ml^{-1}), and HEK-Blue Selection (Invivogen) and maintained at 37°C in a humidified incubator containing 5% CO_2. Cells (100 µl) were seeded into 96 well plates at a concentration of 0.5 x 10^6 cells ml^{-1} and incubated for 48 hours until approximately 90% confluent. Media was removed from adherent cells and replaced with 100 µl concentrated (x2) DMEM (with no FBS, normocin, or selective marker) which was diluted with 100 µl sample/control. A standard curve was generated by stimulating the cells with a six-point serial dilution (0.1 -50 EU ml^{-1}) of the same endotoxin standard as the rFC assay (*Escherichia coli* O55:B5, lot 0000 441 186; Lonza Walkersville Inc., MD, USA). After 20 h incubation, 50 µl-supernatant was transferred in duplicate to a new 96 well plate, upon adding 100 µl of freshly prepared substrate solution (final concentration of 1 mg ml^{-1} pNPP in 100 mM Tris-HCl, 100 mM NaCl, 5 mM $MgCl_2$, pH 9.5 buffer). After a 20 min incubation at 23°C, the absorbance was measured at 405 nm. From the standard curve (Fig 3.9) and sampling efficiency (300 L min^{-1}; 15 ml), the predicted endotoxin concentrations (EU m^{-3}) could be calculated.

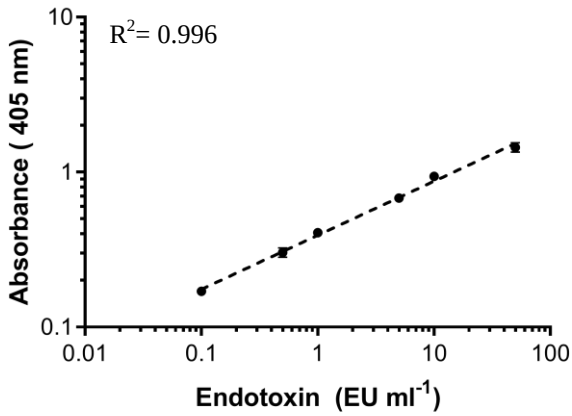

FIG 3.9: Standard curve of logarithm-transformed endotoxin concentration and absorbance. Cells were stimulated in triplicate with six different concentrations of endotoxin (0.5, 1, 5, 10, 50 EU ml^{-1}) and the resulting SEAP activity was measured at an absorbance of 405 nm. Standard deviation is shown in error bars.

This experiment was optimized for:

- ✓ 96 well plates so as to process more samples and repeats
- ✓ Amount of sample needed to give a response within standard curve range
- ✓ The incubation period (8, 16, 20, 24 h) which yields the best standard curve

Special FBS was purchased that was guaranteed to have <1 EU ml^{-1}, and with the measured endotoxin concentrations indicated on the certificate of analysis

3.3.3 Monitoring of pro-inflammatory response genes at mRNA level

The human monocyte cell line U937 (kindly donated by Prof. Cos, Laboratory for Microbiology, Parasitology and Hygiene, UAntwerpen) was cultured in Roswell Park Memorial Institute (RPMI) medium (Gibco, Life Technologies, Grand Island, New York, USA) supplemented with 10% heat-inactivated FBS (Hyclone, GE Healthcare, Little Chalfont, UK), streptomycin (100 µg ml^{-1}) and penicillin (100 units ml^{-1}; Gibco), and maintained at 37°C in a humidified incubator containing 5% CO_2. Cells were seeded in 12-well plates at a concentration of 5 x 10^5 cells ml^{-1} in complete growth medium with phorbol 12-myristate 13-acetate (PMA, 100 ng ml^{-1}; Sigma Aldrich, St. Louis, Michigan, USA) to allow for differentiation to an adherent macrophage-like stage for 48 h. Thereafter, PMA and non-adherent cells were removed by replacing the RPMI medium (without supplements) for a further incubation of 24 h. Medium was removed and cells were co-incubated for 3 h with a 10x RPMI media (Sigma Aldrich, St. Louis, Michigan, USA) diluted out with the supplements sodium bicarbonate (2 g l^{-1}), folic acid (1 mg l^{-1}), GlutaMAX (2 mM) and sample (at a 1:1 ratio), a positive control (100 ng/well lipopolysaccharide from *E. coli* 0111:B4; Sigma Aldrich) or the negative control (unsupplemented RMPI).

After co-incubation, total RNA was isolated with the RNeasy Mini kit (Qiagen, Hilden, Germany) following the manufacturer's instructions and stored at -80°C. RNA integrity was verified on a 1% (v/v) bleach gel as described by Aranda *et al.* (2012). One µg of RNA

(quantified with Qubit 3.0; Thermo Fisher, Waltham, Massachusetts, USA) was used for cDNA synthesis with the ReadyScript® cDNA Synthesis Mix (Sigma Aldrich). The expression of three selected pro-inflammatory markers IL-8, IL-1β and TNFα, and two reference genes (M=0.258, CV=0.09) was quantified by reverse transcription quantitative PCR (RT-qPCR) on a StepOne Plus Real-Time PCR System (v.2.0; Applied Biosystems, Foster City, California, United States). *Guanine nucleotide binding protein beta polypeptide 2-like 1 (GNB2L1)* and *cytochrome c-1 (CYC1)* were selected as the best reference genes, following the GeNorm analysis in Qbase^{+} (Vandesompele *et al.*, 2002). All primers were tested for efficiencies between 90-110% and their sequences can be found in Table 3.1.

Table 3.1: Primer sequences of gene expression from U937 cells.

Gene	Forward primer (5 – 3')	Reverse primer (5 – 3')	nt
IL-8	TGGCAGCCTTCCTGATTTCT	TTAGCACTCCTTGGCAAAACTG	61
TNFα	TCTTCTCGAACCCCGAGTGA	CCTCTGATGGCACCACCAG	151
IL-1β	TTGCTCAAGTGTCTGAAGCAGC	CAAGTCATCCTCATTGCCACTG	89
GNBL	CACTGTCCAGGATGAGAGCCA	CATACCTTGACCAGCTTGTCCC	111
CYC1	CATGTCCCAGATAGCCAAGGA	CTTGTGCCGCTTTATGGTGTAG	145
GAPDH	GAAGGTGAAGGTCGGAGTC	GAAGATGGTGATGGGATTTC	226
ATP5B	GCAGGAAAGAATTACCACTACCAAG	TGGTAGCATCCAAATGGGCAA	122

Every cDNA sample was used in duplicate, each 20 µL reaction consisting of Power SYBR® Green PCR Master Mix (Applied Biosystems), 0.3 µM of each primer, 31.25 ng of diluted cDNA, and nuclease-free water. The resulting data were analyzed using the Qbase^{+} software package (Hellemans *et al.*, 2007) for inter-run calibrations, calculating relative expression levels of the cytokines as compared to the reference genes, and statistical analysis for comparison amongst groups (One-way ANOVA, corrected for multiple testing).

"RT-qPCR is considered today as the gold standard for accurate, sensitive and fast measurement of gene expression. Unfortunately, what many users fail to appreciate is that numerous critical issues in the workflow need to be addressed before biologically meaningful and trustworthy conclusions can be drawn" Derveaux *et al.* (2010).

Set with the task of establishing RT-qPCR within our new laboratory, multiple steps were taken to ensure the integrity of the data. Due to their importance, these steps are briefly mentioned below.

RNA quality

As the saying goes "garbage in, garbage out". For this reason it was of utmost importance that the RNA purity (no contaminants) and integrity (not degraded) was of good quality for RT qPCR applications. Proper sample handling was also employed, this included the prevention of nuclease contaminants, working fast and keeping RNA cold, and storing RNA at -80°C. Furthermore, equal quality between samples is very important. For this reason, the RNeasy Mini kit (Qiagen) was used together with an on-column DNase treatment. Since RNA was extracted from cell lines rather than complex tissues (e.g. formalin fixed paraffin embedded tissues), RNA integrity was validated by visualizing the intact 28S and 18S bands on a bleach gel (Fig 3.10), which is both rapid and inexpensive (Aranda *et al.*, 2012).

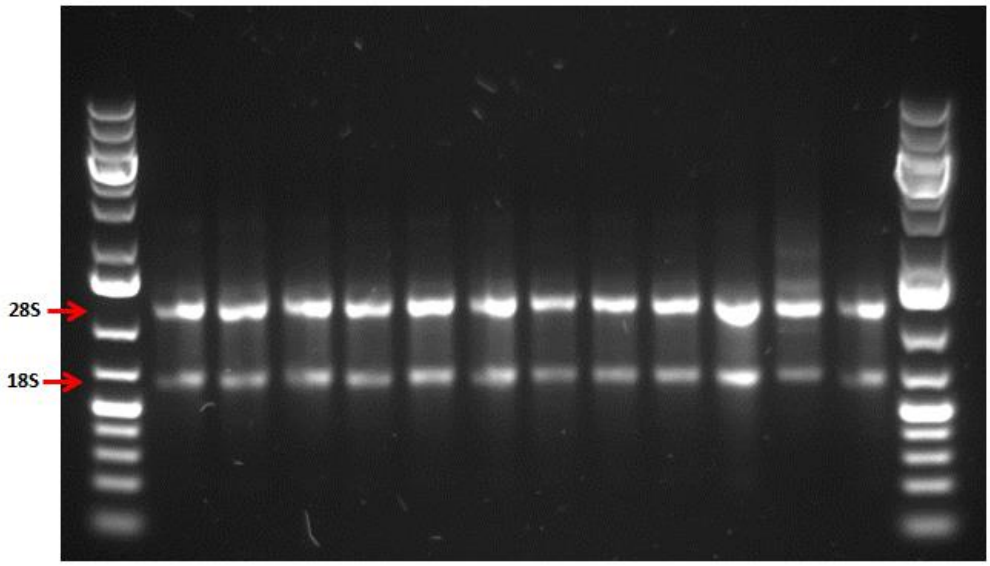

FIG 3.10: Bleach gel used to assess the integrity of RNA by visualizing of the compactness of 28S and 18S bands which should be in a 2:1 ratio

Reverse transcription (RT)

A study by Bustin *et al.* (2015) investigated the reproducibility of the RT step with several commercial reverse transcriptases (RTase) and RNA samples of variable quality and concentrations. The study found that the resulting variability (generally between 2- and 3-fold) could be minimized by choosing an appropriate RTase (e.g. ReadyScript) and using high concentrations of RNA (1µg). ReadyScript also uses a combination of oligo(dT)s and random primers for cDNA synthesis. Oligo(dT)s initiate RT at the 3'end of the transcript (where secondary structures may lead to incomplete cDNA generation) whereas random primers anneal throughout the transcript and are less affected by degraded transcripts and secondary structures.

Primers

Primers need to be carefully selected and rigorously tested for their specificity, sensitivity, and efficiency. In my personal experience, I've learnt to always check the primers – whether they

come from a well-established laboratory, or highly cited articles in high impact journals. Primer specificity was tested *in silico* using Primer-BLAST, and further information was also gathered, such as, presence of SNPs in annealing sites, presence of alternatively spliced isoforms, primer dimers and hairpins, whether primers anneal over exons (preferably), and if not what the band size of gDNA amplification would yield (check for gDNA contamination on melt curve or agarose gel).

Testing the efficiency of the primers is one of the foundations for RT qPCR validation, although it is often neglected. Without the primer efficiencies, you cannot say whether the fold change between samples came from differential gene expression or simply difference in the efficiency of the primers. For this reason, a mixture of cDNA from representative samples are used for a dilution series spanning all sample Cq values. The PCR efficiency can be calculated from the slope of the serial dilution and should be within 90-110%. The theoretical maximum of 100% means the template doubles with each cycle.

$$PCR\ efficiency = 10^{(-1/slope)} - 1$$

A bad primer efficiency may result from poor primer design, presence of inhibitors, secondary structure of the amplicon, etc.

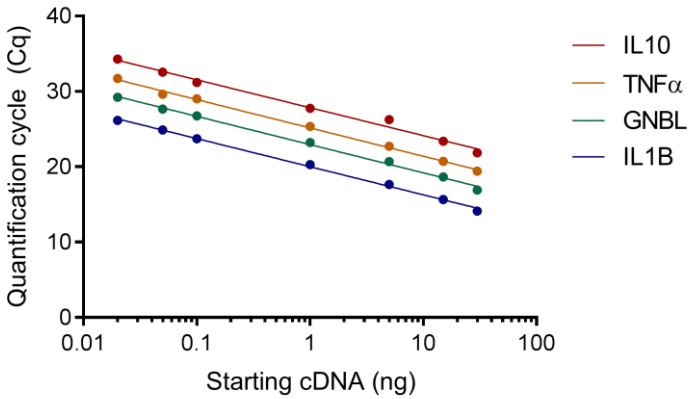

FIG 3.11: PCR efficiency is determined by constructing a standard curve, where log template amount is plotted against the corresponding Cq value, and then determining the slope. The slopes of various target genes are indicated

Selection of proper reference genes

Normalization is an essential component of a reliable qPCR assay because this process controls for variations in extraction yield, reverse-transcription yield, and efficiency of amplification, thus enabling comparisons of mRNA concentrations across different samples. The use of reference genes as internal controls is the most common method for normalizing cellular mRNA data. Selection of reference genes and proper assessment of the stability of selected genes is a circular problem since normalization is required in order to verify the stability of expression of a particular gene. This problem can be circumvented by using several reference genes in combination. For this study, GeNorm analysis (Vandesompele *et al.*, 2002) was carried out on ten representative cDNA samples (from each sampling location) using a selection of eight potential human reference genes selected for SYBR green applications (Primerdesign Ltd, UK). These references genes were selected from twelve potential genes based on their expression stability using the RefGenes function (Fig 3.12) in the Genevestigator database (Hruz *et al.*, 2011). From geNorm analysis, the most stability expressed genes (lowest M score) were CYC1, GNBL, GAPDH, ATP5B (Fig 3.13).

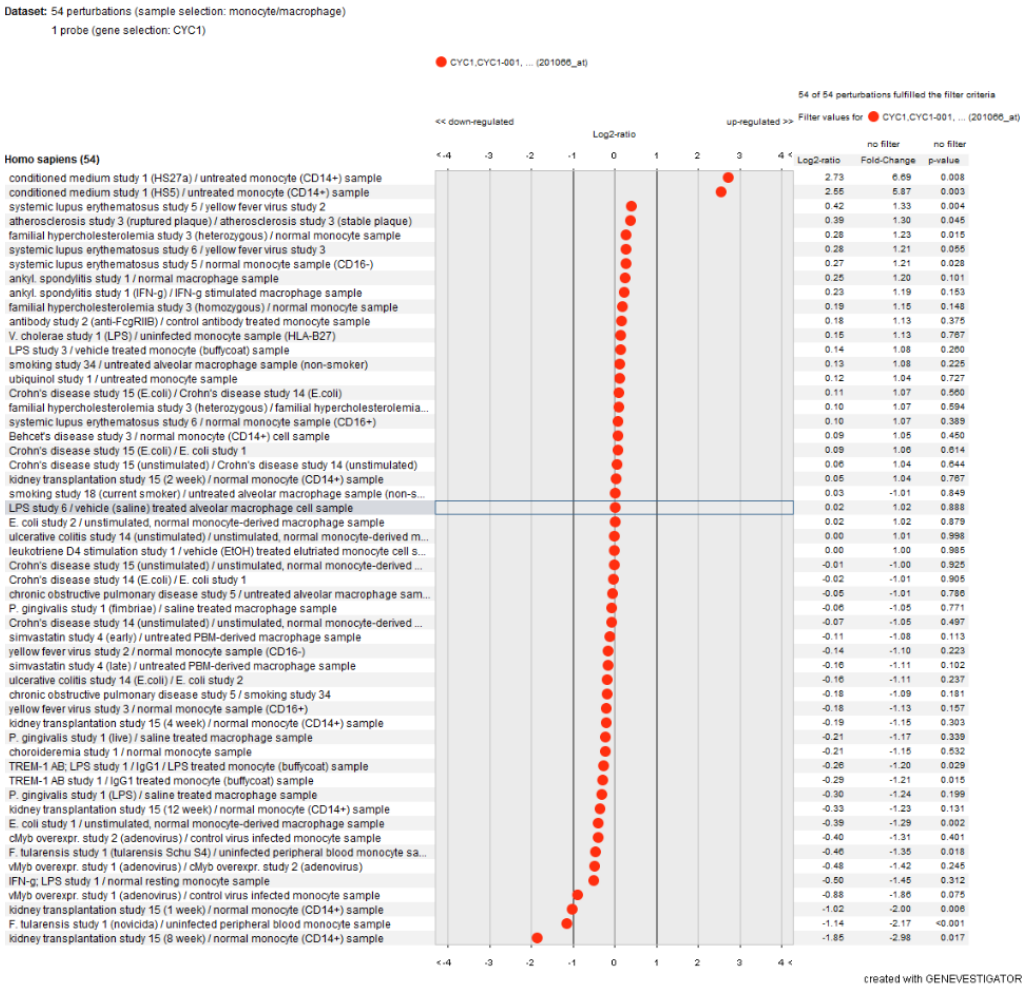

FIG 3.12: Example of RefGenes function which shows the stability of a selected gene (e.g. CYC1) in a specific tissue type (e.g. monocytes) under various conditions using the Genevestigator database of normalized and well-annotated and quality controlled microarray experiments.

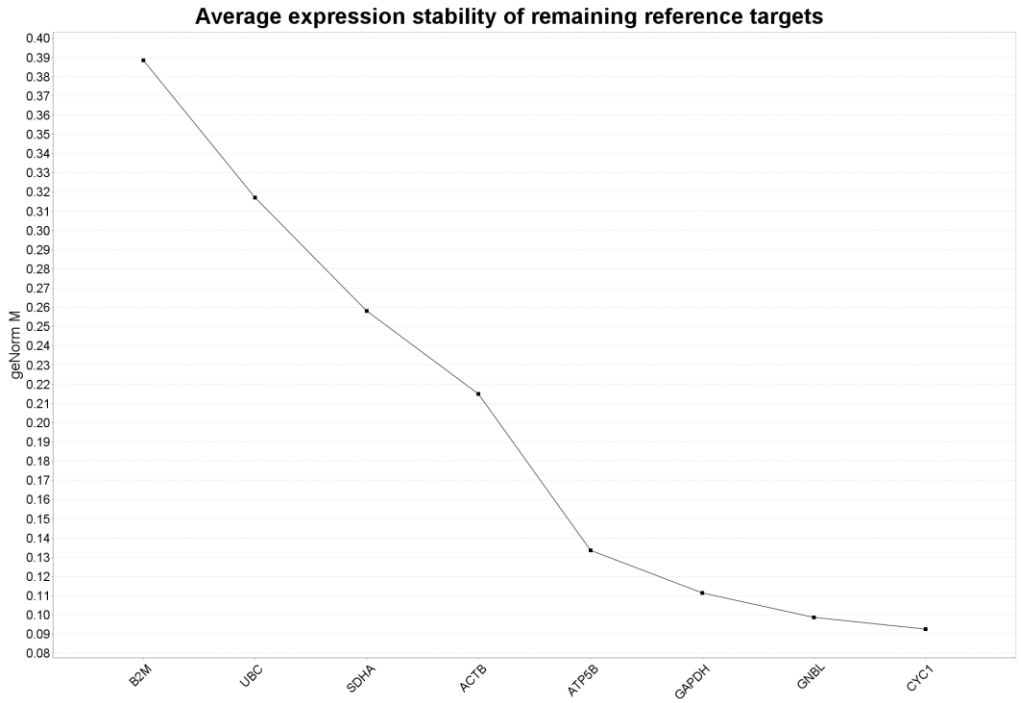

FIG 3.13: GeNorm analysis from ten representative cDNA samples showing the M score (expression stability value) for each target reference gene. The M score is calculated based on the pairwise variations of the reference genes. For every combination of two reference genes, log_2-transformed ratios of relative quantities are calculated for each sample. The M-value of a reference gene is then calculated as the arithmetic mean of all pairwise variations of all combinations in which the reference gene participates.

3.3.4 Statistical analyses

In Graphpad Prism v6.05 the logarithm-transformed data that were normally distributed were analyzed for significance by one-way ANOVA followed by the Tukey test to correct for multiple comparisons, unless otherwise stated. Welch's t-test was used for unequal variance. $P<0.05$ was judged to be statistically significant.

3.4 Results & Discussion

3.4.1 Atmospheric endotoxin concentration

From chapter 2 we monitored the airborne endotoxin concentrations over the different urban land-use classes (all within 15 km distance), categorized as green, traffic, and industrial, based on the expected dominant local emission source. As measured by the rFC assay, endotoxin concentrations ranged from 0.65 to 11.72 EU m^{-3}. Although greener urban areas have many microbial sources (from plants, soil, and animals), the green areas studied here did not show significantly higher concentrations of airborne endotoxins (geomeans (GM) 2.79 EU m^{-3}; 95% confidence interval 1.93-4.04) than the industrial (GM 1.92 EU m^{-3}; 95% confidence interval: 1.21-3.02) or the urban traffic locations (3.68 EU m^{-3}; 95% confidence interval 2.59-5.23). In fact, the traffic locations showed the highest GM (Fig 3.14).

3.4.2 Biological recognition of endotoxin through human TLR4/MD-2

Samples were tested for their biological recognition of endotoxin to human TLR4 using the HEK293 hTLR4 reporter cell line. A standard curve was generated from the same endotoxin stock as used in the rFC assay to predict the endotoxin units per ml (EU ml^{-1}). In terms of this TLR4 bio-assay, the biological recognition of endotoxin differed significantly between the land-use classes (Fig 3.14). Furthermore, the traffic areas studied here showed the highest response. Moreover, the methods for endotoxin quantification differed significantly for the green locations, where recognition of endotoxin by TLR4 stimulation was significantly lower than the rFC-determined endotoxin concentrations ($p=0.0023$). Subsequently, the TLR4 bioassay showed the green areas to have the lowest concentrations of endotoxins, significantly lower than the traffic sites.

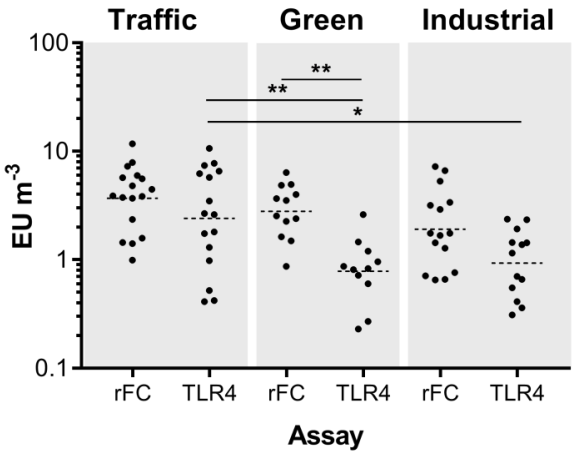

FIG 3.14: The comparison of endotoxin quantification by the rFC assay and via TLR4 stimulation through the HEK-Blue^{TM} hTLR4 cell line. Endotoxin concentrations from the separate locations within each land-use class were not significantly different and further comparisons were thus made between the three land-use classes (traffic, green and industrial) with each sample represented by a black dot. Statistical significance indicated by * $p<0.05$, ** $p<0.01$

3.4.3 Relationship between the rFC assay and TLR4 recognition

Although endotoxin has typically been quantified with the LAL assay, we choose the rFC assay to analyse these environmental samples since its simplified reaction pathway offers reduced likelihood of interference from other PM components, such as the false activation by yeast glucans (Roslansky and Novitsky, 1991; Vassallo and Limper, 1999). Despite this, the rFC assay still displayed higher endotoxin concentrations than the TLR4 assay for 34 out of 41 samples (Fig 3.15B), suggesting the difference between Factor-C based assays and the TLR4 bioassay to be attributed to more than yeast glucans as suggested by Peters *et al.* (2012). The relationship between these assays was investigated using linear regression analysis and initially showed a moderate correlation ($R^2=0.55$, $n=41$, $p<0.001$) (Fig 3.15A). However, when both land-use class and the interaction effect between the latter and rFC measurements (i.e. change in gradients) were included in the model, the fit significantly improved ($R^2=0.73$, $n=41$, $p<0.0001$). The land-use class of the collected air sample therefore seemed to affect the reactivity of the quantified endotoxin to the human host receptor, with endotoxin from the

traffic areas being most reactive and the green areas showing a generally low response ratio (Fig 3.15B).

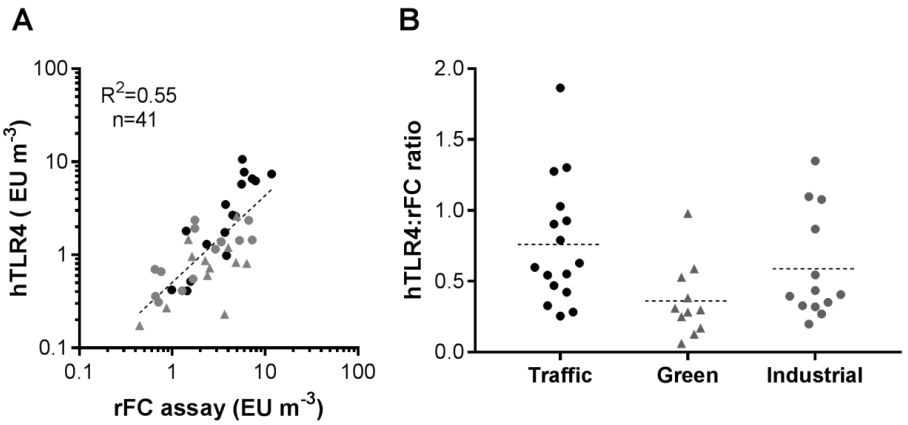

FIG 3.15: (**A**): The correlation between the rFC assay and the HEK-Blue^{TM} hTLR4 cells for samples in the land-use classes: traffic ●, urban green ▲, and industrial ●. (**B**): The response ratio of the hTLR4 stimulation to the rFC assay for the considered urban land use classes.

3.4.4 Immune response of collected urban air samples

Messenger RNA levels of the major pro-inflammatory markers IL-8, IL-1β, and TNFα were measured with RT qPCR after a three hour co-incubation of a sample with the model human monocytic U937 cells. These cytokines were chosen since they represent key extracellular signalling proteins underlying the pathogenesis of various PM-related diseases. For example, TNFα has been implicated in the progression of asthma, chronic bronchitis, chronic obstructive pulmonary disease, acute lung injury, and acute respiratory distress syndrome (Mukhopadhyay *et al.*, 2006). Additionally, IL-1β, IL-8 and TNFα increase in the sputum of patients with chronic obstructive pulmonary disease, and contribute to small airway inflammation (Chung, 2006). Monitoring of mRNA levels, instead of protein levels, was preferred here in order to detect early-response signals and to avoid cross-reaction with unknown contaminants in these environmental samples (Grosse *et al.*, 2016; Seagrave *et al.*, 2004).

In general, the urban traffic and industrial areas showed a heightened and varied pro-inflammatory response for the three markers, in contrast to the urban green area samples which showed relatively low and stable responses (Fig 3.16). The two industrial locations differed clearly for the IL-1β and TNFα mRNA responses, with the harbour location showing a significantly higher immune response for TNFα mRNA, while no difference was seen for IL-8. Despite both being industrial sites, this suggests the activation of different inflammatory pathways based on the unique composition of the samples. Consequently, for all the locations, IL-1β and TNFα are better correlated to each other (R^2= 0.84, n=42, $p<0.0001$) than to IL-8 (R^2= 0.61; R^2= 0.41, $p<0.0001$, respectively).

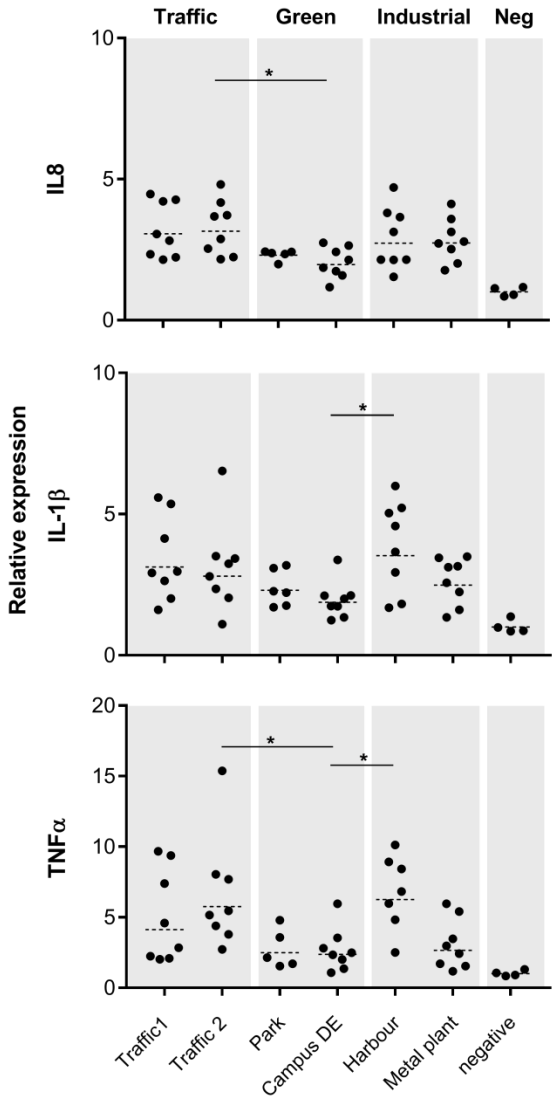

FIG 3.16: mRNA levels of the pro-inflammatory markers IL-8, IL-1β, and TNFα measured in human macrophage-like U937 cells after 3 h exposure with collected air samples. Values are expressed relative to the negative control, represented by an expression of one, and the geometric means of the locations are shown in dotted lines, while each sample is represented as a dot. The land-use classes: traffic, green and industrial each comprise two different sampling locations. The relative expressions for these pro-inflammatory biomarkers were significantly higher than the negative control for all locations (Welch's t-test for unequal variance). Statistical significance indicated by * $p<0.05$, ** $p<0.01$

3.4.5 Association between endotoxin quantification, host reception and pro-inflammatory response.

Typically, isolated LPS is very strongly correlated to the IL-8 mRNA response in the U937 cell model (Fig 3.17). However, this is more complicated for environmental samples where many

other components are capable of contributing to the IL-8 response and where different forms and thus potencies of LPS are present.

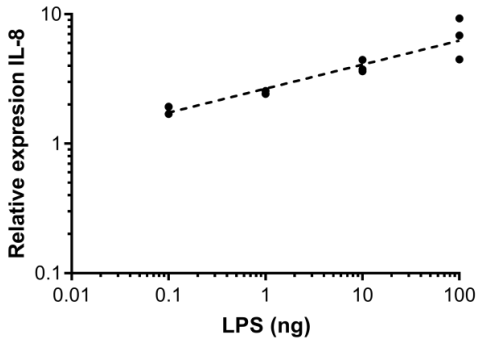

FIG 3.17: Correlation of LPS to IL-8 mRNA expression
Varying concentrations of *E.coli* LPS (0.1-100 ng ml^{-1}) were used to stimulate U937 cells in triplicate for the expression of IL-8 mRNA.

Here, endotoxin concentrations as determined by the rFC assay were only weakly correlated with the IL-8 response (R^2=0.2, p=0.003). Although, when taking the land-use classes into account, we found a positive correlation originating for the industrial (R^2=0.15, p=0.1775) and traffic locations (R^2=0.35, p=0.017). Despite a wide range of endotoxin concentrations found in the green locations, the IL-8 mRNA response remained relatively low (below 2.9 relative expression, Fig 3.18). However, endotoxin concentrations as measured by the rFC assay - specifically in the green locations - were observed to be less capable of stimulating the hTLR4 model (Fig 3.10), likely also explaining the lack of activation of the pro-inflammatory response compared to the other locations. Subsequently, by rather using the bioassay of TLR4 stimulation as a proxy for bioactive endotoxin concentration, the correlation significantly improved for the prediction of the IL-8 response (R^2 =0.38, p<0.0001), no longer with significant effects or interactions from the areas.

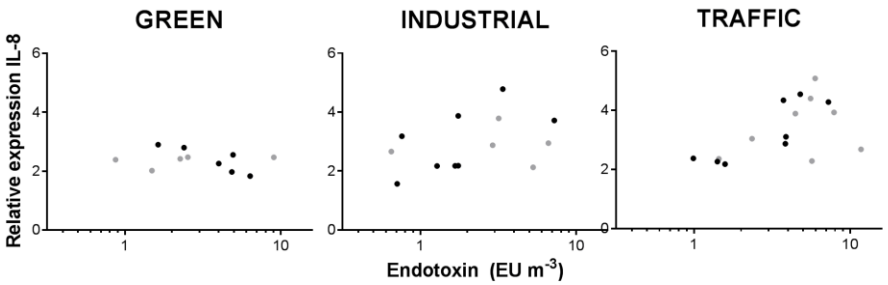

FIG 3.18: Scatter plot of endotoxin concentration as determined with the rFC assay (EU m^{-3}) vs the relative expression in mRNA IL-8 expression, with each dot representing a sample from either the green, industrial and traffic locations. Grey points represent Campus, Metal recycling plant, and Traffic 2, respectively.

While the HEK hTLR4 reporter cell line may offer a more accurate model than the rFC assay for predicting the inflammatory potential of PM associated endotoxin, the bioassay is not without its limitations. Although TLR4 is not sensitive to fungal glucans (as with the LAL assay), fungal overgrowth of an environmental sample during co-incubation usually decreases the acidity (phenol red indicator turns yellow) and is a problem for the cell line viability. Here, the cell viability of 3/50 samples was severely affected in all three technical repeats and results were excluded, while another 8 samples showed fungal contamination in only one of the technical repeats and results were still included in further analyses after the samples were repeated in another independent experiment. To prevent fungal growth, problematic samples were heated at 90°C for 2 min, but some fungal spores still survived and TLR4 stimulation was significantly reduced in all samples. We therefore suggest that a shorter incubation period of the sample with the cell line may help to minimize the problem.

3.5 Conclusion

In this chapter, we applied detection assays that were more related to the molecular recognition of endotoxin in the human body (by mainly focusing on hTLR4) and its inflammatory response (including induction of cytokines) than the standard rFC or LAL assay. Of interest, this hTLR4 stimulation in the HEK-Blue reporter cell line did provide new insights, since it did not always correspond to the endotoxin concentration quantified with the rFC assay in Chapter 2.

Surprisingly, for 83% of the samples, concentrations determined by hTLR4 stimulation in the HEK-Blue reporter cell line were lower than with the rFC assay, despite the improvements of the latter over the commonly used LAL assay (simplified pathway offers less likelihood of interferences, and no false activation by yeast glucans). As expected, the hTLR4-based assay was found to be a better biomarker for the IL-8 response to PM. Furthermore, the ability of the quantified endotoxin (rFC assay) to stimulate the TLR4/MD-2 complex was found to be affected by the urban land-use class from where the samples were collected. In the urban locations studied here, the traffic locations were found to be significantly higher in bioactive endotoxin than the industrial and green locations, despite all areas having similar rFC-determined endotoxin concentrations. In the subsequent chapter we therefore turned our attention to the composition of PM to explain the disparity between the rFC assay and TLR4 stimulation for the different urban land-use classes.

Chapter 4

PM concentration &

transition metal composition

"Science never solves a problem without creating ten more"

-- George Bernard Shaw

4.1 Introduction

As mentioned in chapter 1, PM encompasses a highly diverse range of components varying in chemical composition (from natural to anthropogenic sources), phase (liquid/solid particles), and particle size, which makes it difficult to pinpoint the components responsible for the adverse effects. Furthermore, although regulatory standards and limits for PM size ranges, PM_{10} and $PM_{2.5}$, and specific particle constituents exist, there is still no threshold below which adverse health effects are no longer observed (WHO, 2016). This drives the urgent need to improve our understanding of the toxicological mechanisms – including synergist effects - of specific PM compounds to provide better air quality management.

Recently it was found that the transition metals nickel and cobalt could specifically activate the human TLR4/MD-2 receptor complex, initially considered to be limited to endotoxin. Three histidine residues are proposed to coordinate the binding of nickel ions between two TLR4 ectodomains (completely independent of endotoxin binding site), which would trigger TLR4 dimerization and then stabilization and activation by MD-2 interactions (Oblak *et al.*, 2015; Rachmawati *et al.*, 2013; Schmidt *et al.*, 2010). Furthermore, nickel was shown to act synergistically with endotoxin in the production of TNFα (Oblak *et al.*, 2015).

4.2 Aim

To investigate the difference in TLR4 recognition of endotoxin from the urban land-use classes, in this chapter, we turned our attention to the concentration and composition of particles from these environments. Transition metals are important atmospheric contaminants which may not only confound responses to airborne microbial endotoxins through oxidative stress, but transition metals such as nickel and cobalt are known to directly activate TLR4. This chapter therefore focussed on the quantification of transition metals in the urban air samples and their potential involvement with TLR4 stimulation and the inflammatory response.

4.3 Materials & Methods

4.3.1 Particle count

Particle size distribution and count as determined by Coulter counter analysis (Beckman Coulter Inc.) in chapter 2 were further analysed in this chapter. Using the Multisizer 3 software, insoluble particles were counted for the coarse fraction (2.5 - 10 µm), which were then calculated to be expressed as particles m^{-3}.

4.3.2 Transition metal analysis

From each of the collected air samples, 2 ml was transferred into polypropylene vials and immediately acidified to 2% using highly purified nitric acid so as to prevent metal adsorption and fully dissolve all particulates to avoid clogging of the spray chamber. Corresponding preparation and reagent blanks were always included. Samples were stored at -20°C until elemental analysis was performed in the laboratory of Prof R. Blust (SPHERE, University of Antwerp). High resolution sector field ICP-MS (Element XR, Thermofisher Scientific, Bremen, Germany) was used to determine elemental concentrations in the samples with speed, accuracy and precision. Briefly, samples are ionized with inductively coupled plasma (ICP) using argon gas, and ions are separated on the basis of their mass-to-charge ratio and quantified using a mass spectrometer (MS), where a detector receives an ion signal proportional to the concentration. The following metals were measured in the Low Resolution: silver (Ag), cadmium (Cd), and lead (Pb), while aluminium (Al), chromium (Cr), manganese (Mn), iron (Fe), cobalt (Co), nickel (Ni), copper (Cu), and zinc (Zn) were measured in the medium resolution. Arsenic (As), which is typically more problematic in matrices containing calcium and chloride, was measured in the highest resolution mode. The three mass resolutions correspond to 300, 4000, and 10,000 as defined by the 10% valley, equivalent to 5% peak height. A NIST standard (SRM 1640a) was used as analytical quality control and the recoveries were consistently within 3% of the certified values for all the measured elements. Metal concentrations (ng m^{-3}) of the blank samples (collection liquid in cone; n=5) were all

below the detection limit except for very low traces of Ag (<0.013), Mn (<0.061), Cu (<0.086), and Zn (<0.068).

In addition, nine transition metals (As, Cd, Pb, Zn, Cu, As, Ni, Cd) from the Traffic 1 and Metal recycling plant locations were reported by the VMM during the sampling period. These samples were collected (24 h) using a SEQ 47/50 sequential gravimetric sampler (Leckel, Germany) with PM_{10} inlet and 2.3 m^3 h^{-1} flow rate, after which ED-XRF analysis was performed (following the EN14902 reference).

4.4 Results & Discussion

4.4.1 Relation of endotoxin to particle concentration

In chapter 2, a weak but significant correlation (R^2=0.24; p<0.0001) was found between the coarse PM fraction particle count and endotoxin concentration (rFC assay). Here, we investigated the concentration of these particles (using a Coulter counter) in the different land-use classes, and secondly determined if the biological reactivity of endotoxin may be correlated to PM particle count. The traffic areas showed a trend to contain the highest number of coarse particles per cubic meter of air (GM: 5.56 x 10^4) compared to the industrial (GM: 4.83 x 10^4) and urban green locations (GM: 3.87 x 10^4), however, not significantly so (p=0.1899; Fig 4.1A). Furthermore, the biological recognition of endotoxin was only significantly correlated to the coarse particle count from the traffic land-use class (R^2=0.51, n=17, p=0.0014) (Fig 4.1C). A similar correlation could not be significantly found for green and industrial locations. This may suggest that dominant particles from the traffic location may be contributing synergistically to the TLR4 stimulation.

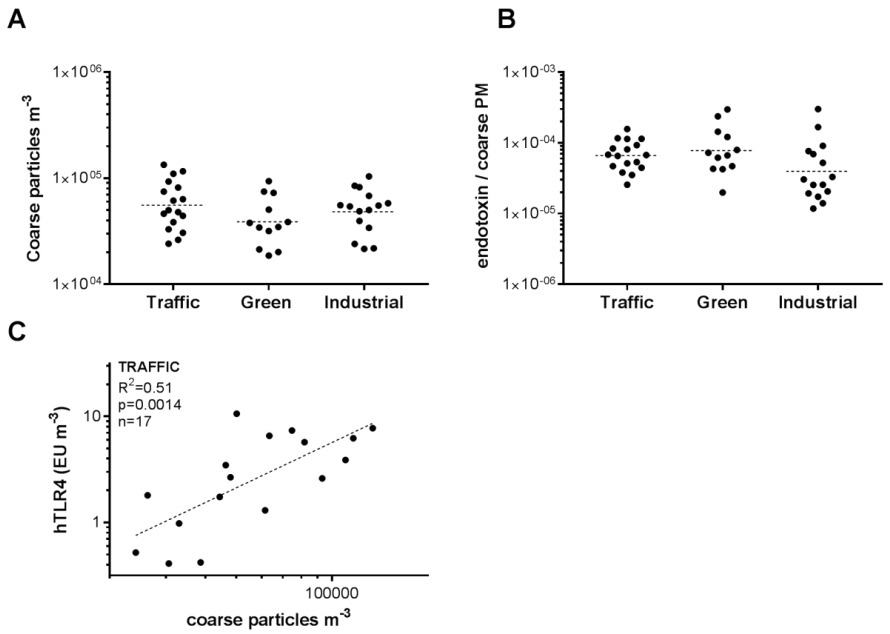

FIG 4.1: Graph demonstrating the coarse particle count (2.5-10 μm) per cubic meter of air from the various land-use classes. Locations within each class (traffic, green, industrial) were not significantly different. **(B)** The ratio of measured endotoxin (rFC assay) per coarse particle count is not significantly different for the various urban settings. **(C)** The biological recognition of endotoxin through hTLR4 was only correlated to the coarse particle count m^{-3} in the traffic locations. Data are logarithm transformed on an anti-logarithm axis to demonstrate original values.

4.4.2 Atmospheric transition metals concentrations

Twelve of the major transition metals were quantified in each sample by ICP-MS and the data was grouped per urban land-use class (Fig 4.2). The concentrations of metals collected over 40 minutes with the Coriolis were found to be comparable with the 24 hour-averaged concentrations reported by the VMM for the corresponding days and locations (Traffic 1 and the Metal recycling plant; Table 4.1).

Table 4.1: A comparison of the median transition metal concentrations (ng m^{-3}), followed by the range (min – max) for the Traffic 1 and Metal recycling plant locations measured on the same days by the Coriolis (40 min) and Leckel SEQ 47/50 sampler from the VMM (24 hr average). Values in bold are significantly higher (two-tailed, paired t-test, $p<0.05$).

	Traffic 1 (n= 9)				Metal recycling plant (n=6)			
	Coriolis		**VMM**		**Coriolis**		**VMM**	
Mn	**17.1**	(5.93 - 31.5)	9.0	(5.2 – 17.6)	15.0	(5.54 - 34.8)	15.05	(11.2 – 22.1)
Cr	3.4	(0.5 - 5.07)	3.5	(2.1 – 10.6)	1.16	(0.55 - 4.12)	**5.05**	(2.0 – 10.2)
Pb	16.4	(7.87 - 109)	12.3	(4.3 – 23.1)	169	(32.1 - 15208)	122	(11.1 – 932)
Zn	59.1	(29.8 - 132)	31.4	(15.5 – 122)	37.3	(23.7 - 1071)	75.6	(15.4 – 159)
Cu	**41.1**	(18.9 - 82.5)	20.7	(9.9 – 38.3)	35.3	(11.9 - 1032)	33.4	(5.0 - 183)
As	0.28	(BMQL - 4)	BMQL	(BMQL - 0.2)	6.40	(0.02 - 280)	7.55	(0.4 – 46.9)
Ni	3.35	(0.85 - 28.3)	BMQL	(BMQL - 2)	11.8	(1.40 - 67.6)	2.45	(0.4 – 9.8)
Cd	0.20	(0.03 - 1.55)	0.30	(0.1 – 3.5)				

From Fig 4.2, there are clear differences in metal concentrations between the traffic, urban green, and metal recycling locations. The two locations representing the urban green land-use class showed similar and relatively low concentrations for all the corresponding transition metals (Table 4.2). In contrast, the traffic locations had significantly elevated concentrations of Fe, Cr, Zn, and Cu compared to the other land-use classes (Kruskal-Wallis test with Dunn's test for multiple comparisons). Furthermore, in comparison to Traffic site 1 (vehicular traffic), Traffic site 2 (which had vehicular and tram traffic) had significantly higher concentrations of Cr, Mn, and Fe, which are relevant indicators for railway abrasion (Gehrig *et al.*, 2007). Lastly, the two industrial locations showed to be the most distinct from each other in terms of their atmospheric metal profiles. The Metal recycling plant (non-ferrous based) displayed an entirely different profile with overall high and variable metal concentrations, dominated by cadmium, cobalt, silver, lead, and arsenic – metals commonly recycled at this plant and often measured to be in exceedance of the European target values by the VMM (2016). Further information of the correlations between the twelve metals for the specific locations may be found in the Appendix (Fig A2.1).

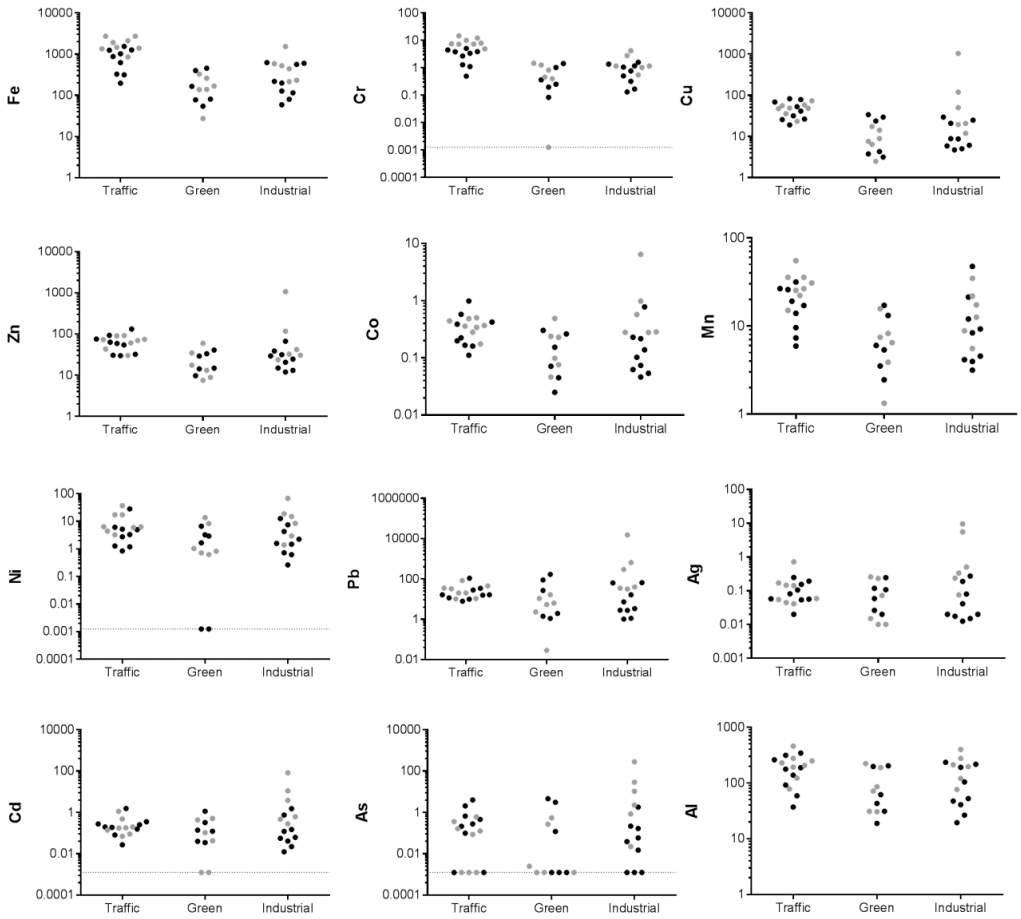

FIG 4.2: Transition metal concentrations (ng m^{-3}) measured with ICP-MS, with each dot represented by a sample from the six sampling sites within the city of Antwerp for urban green, traffic and industrial locations. Black dots represent Traffic 1, Park, and Harbour; grey dots represent Traffic 2, Campus, and Metal recycling plant respectively. Note the differences in the vertical axes. Points on dotted horizontal line were samples below the minimum detection limit.

Table 4.2: Median transition metal concentrations (ng m^{-3}), followed by the range (min – max) reached within the locations in Antwerp for the sampling period July – September 2015. Values in bold and grey represent the highest and lowest values measured, respectively, for the particular metal over the six locations. Arsenic, highlighted in red for the Metal recycling plant, is currently in exceedance of the EU legal limit of 6 ng m^{-3} (1 year)

	TRAFFIC				GREEN				INDUSTRIAL			
	Traffic 1		Traffic 2		Park		Campus		Harbour		Metal recycling plant	
Fe	874	(197 - 1545)	**1692**	(852 - 2730)	123	(54.3 - 455)	154	(27.5 - 326)	198	(59.1 - 622)	482	(214 - 1535)
Al	178	(37.1 - 343)	**218**	(78.5 - 460)	52.5	(18.9 - 203)	78.9	(30.7 - 223)	52.5	(19.5 - 236)	204	(76.4 - 400)
Mn	17.1	(5.93 - 31.5)	**28.6**	(15.1 - 55.1)	5.69	(2.45 - 17.1)	6.96	(1.33 - 15.7)	8.37	(3.16 - 47.3)	15.0	(5.54 - 34.8)
Cr	3.36	(0.5 - 5.07)	**7.69**	(4.87 - 14.5)	0.30	(0.08 - 1.42)	0.64	(BMQL - 1.45)	0.76	(0.13 - 1.58)	1.16	(0.55 - 4.12)
Zn	59.1	(29.8 - 132)	**71.2**	(30.2 - 91.5)	22.1	(9.74 - 41.0)	15.4	(7.56 - 59.3)	24.6	(12.0 - 66.9)	37.3	(23.7 - 1071)
Cu	41.1	(18.9 - 82.5)	**48.4**	(23.3 - 73.1)	14.0	(3.15 - 33.9)	8.23	(2.49 - 17.5)	8.67	(4.69 - 29.4)	35.3	(11.9 - 1032)
As	0.28	(BMQL - 4.00)	0.11	(BMQL - 0.60)	0.12	(BMQL - 4.60)	BMQL	(BMQL - 0.55)	0.04	(BMQL - 0.04)	**6.38**	(0.02 - 280)
Ni	3.35	(0.85 - 28.3)	6.32	(3.25 - 37.1)	2.31	(BMQL - 6.62)	0.93	(0.63 - 13.7)	1.59	(0.27 - 12.6)	**11.8**	(1.40 - 67.6)
Pb	16.4	(7.87 - 109)	26.3	(10.3 - 83.2)	14.4	(1.11 - 170)	5.91	(0.03 - 16.6)	3.41	(1.03 - 65.7)	**169**	(32.1 - 15208)
Cd	0.20	(0.03 - 1.55)	0.18	(0.07 - 1.12)	0.13	(0.04 - 1.14)	0.07	(BMQL - 0.51	0.06	(0.01 - 1.53)	**2.21**	(0.28 - 82.5)
Ag	0.08	(0.02 - 0.25)	0.10	(0.04 - 0.72)	0.08	(0.02 - 0.25)	0.04	(0.01 - 0.26)	0.02	(0.01 - 0.27)	**0.42**	(0.08 - 9.61)
Co	0.23	(0.11 - 0.99)	0.36	(0.18 - 0.5)	0.11	(0.03 - 0.30)	0.16	(0.05 - 0.49)	0.10	(0.05 - 0.78)	**0.43**	(0.28 - 6.44)

4.4.3 Associations between source composition and immune response

Consequently, we explored the correlations between the endotoxins, metals and inflammation markers. Although nickel and cobalt have previously been shown to directly activate hTLR4/MD-2, their effect in this study was negligible in comparison to the surprisingly strong correlation of iron with the stimulation of TLR4 in the HEK293 cell line (R^2=0.50; n=41; p<0.0001), with no significant interaction effect of the considered monitoring locations/land-use classes. Subsequently, we found that by adding iron concentrations together with rFC assay as factors in the linear regression model predicting TLR4 stimulation (HEK assay), the model was significantly improved (R^2=0.77, n=41; p<0.0001). This raised the question of whether iron may act synergistically with LPS stimulation. Interestingly, in a study by Becker *et al.* (2005a), iron concentrations quantified from coarse PM fractions correlated well with the IL-6 release in alveolar macrophages (from normal individuals through bronchial brushings), while no correlation was found in ultrafine particles. Although endotoxin was not quantified in the study, it is interesting to note that the inflammatory potential of iron was best correlated in the coarse PM fraction where endotoxin is predominantly found.

Multivariate analysis was performed in JMP Pro (v13.0.0) to determine the correlation of the measured factors to the immune response markers. IL-8 was best correlated to the TLR4 bioassay, in addition to Mn, Fe and Cr (r=0.64, 0.63, 0.57; p≤0.0001). The IL-1β response was best correlated with Mn (r=0.55; p=0.0002), especially in the traffic locations - Traffic 1 (r=0.88, p<0.0001) and Traffic 2 (r=0.94, p<0.0001) - and also the TLR4 bioassay (r=0.52, p=0.0005). Furthermore, the metals Mn, Fe and Cr were often very strongly correlated with each other, likely a metal alloy or originating from vehicular combustion and wear (Fig A2.1). Furthermore, in the Traffic 1 location, the VMM measured nitrogen oxides (NOx) and black carbon (BC) concentrations, which are by-products for fossil fuel combustion. NOx and BC were both significantly (p<0.05) correlated to Cr, Mn, and Fe. Particle concentration was also best correlated to Mn for the various locations (Fig 4.3). Lastly, the TNFα response was better associated to the TLR4 bioassay (r=0.5, p=0.0007).

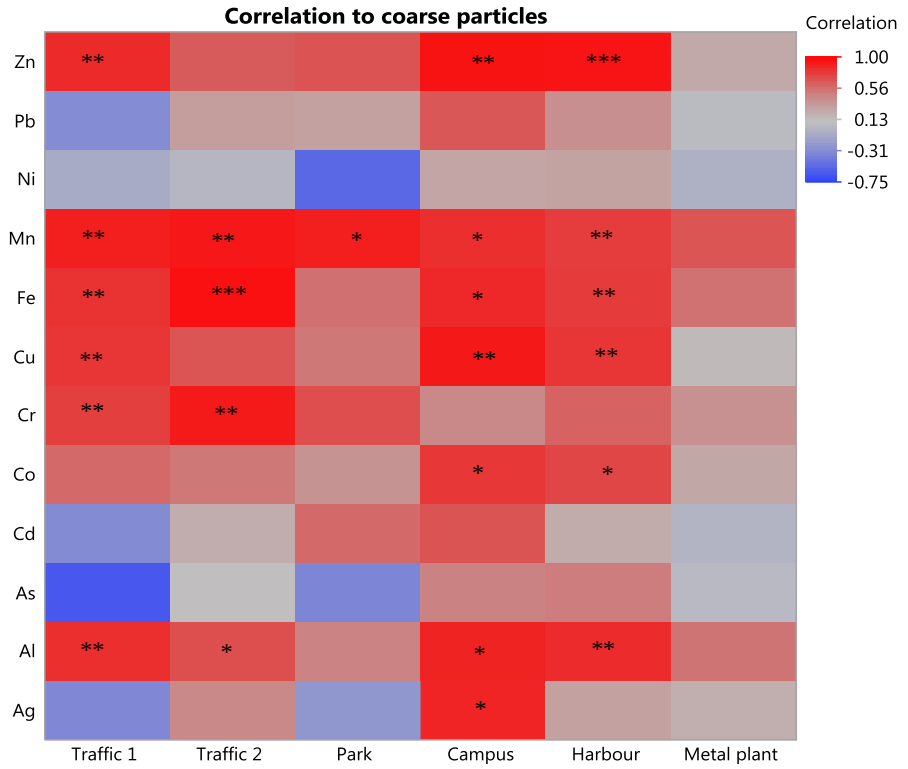

FIG 4.3. Heat map of the correlation coefficients (r) between the logarithm of coarse particles m^{-3} and the corresponding transition metals per sampling location. Statistical significance indicated * $p<0.05$, ** $p<0.01$ *** $p<0.0001$

4.5 Conclusion

In this chapter, samples were characterized based on their transition metal concentrations. Although we were not sure what to expect regarding metal collection using the Coriolis sampler, the 40-minute Coriolis samples were comparable to the 24 hour-averaged VMM samples. Subsequently, we could conclude that the collected metals were in a realistic range. In this study, we managed to collect a considerable variation of metal concentrations, not only amongst land-use classes, but also between and within locations. Generally, the urban green land-use class had relatively low concentrations of transition metals, while the traffic locations often had elevated concentrations of iron (amongst other metals). Initially, we found that the

stimulation of the HEK hTLR4 model correlated to the coarse particle count only in the traffic land-use class. Furthermore, iron concentrations were also well correlated to the coarse particle count, especially in the urban locations. In turn, iron was correlated to the stimulation of the HEK hTLR4 model. Through all these correlations, the ultimate question of "correlation or causation?" arises.

In chapter 3 we found that the ability of the quantified endotoxin (rFC assay) to stimulate the HEK hTLR4 model was affected by the urban land-use class. We initially proposed that the linear regression model would improve upon taking into account the concentrations of nickel and cobalt, which were previously reported to activate the hTLR4/MD2 complex. Surprisingly, we found the effects of nickel and cobalt to be negligible in comparison to that of iron. In fact, the addition of iron concentrations as a factor significantly improved the regression model between the two endotoxin quantification assays, explaining 77% of the variation of HEK hTLR4 model stimulation and excluding the significant effect of land-use class. As one of the most abundant transitional metals in urban PM, in chapter 5 we further explore the immunoregulatory effects of iron during endotoxin exposure.

Chapter 5

Modulation of LPS immune response by iron

“Your assumptions are your windows on the world. Scrub them off every once in a while, or the light won't come in.”

— Isaac Asimov

5.1 Introduction

Iron is typically one of the most abundant transition metals found in urban PM (Michael et al., 2013), which was also confirmed in our own analysis in chapter 4. Various forms/speciations of iron may originate from crustal matter (Fe_2O_3 and Fe_3O_4), iron industries (metallic iron and its alloys with Mn, Cr, etc), traffic ($Fe_2(SO_4)_2$ from doping fuel with ferrocene) and railway related sources (metallic iron and iron oxides) (De Kok *et al.*, 2006; Jung *et al.*, 2012; Srimuruganandam and Shiva Nagendra, 2012). Once inhaled, iron can be taken up by the innate immune system where it may modulate intracellular signalling pathways, many of which are related to oxidative stress (see chapter 1 for more details). As presented in chapter 4, we found a clear correlation of iron with the stimulation of the HEK hTLR4 bioassay. Although iron may exist in numerous compounds and originate from different sources in urban environments, our own data measuring total iron concentrations with ICP-MS indicated that these land-use classes per se (*i.e.* location) had no significant effect on this association. Subsequently, the effect of iron is likely owing to its oxidized forms (i.e. ferric and ferrous ions), rather than specific compounds.

Despite the compelling correlation found in our own data between iron and TLR4 activation, other studies have repeatedly shown that iron cations are not capable of independently stimulating the TLR4/MD-2 complex, unlike nickel and cobalt (Oblak et al., 2015; Rachmawati et al., 2013). However, the ability of iron to act synergistically with LPS (ubiquitously present in urban air) to stimulate the TLR4/MD-2 complex has not yet been investigated. Since iron is well known for the production of ROS (as reviewed in chapter 1), it may function by boosting TLR4 signalling through MD-2 upregulation. This could be similar to lactate, which has been shown to boost TLR4 signalling via ROS production and MD-2 upregulation in macrophages (Samuvel *et al.*, 2009). In addition, Toll-like receptors such as TLR2 have already been shown to be enhanced (both mRNA and protein levels) by LPS exposure in alveolar macrophages *in vitro* (Oshikawa and Sugiyama, 2003) and *in vivo* (Maris *et al.*, 2006). Furthermore, a form of transcript regulation between function and non-functional splice variants of TLR4 has been found to control signal transduction in mouse models (Iwami

et al., 2000). In humans, TLR4 contains four splice variants: TLR4 v1-v4. TLR4 v1 (NM 138554) is involved in LPS binding and triggering of intracellular signal transduction cascades, while TLR4 v3 (NM 003266) and TLR4 v4 (NM 138557) lack residues which are essential for MD-2 binding and LPS signalling (Jarešová *et al.*, 2007; Maris *et al.*, 2006). As for the TLR4 v2 (NM 138556), there is currently insufficient support for the transcript, and the protein is not supported by current protein homology data. A similar form of transcript regulation has not yet been explored for exposure to air pollutants in humans. For this reason, we explored if iron could modulate LPS recognition through the transcriptional regulation of TLR4 itself, together with associated signalling molecules (e.g. MD-2).

5.2 Aim

In this chapter, we investigated whether the correlations of iron to SEAP production in the HEK hTLR4 model may be linked to causative and potential synergistic effects between LPS and iron. Furthermore, we investigated whether these effects are present in other cell types (i.e. macrophages) by monitoring transcriptional regulation of various genes involved in the pro-inflammatory and oxidative stress responses, TLR2, TLR4 splice variants and MD-2 accessory protein.

5.3 Materials & Methods

5.3.1 TLR4 stimulation in HEK293 cells

HEK-Blue^{TM} hTLR4 cells were cultured as mentioned in chapter 3. Cells were seeded into opaque white 96 well plates at a concentration of 0.5 x 10^6 cells ml^{-1} and incubated for 48 hours until approximately 80% confluent. Media was removed from adherent cells and replaced with 5 EU ml^{-1} endotoxin well vortexed in DMEM media and for the negative control just DMEM. Varying concentrations of iron chloride, nickel chloride or magnesium chloride were added to the corresponding wells. A standard curve was generated by stimulating the cells with a five-point serial dilution (0.5 -50 EU ml^{-1}) of endotoxin (*E. coli* O55:B5, lot 0000 441 186; Lonza Walkersville Inc., MD, USA) as illustrated in Fig 5.1A. After 20 h incubation, 50

µl-supernatant was transferred in duplicate to a new clear 96 well plate where SEAP activity was determined upon adding 100 µl of freshly prepared substrate solution (final concentration of 1 mg ml^{-1} pNPP in 100 mM Tris-HCl, 100 mM NaCl, 5 mM $MgCl_2$, pH 9.5 buffer). After a 20 min incubation at 23°C, the absorbance was measured at 405 nm (Fig 5.1). From the standard curve and sampling efficiency, the predicted endotoxin concentrations (EU m^{-3}) could be calculated.

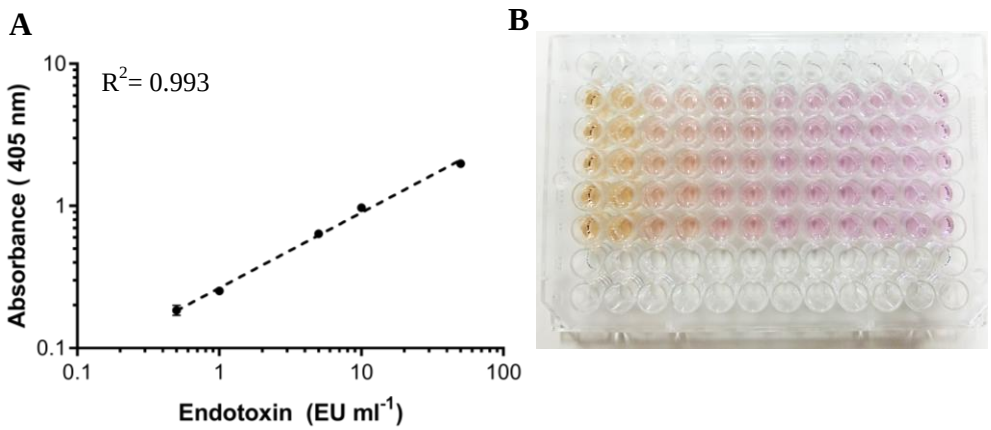

FIG 5.1: A) Standard curve of logarithm-transformed endotoxin concentration and absorbance. Cells were stimulated with five different concentrations of endotoxin (0.5, 1, 5, 10, 50 EU ml^{-1}) in four technical repeats and the resulting SEAP activity was measured at an absorbance of 405 nm. Standard deviation is shown in error bars. **B) Representative examples of the colour changes observed due to SEAP activity.** Levels of NF-κβ-inducible SEAP secreted into the culture medium are determined by measuring the absorbance (405 nm) of p-nitrophenyl (yellow) from the hydrolysis of p-nitrophenyl phosphate (pNPP) by the alkaline phosphatase.

After removing 100 µl of the supernatant to test extracellular SEAP activity, cell viability was assessed on the remaining cells using the CellTiter-Glo 2 Assay (Promega). The assay quantifies the amount of ATP present in metabolically active cells through the generation of a luminescent signal as illustrated in Fig 5.2.

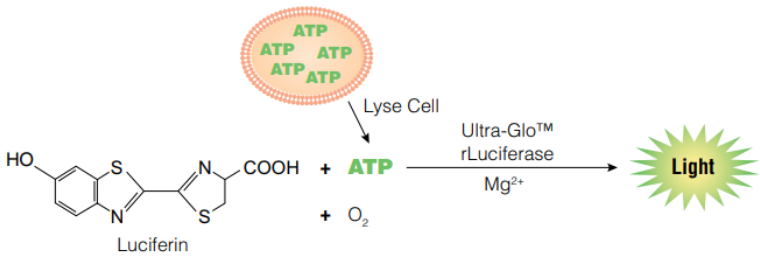

FIG 5.2: Overview of CellTiter-Glo 2.0 Assay principle as illustrated by the manufacturer, Promega.

5.3.2 Gene expression in monocyte cell line (U937)

The human monocyte cell line U937 was cultured as mentioned in chapter 3. Cells were seeded in 12-well plates at a concentration of 5 x 10^5 cells ml^{-1} in complete growth medium with 100 ng ml^{-1} PMA to allow for differentiation to an adherent macrophage-like stage for 48 h. Thereafter, PMA and non-adherent cells were removed by replacing the RPMI medium (without supplements) for a further incubation of 24 h. Medium was removed and cells were co-incubated for 3 h with 5 ng ml^{-1} LPS (phenol extraction from *E. coli* 0111:B4; Sigma Aldrich) thoroughly vortexed in RPMI media with or without 0.1 mM $FeCl_2$. A negative control with cells only exposed to RPMI medium was also included. After co-incubation, total RNA was isolated, cDNA was synthesized and qPCR was carried out as previously mentioned in chapter 3. In addition to the expression of three selected pro-inflammatory markers (IL-8, IL-1β and TNFα) and two reference genes (*GNB2L1* and *CYC1* as in chapter 3), an oxidative stress marker (HO-1), TLR4 splice variants, and MD-2 accessory protein were monitored by RT-qPCR on a StepOne Plus Real-Time PCR System. All primers were tested for efficiencies between 90-110% and their sequences can be found in Table 5.1.

Table 5.1: Primer sequences of gene expression with the product size (nucleotides) indicated

Gene	Forward primer (5 – 3')	Reverse primer (5 – 3')	nt
HO-1	GGCTTCCCTCTGGGAGTCT	AGCTGCTGACCCATGACAC	115
TLR2	AACCGGAGAGACTTTGCTCA	CCACTGACAAGTTTCAGGCA	91
MD-2	ACACCATGAATCTTCCAAAG	TATTCACAGTCTCTCCCTTC	96
TLR4 v1	GCTCACAGAAGCAGTGAGGATG	TAGGAACCACCTCCACGCAG	133
TLR4 v3	TTGGCCCTAAACCACACAGAA	TTAGGAACCACCTCCGTGATAA	129
TLR4 v4	GCTCACAGAAGCAGTGAGGATG	ATTTCACACCTCCACGCAGG	132

5.4 Results

5.4.1 HEK hTLR4 cell model

To investigate a potential direct effect of iron during LPS stimulation, the complexity of the environmental samples was simplified by treating HEK hTLR4 cells with a constant LPS concentration, yet with increasing concentrations of iron. In this chapter, HEK hTLR4 cells treated with 5 EU ml^{-1} LPS and increasing concentrations of $FeCl_2$ showed a significant increase in SEAP production at iron concentrations of 0.1 and 0.2 mM (60 and 64% increase respectively in terms of EU ml^{-1}), while the iron itself (in absence of LPS) did not stimulate a response that was significantly higher than the negative control (Fig 5.3). Consequently, these data also showed that the iron solution was not contaminated with LPS, and was not able to independently stimulate SEAP production.

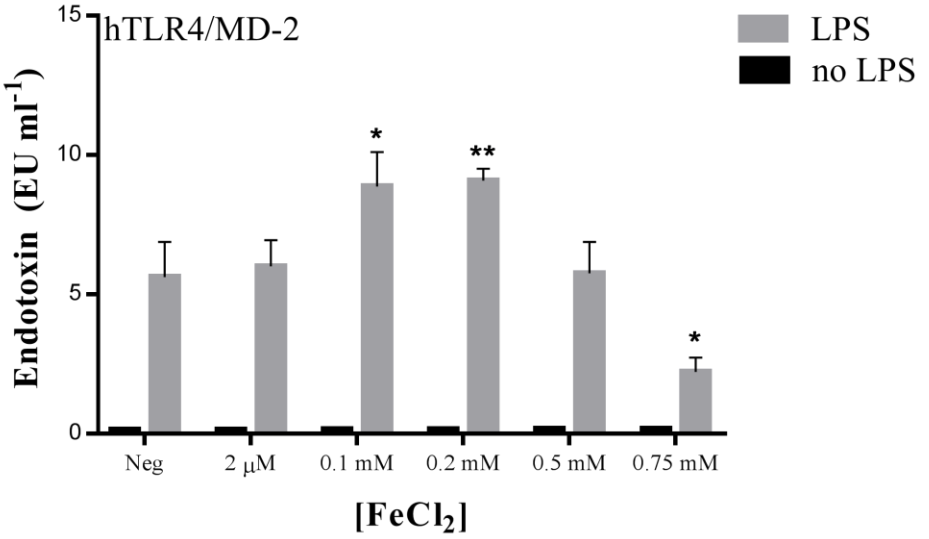

FIG 5.3: HEK-Blue hTLR4 cells were stimulated in triplicate with LPS (5 EU ml^{-1}) and/or increasing iron concentrations (2 μM to 0.75 mM) for 20 hours. Results shown are from one experiment (standard deviation shown for three technical repeats) representative of three independent experiments. The resulting SEAP activity was converted to EU ml^{-1} with a standard curve. The "no LPS" control tested the response of the iron solutions in the absence of LPS. For statistical analysis, the Fe doses were compared to the negative control (* $p<0.05$, ** $p<0.01$).

From Fig 5.3 a drop in SEAP production was observed from 0.5 mM $FeCl_2$ with LPS. Cell viability was tested with the CellTiter-Glo 2.0 assay and a corresponding drop in viability was observed when the iron concentrations (in the absence and presence of LPS) exceeded 0.5 mM (Fig 5.4), as similarly seen in the study of Rachmawati et al. (2013). Of note, the environmental samples did not reach these iron concentrations when treating the HEK hTLR4 model in chapter 2, and were in the range of 0.39 μM to 20 μM.

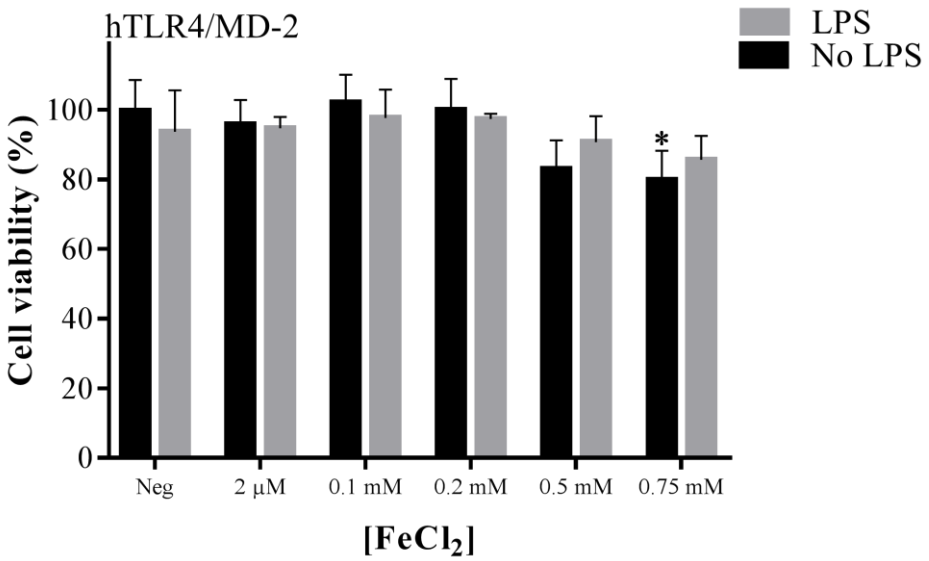

FIG 5.4: Viability of HEK-Blue hTLR4 cell line measured with the CellTiter-Glo 2.0 Assay after cells were stimulated in triplicated for 20 hours with LPS (5 EU ml^{-1}) and/or increasing iron concentrations. For statistical analysis, the iron doses were compared to the negative control (* $p<0.05$, ** $p<0.01$).

Furthermore, since alkaline phosphatases depend on Zn^{2+} and Mg^{2+} divalent cations for their enzymatic activity (Bucevic-Popovic *et al.*, 2004), we established that the increasing concentrations of Fe^{2+} had no significant effect on the activity of the SEAP reporter enzyme in this study.

To further test the HEK hTLR4 cell model, other divalent cations, such as $MgCl_2$ and $NiCl_2$ were used together with LPS. As expected, Mg^{2+} (0.1 µM -1 mM) showed no significant effect on LPS stimulation (or cell viability) compared to the negative control. As previously stated, nickel is reported to independently activate the hTLR4/MD-2 complex and increase TNFα production in undifferentiated monocytes (THP-1 cells) through synergistic effects with LPS (Oblak *et al.*, 2015). Here, we could confirm the independent stimulation of the hTLR4/MD-2 complex with increasing concentrations of nickel (Fig 5.5). The viability of the cells was affected at 0.75 mM $NiCl_2$ after incubation for 20 h. Although large synergistic effects were

previously reported for the production of TNFα after 6 h, SEAP production from the co-stimulation of the HEK hTLR4 model by LPS and nickel (0.5 mM) was less than an additive effect (although significantly different) when compared to nickel alone after 20 h.

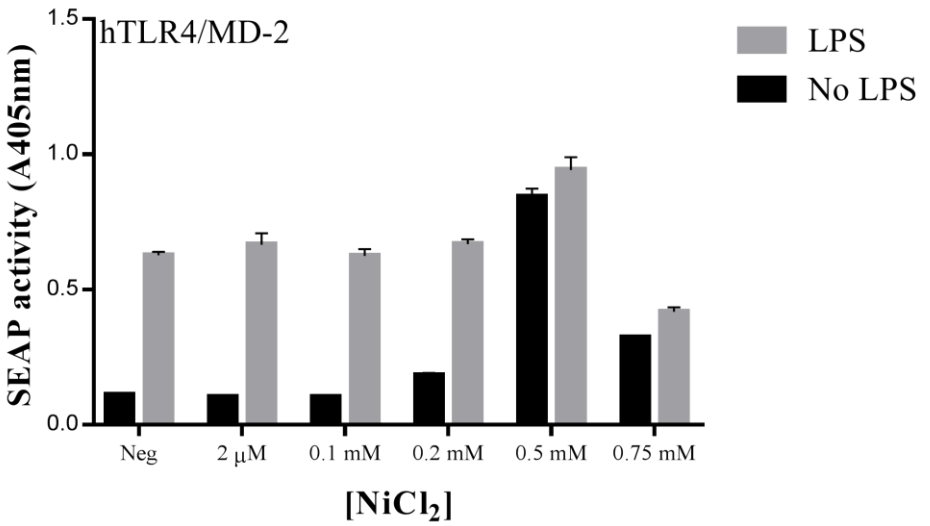

FIG 5.5: HEK-Blue hTLR4 cells were stimulated in triplicate with LPS (5 EU ml^{-1}) and/or increasing $NiCl_2$ concentrations (2 μM to 0.75 mM) for 20 hours. The resulting SEAP activity was measured at an absorbance of 405 nm after 20 min incubation with substrate pNPP. The "no LPS" control tested the response of the nickel solutions in the absence of LPS.

5.4.2 Gene expression in U937 cell lines

The stimulatory effect of co-exposure to iron and LPS observed in the HEK cell line was further investigated in the human macrophage-like U937 cell line by monitoring changes in gene expression. Figure 5.6 shows that the addition of 0.1 mM $FeCl_2$ to 5 ng ml^{-1} LPS after 3 h co-exposure lead to a significant reduction in the expression of TNFα, which was similar for IL-8 and IL-1β (Fig 5.6).

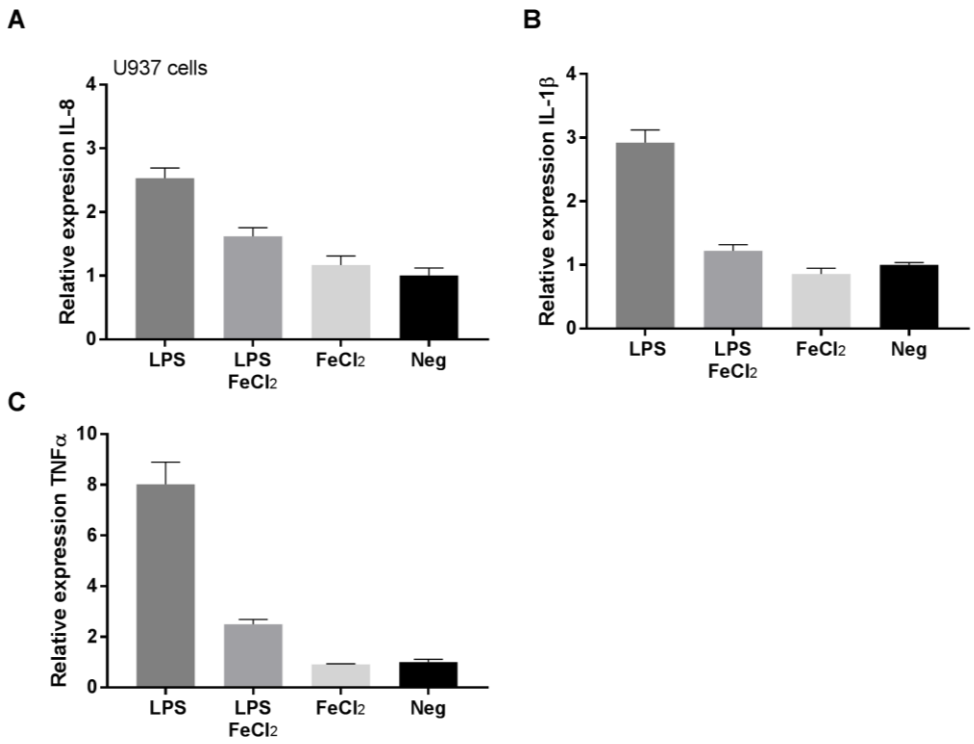

FIG 5.6: mRNA levels of the pro-inflammatory markers **A)** IL-8**, B)** IL-1β, **C)** TNFα measured in human macrophage-like U937 cells after 3 h exposure with 5 ng ml^{-1} LPS with or without 0.1 mM $FeCl_2$ (in triplicate and in two independent experiments). Values are expressed relative to the negative control, represented by an expression of one.

In addition to the expression of pro-inflammatory cytokines, the *hemoxygenase-1* (*HO-1)* gene was measured as a marker of oxidative stress (see chapter 1). In response to ROS production, the transcriptional factor Nrf-2 activates the antioxidant response element (ARE) found in the promoter region of many genes that control the expression of antioxidant defence pathways, such as HO-1 and glutathione S-transferase (GST) as discussed in chapter 1. HO-1 catalyzes the oxidative degradation of free heme and releases Fe^{2+}, biliverdin and carbon monoxide (CO), which when exhaled is a sensitive *in vivo* marker for PM-induced oxidative stress. Furthermore, HO-1 expression has been shown to correlate with dithiothreitol (DTT)-activity, which is commonly used to measure the oxidative potential of PM (Li *et al.*, 2003).

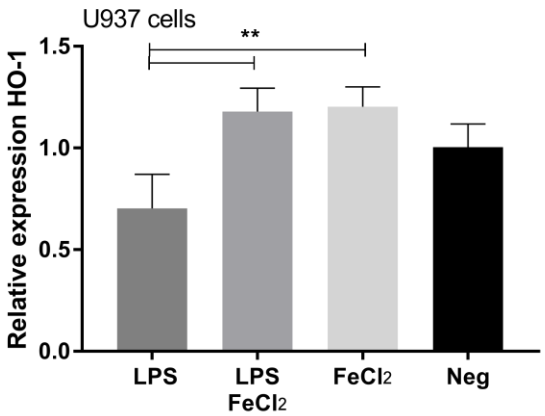

FIG 5.7: mRNA levels of the oxidative stress marker HO-1 measured in human macrophage-like U937 cells after 3 h exposure with 5 ng ml^{-1} LPS with or without 0.1 mM $FeCl_2$ (in triplicate and in two independent experiments). Values are expressed relative to the negative control, represented by an expression of one. Statistical significance is indicated for $p \leq 0.01$

Although only small changes in the relative expression were observed (two independent experiments), LPS lead to a significant ($p \leq 0.01$) decrease in the expression of HO-1, while no significant difference was seen between treatments with $FeCl_2$ (with and without LPS) and the negative control (Fig 5.7). This once again highlights the modulatory effects of iron with LPS. Interestingly, there exists a regulatory pathway between LPS stimulation and HO-1 expression which has been reported in multiple cellular and animal models (Li *et al.*, 2002). The HO-1/CO pathway exerts an anti-inflammatory activity, however may in turn be regulated when activator protein-1 (AP-1) binds to the ARE site, thus inhibiting its activation and preventing the upregulation of antioxidant defences, including HO-1. This may potentially explain the down regulation of HO-1 expression by LPS observed here.

Subsequently, we monitored the transcriptional regulation of MD-2, TLR2 and the TLR4 splice variants (Fig 5.8). Unfortunately no significant differences were seen between the negative controls and samples with 5 ng ml^{-1} LPS (with and without $FeCl_2$) and $FeCl_2$ alone, thus suggesting the transcriptional regulation of these genes are not involved in the synergistic effects of iron and LPS (or at least at this time interval and concentration). Although we expected the upregulation of TLR2 by LPS, as previously stated in literature (Maris *et al.*,

2006; Oshikawa and Sugiyama, 2003), we found a relative expression of approximately two when treating cells with higher concentrations of LPS, i.e.10 ng ml^{-1}.

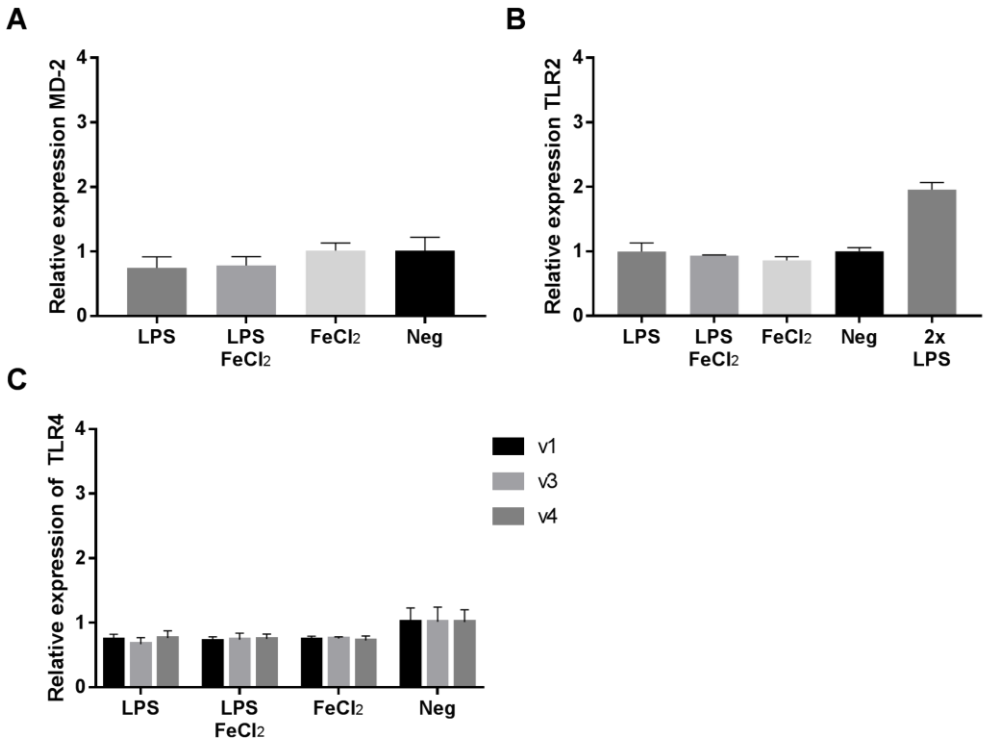

FIG 5.8: mRNA levels of **A)** MD-2**, B)** TLR2, **C)** TLR4 splice variants (v1, v2, v3) measured in human macrophage-like U937 cells after 3 h exposure with 5 ng ml^{-1} LPS with or without 0.1 mM $FeCl_2$ (in triplicate and in two independent experiments). Values are expressed relative to the negative control, represented by an expression of one.

5.4.3 Urban air samples: gene expression in U937 cell line

To access the possible transcriptional regulation of the MD-2, TLR2, and HO-1 genes from exposure to complex mixtures of ambient urban pollutants, we subsequently screened the air samples (July until September 2015) for their relative expression profiles in the macrophage-like U937 cell line (Fig 5.9). For the expression of MD-2, there was both downregulation (below the negative control) which was prevalent for many of the traffic samples, and upregulation which was especially prevalent in samples from the harbour. Surprisingly, the expression of MD-2 did not correlate with any of the measured variables described in the

previous chapters (i.e. metal concentrations, particle count, endotoxin quantification, TLR4 stimulation) in this study. For the expression of TLR2, we observed mostly upregulation, with the harbour again showing a rather large range of variation. As for the expression of HO-1, only small changes in gene expression could be detected, except for one of the metal recycling plant samples. This sample showed a relative HO-1 expression of 10.9 and notably also had the highest measured concentrations of As, Ag, Cd, Pb, Ni, Co, Cu, and Zn (Fig A2.2). Nevertheless, the fact that only small changes in gene expression were observed is likely due to the fact that new cDNA was synthesized for this qPCR analysis and the RNA integrity was likely diminished after their storage of 11 months. Similarly, the samples were also not fully screened for the TLR4 splice variants, since no significant differences were observed with the new cDNA.

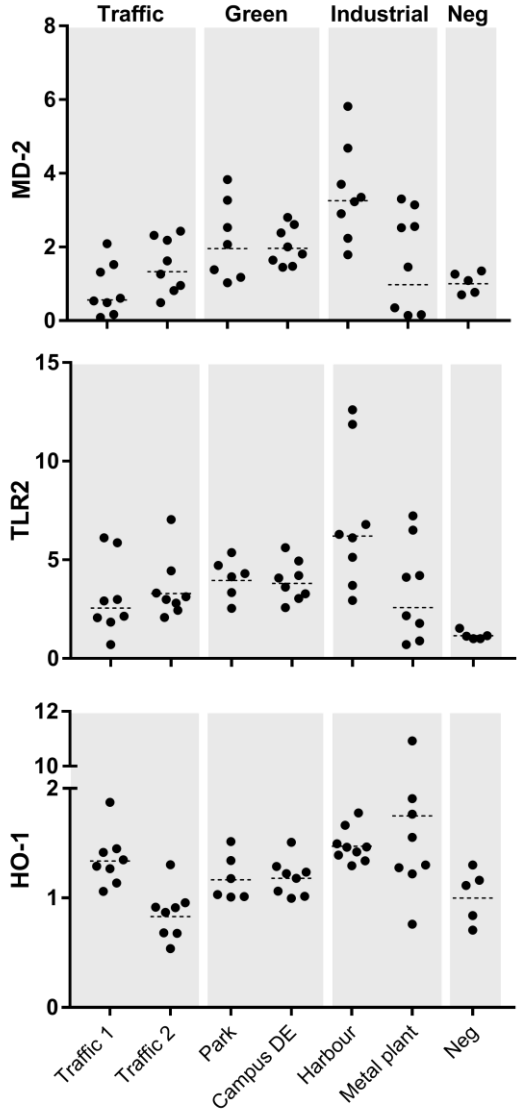

FIG 5.9: mRNA levels of MD-2, TLR2, and HO-1 genes were measured in human macrophage-like U937 cells after 3 h exposure with collected air samples (2015). Values are expressed relative to the negative control (RPMI media), represented by an expression of one, and the geometric means of the locations are shown in dotted lines, while each sample is represented as a dot. The land-use classes: traffic, green and industrial each comprise two different sampling locations.

5.5 Discussion & Conclusion

In this chapter, we set out to investigate whether the correlation found in the environmental samples between iron and the stimulation of the HEK hTLR4 cell model was indeed causative and possibly synergistic with LPS exposure. As expected, iron alone could not elicit SEAP production, however significantly increased the response during co-exposure with LPS. Since the purpose of the HEK hTLR4 cell model is to report hTLR4 activation, the results would suggest that Fe^{2+} may in some way enhance the host recognition of LPS at the TLR4/MD-2 complex.

However, it is also possible that NF-κβ activation may be independent of TLR4/MD-2 stimulation. For which, we propose that the IL-1β pathway may be responsible, as explained as follows. The secretion of IL-1β is unique in that it involves two processes, i.e. (1) NF-κβ activation - which is induced by TLR ligands such as LPS – resulting in the upregulation of pro-IL-1β, and (2) inflammasome assembly, which activates caspase-1 to cleave pro-IL-1β into the mature form which is released in to the cytoplasm (Fig 5.9) (Lamkanfi and Dixit, 2014). Once released, IL-1β may in turn bind to IL1R on the cell surface and potentiate the NF-κβ signal. This may also explain why iron alone does not stimulate SEAP production, since there is no NF-κβ activation or no pro-IL-1β to process. In the future, blocking the IL-1β pathway may help elucidate the role of iron during LPS exposure.

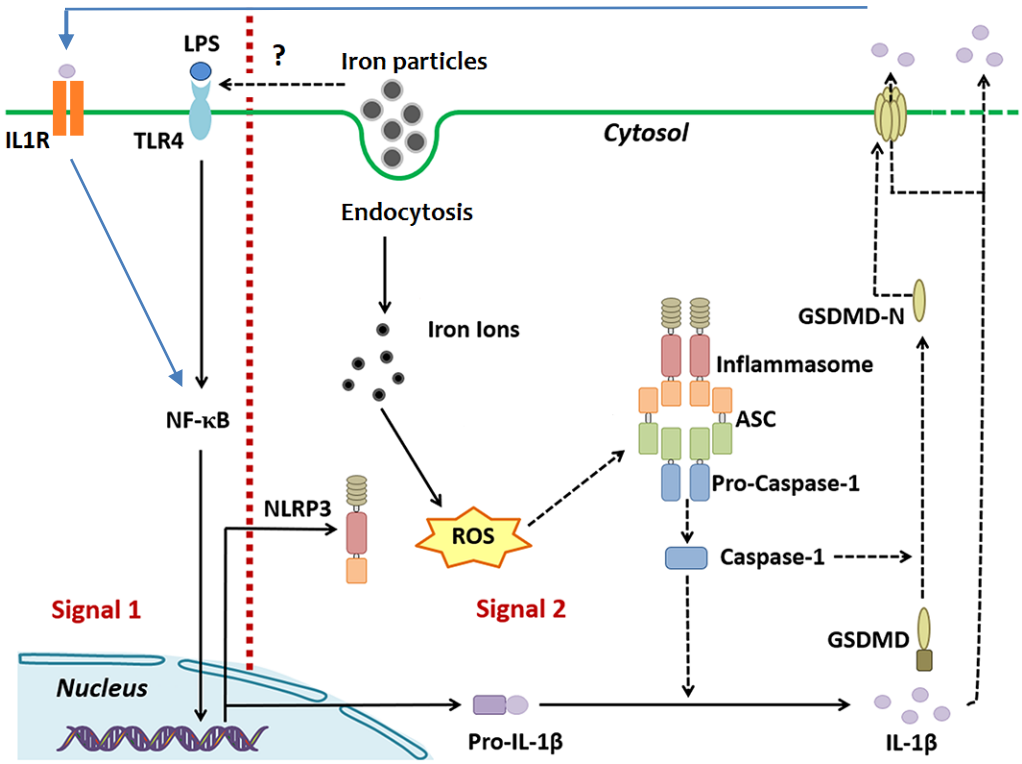

FIG 5.9: Scheme showing the possible synergistic interaction between iron and LPS/TLR4 recognition, and the production and maturation of IL-1β from host cell. Pro-IL-1β expression is induced by NF-κB activation via LPS exposure (Signal 1). Iron is taken up by the cell where the ions lead to ROS production through the Fenton reaction. In turn, the assembly of the NLRP3 inflammasome is activated to cleave pro-caspase-1 to induce IL-1β maturation. Gasdermin D (GSDMD) is another substrate of active caspase-1 that the cleaved N-terminal fragment (GSDMD-N) oligomerizes to form pores in the cell membrane, which facilitate the release of mature IL-1β. Subsequently, extracellular IL-1β may bind to IL1-receptor and induce NF-κB production as highlighted with the blue arrows. Adapted from Chen *et al.* (2018).

By studying the early response of mRNA regulation in the U937 macrophages, we noticed that the immune response (measured via TNFα, IL-1β, IL-8, HO-1) to LPS was modulated by the addition of Fe^{2+}. However, the decreased expression of the pro-inflammatory markers upon co-exposure in macrophages is seemingly contradictory to the increased NF-κB stimulation seen in the HEK hTLR4 cell line. Differences between the experiments are summarised in Table 5.2. Although the same $FeCl_2$ concentration was used as in the HEK experiment (showing maximal SEAP production without loss in cell viability), the LPS dose had to be

increased tenfold in the U937 experiment due to different sensitivity between the cell models. Furthermore, while the HEK experiment relied on the accumulation of the response over 20 h, the U937 experiment simply gives a snapshot of the mRNA expression levels at 3 h. In future experiments, it would therefore be useful to use an ELISA to measure cytokine production at the same time interval, i.e. 20 h.

Table 5.2: Difference between experiments with the HEK hTLR4 reporter cell line and gene expression in U937 cells.

	HEK hTLR4 model	**U937 cell line**
Cell type	human HEK293	human macrophage-like
Co-exposure time	20 h	3 h
Measurement	Accumulated SEAP production	mRNA gene expression
LPS dose	5 EU ml^{-1}	5 ng ml^{-1} (1 ng = 10 EU)

Nonetheless, the lower gene expressions of pro-inflammatory markers after co-exposure gives us insight into the possible hindered host recognition of LPS in the human macrophage cell line. Divalent cations have previously been shown by Garidel *et al.* (2005) to affect the aggregate structure of LPS, leading to lower IL-6 production after 24 hours incubation in human mononuclear cells, likely due to the impediment of interactions between LPS with LPS-binding protein (LBP) and CD14. While we found Mg^{2+} to have no significant effect on SEAP production during LPS exposure, the Mg^{2+} salt form of LPS in the study of Geridel *et al.* showed only a moderate decrease in IL-6 production compared to other tested salts (Ca^{2+} and Ba^{2+}). Perhaps Fe^{2+} may similarly bind to LPS and modulate the aggregate structure.

Although the transcriptional regulation of MD-2 and TLR4 splice variants were not seen to be significantly affected during co-exposure of LPS and iron, in the future, a PCR array of the TLR4 pathway may provide more details at which point iron affects LPS stimulation. Furthermore, monitoring the immune response over time may also show if iron simply delays the LPS response of the cells. Finally, we observed a wide transcriptional modulation of MD-2 (facilitating TLR4 stimulation) and TLR2 (mediating host response to gram-positive bacteria

and yeast) from the urban air samples. No doubt there are still many secrets left to explore regarding the interactions of air pollutants and human immune responses.

Chapter 6

General conclusions & Perspectives

"Look wide, and even when you think you are looking wide – look wider still"

-- Robert Baden-Powell

This PhD thesis investigated the relative contribution of bacterial endotoxins and transition metals in the pro-inflammatory immune responses induced by particulate matter (PM). Endotoxins (LPS) belong to the strongest elicitors of the mammalian immune system (Alexander and Rietschel, 2001), which may result in either a beneficial or detrimental outcome depending on various factors. For example, very high concentrations of endotoxin in the bloodstream are well-known to induce septic shock syndrome (Tsujimoto *et al.*, 2008), while inhalation of rather high concentrations of endotoxin from more rural and farming areas have shown a lower prevalence of allergy and asthma in children when compared with urban populations (Liebers *et al.*, 2008; Mutius, 2000; Schuijs *et al.*, 2015). Co-exposure of endotoxin together with other environmental compounds is another important factor influencing the type and height of our immune response (Liu, 2002). In an urban environment, endotoxin forms part of a complex mixture of airborne pollutants such as PM. As natural adjuvants, endotoxins are apt candidates for the PM-induced health effects, as they may amplify or modulate the immune response of co-pollutants (Degobbi *et al.*, 2011; Delfino, 2009; Imrich *et al.*, 1999; Long *et al.*, 2001; Ryan *et al.*, 2009). However, these effects have barely been explored at a mechanistic level, such as done in this PhD work.

A new approach to sampling of urban endotoxins

Since the aim of this PhD was to focus on the role of bacterial endotoxins in PM-related health effects, we first explored a dedicated approach for the sampling of ambient endotoxins in an urban environment (chapter 2). With our more microbial-targeted approach using a Coriolis µ sampler, endotoxins were detected at approximately 10-fold higher concentrations in Antwerp (GM 4.49 EU m^{-3}) compared to the urban air of other cities using filter-based samplers (average of 0.44. EU m^{-3} in PM_{10}). Additionally, metal concentrations collected with this sampler (reported in chapter 3) were detected in comparable concentrations to those reported by the Flemish Environmental Agency (VMM) using filter-based samplers (e.g. table 4.1), which formed an important validation for our sampling approach. Impingers, such as the Coriolis µ sampler, offer a distinct advantage over filter-based samplers by bypassing the lengthy and problematic filter-extraction procedures which often lead to variations and

endotoxin loss. Hereby, (i) the use of plastics is minimized, which is important since the lipid portion of endotoxin molecules tends to make them very adherent, especially to plastics (Novitsky *et al.*, 1986; Roslansky *et al.*, 1991), (ii) the use of detergents (e.g. Tween 20, 0.01% triethylamine) is no longer needed for the recovery of particles from the filter, as they interfere with endotoxin quantification (Spaan *et al.*, 2007), and (iii) a minimized number of steps prevent contamination and reduce endotoxin loss. The shorter sampling time – which we initially thought to be the main disadvantage of the approach, actually also had the advantage that we are able to detect real-time concentrations and fluctuations. In chapter 2, impinger collection also allowed samples to be cultivated, where numerous colonies were identified by 16S rDNA sequencing. Many of these identified colonies were also isolated and stored at -80°C, as reservoirs of airborne bacteria to be later screened in projects for their bioremediation potential (e.g. as done by colleague Wenke Smets in her PhD thesis, Smets, 2018). Nevertheless, because of the shorter sampling time and the general low activity of microbes in the air, optimizations are still warranted to obtain sufficient total microbial DNA and RNA material for next-generation-sequencing approaches such as done by Franzetti and co-workers from filter-based samples (Franzetti *et al.*, 2011). Yet, the overall advantages encourage future studies to definitively assess the use of impingers over filter-based samplers for ambient endotoxin collection, specifically in an urban environment.

Does endotoxin quantification by Factor C from the horseshoe crab relate to human TLR4 recognition for environmental samples?

Due to the complexity of the environmental samples, we choose to use the rFC assay with its simplified enzymatic reaction for endotoxin detection, reducing the likelihood of interference from other PM components. This assay is genetically engineered from the endotoxin-sensitive Factor C, the first of a cascade of enzymes in the limulus amybocyte lysate (LAL) assay which is *the* golden standard in pharmaceutical testing and is based on the innate immune response of the horseshoe crab (Ding and Ho, 2001). As mentioned in chapter 1 (section 1.3.2) studies have investigated differences in the activation of the LAL assay compared to that of the human immune response and the structural motifs necessary for each (Brandenburg *et al.*, 2009;

Dehus *et al.,* 2006; Schromm *et al.,* 2000). Nevertheless, environmental samples may complicate this comparison by hosting a variety of different bacteria with their respective LPS motifs, together with the possibility of interactions with other PM components. We therefore went on to investigate human recognition of endotoxins using a HEK-Blue reporter cell line in which the key human innate immune receptor Toll-like receptor 4 (hTLR4) is overexpressed and in which its associated immune signalling pathway could be easily monitored. We observed that the response in the HEK hTLR4 cell line did not always correspond to the endotoxin concentrations measured with the rFC assay (chapter 3). Furthermore, endotoxin concentrations calculated from a standard curve in the HEK hTLR4 cell line generally gave lower values than those determined with the rFC assay. These data suggest that LPS from the environmental samples is simply not as potent as the *E.coli* LPS used to construct the standard curve in the HEK hTLR4 bioassay, thus underestimating the endotoxin concentration of the environmental sample. This is highly plausible, as mentioned in chapter 1, the hexa-acylated LPS structure of *E.coli* is considered to be close to that optimally recognised by human cellular LPS receptors such as TLR4, while many environmental gram-negative bacteria other than *E. coli* appear to have other LPS structures which are less stimulatory for TLR4 (e.g. penta-acylated and 1'-phosphorylated LPS of *Bacteroides* strains) (Coats *et al.*, 2011). Nevertheless, even when considering that ambient environmental LPS might be less pro-inflammatory than pathogenic LPS from bacteria such as *E. coli*, synergistic effects between environmental LPS and other PM components likely also affected the hTLR4 interactions in our assays. This was apparent by the correlation of the endotoxin assays being significantly dependent on the land-use class.

In chapter 4, after quantifying the transition metal concentrations in the urban air samples, we found that especially iron concentrations could explain why the relation of rFC-quantified endotoxin to the HEK hTLR4 response was dependent on the land-use class. Iron concentrations were surprisingly correlated to the stimulation of the HEK hTLR4 cell line: samples from the traffic land-use class which had significantly higher iron concentrations, also showed a high HEK TLR4 response. Coarse particle counts from the Coulter counter further implicated iron particles, since iron was well correlated to the particle count in the traffic land-

use class samples, and only the coarse particles from the traffic land-use class were correlated to the stimulation of the HEK hTLR4 cell line. Iron particles in urban air are well known for their oxidative potential through ROS-generating Fenton reactions (Valko *et al.*, 2005), however much less is known in literature how they may modulate the pro-inflammatory response of endotoxin.

Iron enhancing endotoxin-TLR4 interaction: correlation or causation?

In chapter 5 we therefore had to simplify the complexity of the environmental samples in order to explore mechanistic/causal interactions between LPS, iron and hTLR activation. In this way, we could show a direct enhancing effect of iron exposure (especially $FeCl_2$) during LPS stimulation in the HEK TLR4 cell line. Additionally, we controlled for cell viability, LPS contamination of metal solutions, potential interference of SEAP activity by Fe^{2+} and Mg^{2+}, and the specificity of the effect caused by iron compared to other metal cations such as Ni^{2+} and Mg^{2+} (Oblak *et al.*, 2015; Rachmawati *et al.*, 2013). To explain this effect in the HEK TLR4 cell line, we hypothesized that iron cations may either influence stimulation at TLR4 (transcriptional regulation or directly play a role in LPS recognition) or may indirectly contribute to SEAP production (reporter of TLR4 activation) through the IL-1β pathway during LPS stimulation. In the future, blocking the IL-1β pathway may help elucidate the role of iron during LPS exposure (see figure 5.9). Although the HEK hTLR4 assay applied does not definitively give us an answer of whether ferrous iron modulates host reception, it does highlight the synergistic effects between iron and LPS in this human cell model.

To the best of our knowledge, such synergistic effects have not been reported before in the literature. Of interest, because of the role of TLR4 as a target for several novel therapeutics, these findings could have important implications outside air pollution research. For example, TLR4 stimulation (agonism) by high-affinity ligands mimicking lipid A can provide vaccine adjuvants with improved specificity and efficacy that have been licensed and entered into the market (Zaffaroni and Peri, 2018). TLR4 inhibition (antagonism) prevents cytokine production at a very early stage, which is in principle a more efficient method to block inflammatory diseases compared to cytokines neutralization by antibodies, e.g. upon septic shock (Ianaro *et*

al., 2009). Because of the potential application of iron derivatives modulating TLR4 receptor interactions, the findings presented in chapter 4 and chapter 5 formed the basis for a 'provisional filing' ENHENDIR (MyIP-2018015, UNA-030, 'IRON-BASED VACCINE ADJUVANTS). Further research in more complex models is needed to validate this and contacts have been initiated with e.g. Prof. P. Delputte, an UAntwerpen colleague and vaccine adjuvant expert to explore this further.

Iron seems to decrease LPS-mediated pro-inflammatory gene expression in human macrophages

We already explored the effect of iron and LPS co-exposure in a more complex cellular model than the HEK hTLR4 cells, namely the U937 macrophage cell line. In this cell line, we monitored the gene regulation for pro-inflammatory markers (TNFα, IL-1β, IL-8) and oxidative stress (HO-1). These results confirmed that iron modulated the immune response to LPS, however the decreased expression of the pro-inflammatory markers seemed contradictory to the increased NFκB production (typically linked to increased production of pro-inflammatory markers) previously detected in the HEK hTLR4 cell line. This may suggest the hindered recognition of LPS by iron in more complex cells such as U937, or the modulation of the LPS response via the MyD88-independent pathway in these cells, which is known to mitigate the production of pro-inflammatory cytokines as discussed in chapter 1. More experiments are needed to explore cytokine production over time and the possible pathways and mechanisms involved through PCR or microarray studies. Furthermore, we observed considerable transcriptional regulation of the MD-2 (accessory protein of TLR4), TLR2, and HO-1 genes in the environmental samples. This reminds us that we still have much to learn regarding the host response to air pollutants such as particulate matter and the responsible components. Even more important considering our previous statement that 'iron might have some potential modulatory role for novel TLR4 targeting therapeutics', a better mechanistic understanding will be warranted before such applications are possible.

Integrating research into a magnetic monitoring study

Lastly, we are currently involved in an ongoing project aimed at integrating these results with a larger PM fingerprinting campaign at the department. As mentioned in chapter 1, one of the key research lines within the department is the biomonitoring of air pollution using urban plants (headed by Prof Roeland Samson). Here, biomagnetic monitoring is typically applied to measure magnetic minerals in urban PM (e.g. iron oxides) deposited onto plant leaves, where higher magnetic concentration values are typically measured with increasing proximity to PM sources and with increasing source strength such as traffic volume (Hofman *et al.*, 2017).

In 2014, a large citizen science project called "AIRbezen" aimed to monitor the spatial distribution of traffic-related PM in Antwerp by the means of strawberry plants as local monitoring stations, while also creating awareness of the urban air PM problem by actively involving citizens. After the distribution of over a 1000 plants to volunteering Antwerp citizens and 2 months exposure to the local air, leaves were collected and magnetically analyzed to yield a detailed biomagnetic map of the different districts within Antwerp. To build upon the success of the AIRbezen project, the Particulate Matter Fingerprinting (PMF) project was initiated in 2017 to further develop, diversify and fine-tune the vegetation-based biomagnetic monitoring of PM pollution in accordance with other PM characterization techniques, in order to obtain more information on PM sources and toxicology. Iron-rich particles exhibit a strong magnetic behavior and iron has previously been shown within the research group to be significantly correlated ($p < 0.01$) to biomagnetic measurements of leaves (Castanheiro *et al.*, 2016). Since iron was linked to modulating the LPS response in human cell lines within this thesis (together with their strong capacity to elicit oxidative stress), we are currently investigating within the PMF study the correlation of biomagnetic monitoring techniques to toxicity biomarkers such as the pro-inflammatory and oxidative stress markers used in this thesis. Additionally, particles from the different sampling locations in the PMF study were visualized using a scanning electron microscope (SEM), which is a complementary technique to the air sampling campaigns of this thesis. This was done by passively collecting particles on an adhesive aluminum stub at the different sampling locations throughout the campaign (16

September - 31 October 2017). After collection, the stubs were vacuum-coated with carbon to be examined with a Quanta 250 field emission gun SEM (Fig 6.1). The backscattered (BS) electron detector was specifically used to identify brighter metallic particles due to its discrimination based on atomic number. From this, different concentrations, shapes and sizes of particles and metals can be seen in the different sampling locations, showing to be promising for the further analyses. However, in order to view bacteria, the samples need to be treated differently for SEM, whereby bacterial cells are fixed (e.g. 3% glutaraldehyde), slowly desiccated with ethanol, and then finally coated with carbon. This is yet another example showing the complexity of studying particulate matter, where numerous approaches are needed to view the full picture.

To conclude, this PhD thesis focused on ambient endotoxins - as a component of PM in an urban environment – and its possible contribution to inflammation-related health risks of air pollution, including further interactions with transition metals. To do so, we investigated several analyses, and those found feasible were further validated (as summarized in table 6.1), and many of which revealed novel insights. Future perspectives include the further elucidation of the mechanistic interactions *in vitro* and *in vivo* between endotoxin and iron for the potential application in the pharmaceutical industry. Furthermore, knowledge of more real-time (or hourly) monitoring of endotoxin fluctuations throughout the day may be gained with the use of the Coriolis sampler, with its shorter required sampling time. To accommodate for more extensive sampling campaigns, a faster and more real-time detection of endotoxin would be advantageous. In the future, this may be achieved with the use of electrochemical LPS biosensors, which are currently in developmental stages (Das *et al.*, 2014; Mayall *et al.*, 2017).

From this work we showed that to understand the toxicity of PM, we need to look beyond the individual effects of PM components, and to better understand the complex interactions between PM components and how they may modulate our immune response during co-exposure.

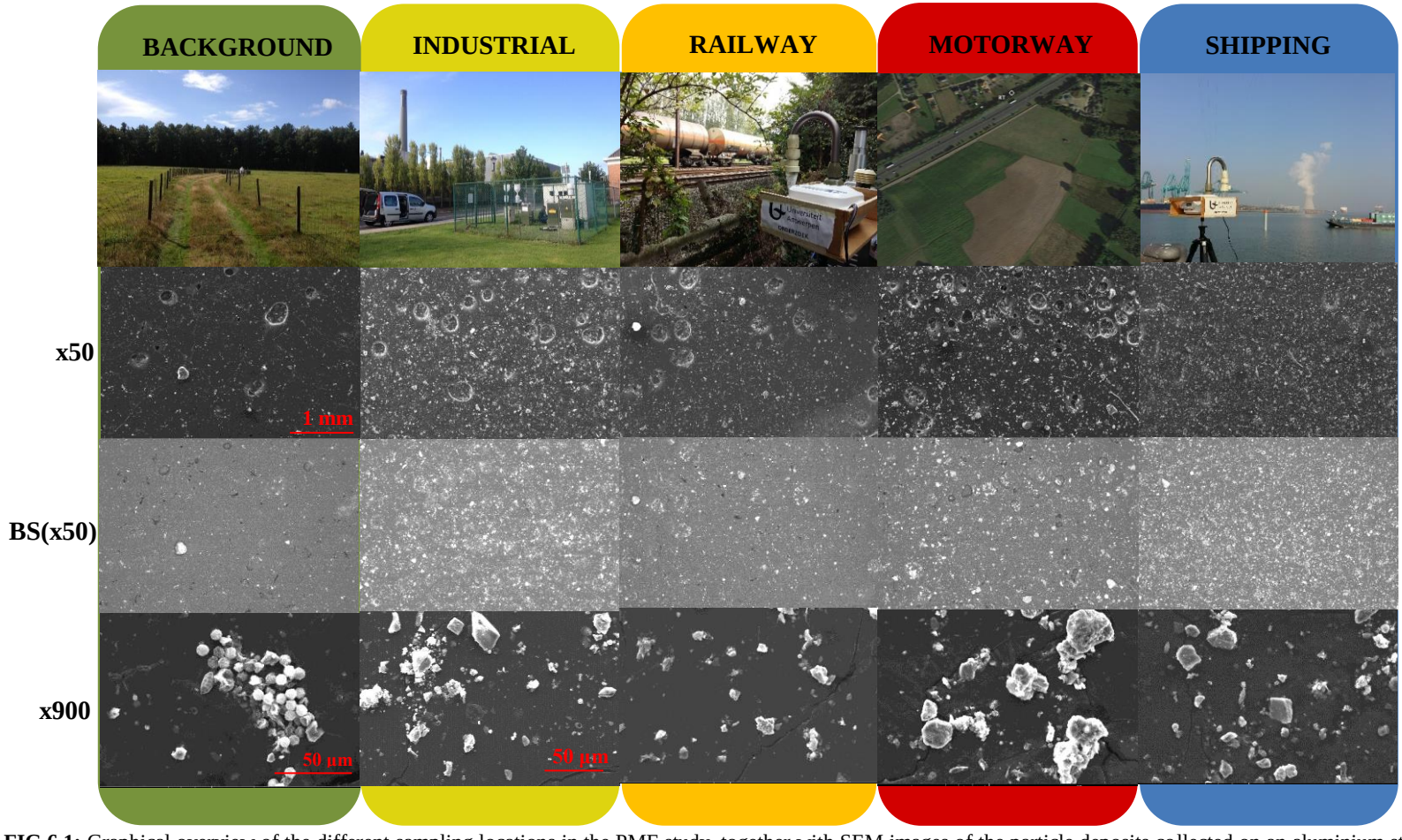

FIG 6.1: Graphical overview of the different sampling locations in the PMF study, together with SEM images of the particle deposits collected on an aluminium stub at different magnifications (x50, x900) and using backscatter (BS) detection to identify brighter metallic particles due to its discrimination based on atomic number.

Table 6.1: Summary of the different analysis carried out in this thesis

Analysis	Measures	Advantages	Disadvantages
rFC assay	Endotoxin quantification	Very sensitive (0.001 EU ml^{-1}). Improvement from the LAL assay (reduction of enzymatic cascade to a single reaction; not activated by fungal glucans, not dependent on blood of horse-shoe crabs, less sensitive lot-to-lot variations)	Enzymatic assay and therefore sensitive to pH, temperature, and cations. Relatively expensive (€15/sample)
HEK-Blue hTLR4 bioassay	Stimulation of human TLR4 through SEAP reporter	Relatively inexpensive Sensitive (based on ligand-receptor interactions)	Cell viability may be affected e.g. by fungal growth Complex biological model with potential interferences
U937 macrophage cell line	Gene expression e.g. pro-inflammatory (IL-1β, IL-8, TNFα) & oxidative stress markers (HO-1)	Sensitive Test wide-array of response Relevant for human biological response	Expensive and time-consuming Results highly dependent on viability, RNA quality and proper validation steps
ICP-MS *Prof R. Blust, SPHERE*	Transition metal concentrations	Sensitive, easily used in combination with Coriolis sampler	Trained personnel required Expensive equipment
Coulter counter *Prof R. Blust, SPHERE*	Particle count and size distribution	Sensitive, inexpensive (cheaper than flow cytometry), quick, easily used in combination with Coriolis sampler	Depends on the stability of the particles in the liquid phase (agglomeration or dissolving)
*HPLC *Dr. Pieter Joos, water-link*	PAH quantification	Sensitive	Expensive (~€130/sample) Trained personnel
*Cyclic voltammetry, Autolab potentiostad *Prof K. De Wael, AXES*	Identify redox-active metals (e.g. Fe^{+2}, Fe^{+3})	Identifies main redox-active compounds	Results not always reproducible (may be linked to longer storage times)
*TOC-$V_{CPH/CPN}$ Analyzer (Shimadzu) *Prof R. Blust, SPHERE*	Total organic carbon	Relatively inexpensive and easy	Requires 20 ml of sample. 5ml of original sample (from 15ml collection liquid) diluted to 20 ml gave readings under 1ppm, at which point reproducibility decreases
*Electron paramagnetic resonance (EPR) *Prof. P. Cos, LMPH*	Detect superoxide radicals in cell models (e.g. RAW264.7 cells)	Sensitive, specific, relatively inexpensive	Addition of the test sample and probe, and detection are time-sensitive and the processing of larger sample numbers will require more than one person.

* Analyses investigate, but not found feasible to use further in this thesis

Appendices

A1: Additional information of air sample collection

Sample	Location	Land-use class	Date	Time	Temp	Humidity	PM_{10} (VMM stations)	Comments
			y/m/d	GMT +1	°C	%	$\mu g/m^3$	
1	Traffic 1	Traffic	2014/08/14	10:46	24	58	57.5	
2	Pasture	Green	2014/08/14	11:48	17	74		
3	Traffic 1	Traffic	2014/08/21	10:45	23	46	31.5	
4	Pasture	Green	2014/08/21	13:33	23	35		
5	Metal plant	Industrial	2014/08/21	15:05	24	37	24.5	
6	Traffic 1	Traffic	2014/08/29	11:07	25	50	34	
7	Harbour	Industrial	2014/08/29	13:50	23	53	21	
8	Pasture	Green	2014/09/01	15:15	23	52		
9	Metal plant	Industrial	2014/09/01	16:20	24	46	16	
10	Traffic 1	Traffic	2014/09/04	10:25	24	52	33	
11	Traffic 3	Traffic	2014/09/04	11:42	29	47	35	
12	Harbour	Industrial	2014/09/04	13:25	27	45	42	
13	Traffic 1	Traffic	2014/09/09	10:41	21	52		
14	Traffic 3	Traffic	2014/09/09	11:50	21	53	12	
15	Harbour	Industrial	2014/09/09	13:03	19	56	19	
16	Metal plant	Industrial	2014/09/12	12:57	23	50	13	
17	Metal plant	Industrial	2014/09/16	12:17	25	53	15	
18	Pasture	Green	2014/09/16	13:20	29	43		
19	Traffic 1	Traffic	2014/09/18	11:09	24	55	20	
20	Traffic 3	Traffic	2014/09/18	12:22	28	60	46	
21	Harbour	Industrial	2014/09/18	13:47	30	47	25	
22	Park	Green	2014/10/07	10:45	15	72		
23	Traffic 4	Traffic	2014/10/07	11:50	17	63		
24	Traffic 2	Traffic	2014/10/07	12:50	16	60		
25	Park	Green	2014/10/30	11:19	16	86		
26	Traffic 4	Traffic	2014/10/30	12:20	17	73		
27	Traffic 2	Traffic	2014/10/30	13:31	19	69		
28	Metal plant	Industrial	2014/11/20	15:05	10	80	46	

29	City campus	Traffic	2014/11/24	12:30	12	58		
30	Campus DE	Green	2014/11/24	13:48	16	64		
31	Campus G	Green	2014/11/24	14:50	11	73		
32	Park	Green	2014/11/25	10:50	9	65		
33	Traffic 4	Traffic	2014/11/25	12:10	12	61		
34	Traffic 2	Traffic	2014/11/25	13:30	11	57		
35	City campus	Traffic	2014/12/03	10:38	2	74		
36	Campus DE	Green	2014/12/03	12:26	2	60		
37	Campus G	Green	2014/12/03	14:35	2	63		
38	Traffic 1	Traffic	2014/12/06	12:42	12	68	19	
39	Traffic 3	Traffic	2014/12/06	14:39	12	63	15	
40	Harbour	Industrial	2014/12/06	16:22	8	84	7	
41	City campus	Traffic	2014/12/09	10:40	9	64		
42	Campus DE	Green	2014/12/09	11:53	8	69		
43	Campus G	Green	2014/12/09	14:04	9	75		
44	Traffic 1	Traffic	2015/07/07	10:30	27	35	32.5	
45	Harbour	Industrial	2015/07/07	13:20	23	63	25.5	
46	Traffic 1	Traffic	2015/07/16	10:00	22	59	23	
47	Harbour	Industrial	2015/07/16	11:33	29	43	18	
48	Park	Green	2015/07/16	12:56	24	50		Discarded: Passing car on sand road
49	Traffic 2	Traffic	2015/07/17	10:20	28	52		
50	Campus DE	Green	2015/07/17	11:35	26	53		
51	Metal plant	Industrial	2015/07/17	14:08	28	45	18	
52	Traffic 1	Traffic	2015/07/22	11:08	22	54	16.5	
53	Harbour	Industrial	2015/07/22	12:35	25	44	12	
54	Park	Green	2015/07/22	13:55	26	40		
55	Traffic 2	Traffic	2015/07/24	09:50	22	48		
56	Campus DE	Green	2015/07/24	11:05	25	40		
57	Metal plant	Industrial	2015/07/24	13:40	29	32	17	
58	Traffic 1	Traffic	2015/07/29	10:40	20	45	9	
59	Harbour	Industrial	2015/07/29	12:15	19	55	21	
60	Park	Green	2015/07/29	13:45	20	46		
61	Traffic 2	Traffic	2015/07/31	10:15	21	32		

62	Campus DE	Green	2015/07/31	11:35	20	36		Discarded: spilled when aliquoting
63	Metal plant	Industrial	2015/07/31	13:45	22	33		Discarded: contaminated with insect
64	Traffic 1	Traffic	2015/08/11	11:35	25	50	36	
65	Harbour	Industrial	2015/08/11	12:55	23	21	9.5	
66	Park	Green	2015/08/11	14:20	26	52		
67	Traffic 2	Traffic	2015/08/13	12:07	28	52		
68	Metal plant	Industrial	2015/08/13	13:20	33	42	38	
69	Campus DE	Green	2015/08/13	14:35	32	44		
70	Traffic 1	Traffic	2015/08/18	11:50	19	54	24	
71	Harbour	Industrial	2015/08/18	13:14	19	64	12	
72	Park	Green	2015/08/18	14:30	21	55		
73	Traffic 2	Traffic	2015/08/21	10:41	27	49		
74	Metal plant	Industrial	2015/08/21	12:55	30	42	16	
75	Campus DE	Green	2015/08/21	14:30	27	43		
76	Traffic 1	Traffic	2015/08/25	11:55	20	49	15	
77	Harbour	Industrial	2015/08/25	13:18	21	56	12	
78	Park	Green	2015/08/25	14:43	22	44		
79	Traffic 2	Traffic	2015/08/28	10:25	19	61		
80	Campus DE	Green	2015/08/28	11:45	21	49		Discarded: contaminated with insect
81	Metal plant	Industrial	2015/08/28	14:00	23	41		Discarded: contaminated with insect
82	Traffic 1	Traffic	2015/08/31	10:30	29	57	25.5	
83	Harbour	Industrial	2015/08/31	11:52	30	54	25	
84	Park	Green	2015/08/31	13:30	30	48		Discarded: Passing car on sand road
85	Traffic 2	Traffic	2015/09/01	10:53	18			
86	Metal plant	Industrial	2015/09/01	12:01	19	85	15	
87	Campus DE	Green	2015/09/01	15:12	22	70		
88	Campus DE	Green	2015/09/11	11:15	20	48		
89	Traffic 2	Traffic	2015/09/11	13:35	23	43		
90	Metal plant	Industrial	2015/09/11	14:50	23	20	14	
91	Traffic 1	Traffic	2015/09/18	10:31	19	64	11	
92	Harbour	Industrial	2015/09/18	12:08	18	66	9	
93	Park	Green	2015/09/18	13:26	18	63		

A2: Analysis of transition metals: extended

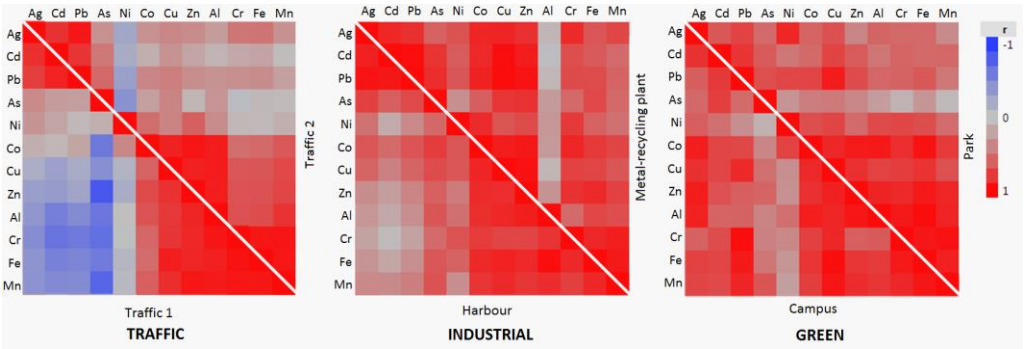

FIG A2.1: Correlation scatter matrix of transition metals from the different land-use classes: traffic, industrial and green

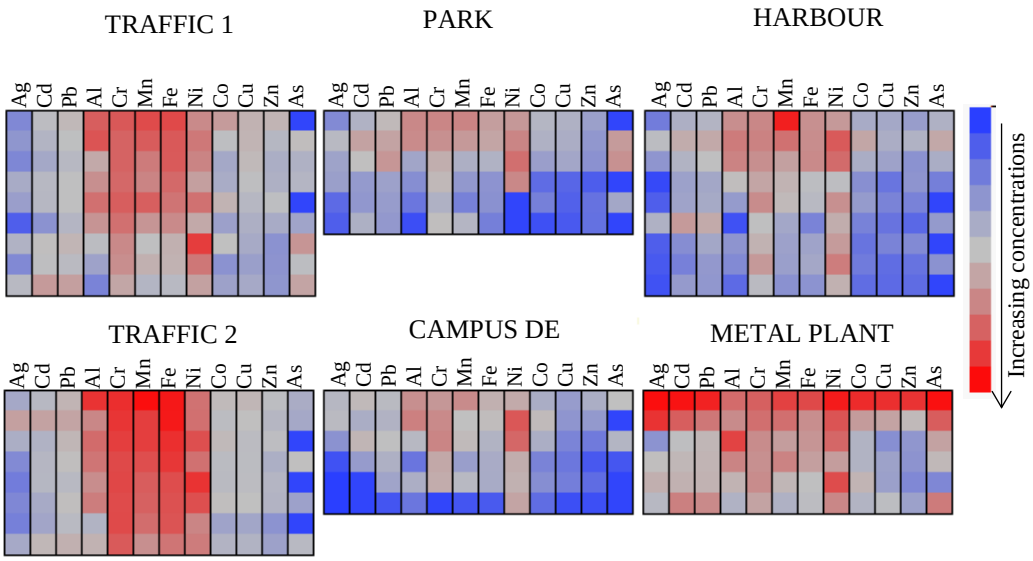

FIG A2.3: Cell plots illustrating a heat map of the concentrations of the logarithm metal concentrations (ng m^{-3}) in the different locations. Each row within the plot represents a sample and its transition metal profile collected at a different time points.

Publications

Moretti S, Smets W, Hofman J, Mubiana KV, Oerlemans E, Vandenheuvel D, Samson R, Blust R, Lebeer S (2018). Host reception of endotoxin through human TLR4/MD-2 complex enhanced by transition metals in urban particulate matter. Submitted to *Environmental Pollution.*

Moretti S, Smets W, Oerlemans E, Blust R, Lebeer S (2018). The abundance of urban endotoxins as measured with an impinger-based sampling strategy. Accepted in *Aerobiologia*

Smets W*, **Moretti S***, Denys S, Lebeer S (2016). Review: Airborne bacteria in the atmosphere: presence, purpose, and potential. *Atmospheric Environment* 139: 214-221.

*equal contribution

Goedhals D, Scott LE, **Moretti S**, Cooper MA, Opperman WJL & Rossouw I (2013). Evaluation of the use of plasma preparation tubes for HIV viral load testing on the COBAS AmpliPrep/COBAS TaqMan HIV-1 version 2.0. *Journal of Virological Methods* 187(2): 248-250.

Moretti S, Boucher CE & Bragg RR (2013). Molecular characterization of Mycoplasma gallisepticum from poultry in Zimbabwe and South Africa. *South African Journal of Science* 109 (11/12)Art. #2013-0117

Smets W, **Moretti S**, Lebeer S (2014). Study of airborne bacteria and their relation to air pollutants. In: The Sustainable City IX: *Urban Regeneration and Sustainability* (Marchettini N, Brebbia CA, Pulselli R, Bastianoni S, ed). WIT press, 1449-1458.

Curriculum Vitae

Smoretti23@gmail.com Serena M0retti serena-moretti

Education

Ph.D Bioscience Engineering 2012-2018
University of Antwerp Belgium

Microbial analysis of airborne Particulate matter from polluted air

Eurosa: (1/10/2012-30/9/2014)
BOF-UA: (1/10/2014-30/9/2015)
FWO fellowship (1/10/2015-present)

M.Sc Microbiology 2010-2012
University of the Free State South Africa

A molecular study of M. gallisepticum isolates from poultry in southern Africa

B.Sc Honours Biochemistry 2009
University of the Free State South Africa

Study of Mycoplasma gallisepticum in southern Africa

B.Sc Microbiology 2006-2008
University of the Free State South Africa

Majoring in: Microbiology, Biochemistry, Molecular Biology

Work Experience

BAP
University of Antwerp 2012-2018
Voluntary employee (2012-2014)
BOF-UA (2014-2015)

Research Assistant 2010-2012
Medical Virology Department
& NHS South Africa

- *HIV genotyping for admission of new ARVs*
- *Genotyping Human Herpesvirus 8 for correlation studies of tissue lesions*
- *Study of Hepatitis E prevalence in SA*
- *Sequence analysis of measles virus causing SSPE with atypical symptoms*

AWARDS

NSABS oral presentation award, 2016
National Symposium on Applied Biological Sciences, 150 participants

Rosa Blanckaert award, 2015
University of Antwerp, encouragement award for young researcher

Poster Prize at Knowledge for Growth conference, 2013
Selected from 160 applicants, Ghent

Best M.Sc Microbiology, 2012
University of the Free State

PPS Award for Exceptional Postgraduate Student, 2012
This award was conferred by the Professional Provident Society.

Kovsie-Alumni Trust Awards for Best B.Sc. Student (89.83%), 2009
The award was conferred by the University of the Free State, from the B.Sc programme of 3 220 graduating students.

Dean's Award, 2009
For the best undergraduate student in the Faculty. The award was conferred by the University of the Free State, from 483 graduating B.Sc students

The Beckman Coulter Award, 2009
For the best national undergraduate student. This award was conferred by the South African Society for Microbiology. The winner was selected from invited submissions from all microbiology departments in South Africa.

Roche Diagnostic Book Prize,2009
For the best final year B.Sc student in biochemistry. The award was conferred by the University of the Free State, from a class of 103 third-year students.

Merck Prize and Achievement Medal, 2009
Best final year B.Sc student in Microbiology. The award was conferred by the University of the Free State, from a class of 66 third-year students.

Assistant Lecturer 2012
University of the Free State South Africa
Pathogens and Immunity: Theory & Practical (3rd year B.Sc)

Lab manager 2011
Veterinary Biotechnology lab South Africa
Ordering of reagents and equipment
Lab administration

Practical Assistant 2007-2011
University of the Free State South Africa
Courses: Microbiology, Physics, Mycology, Biochemistry

COURSES

Method in Research Design
StatUa, 2014

Applied communication skills
Gerrit van Aken, 2014

qPCR data analysis in Qbase+
VIB BITS, 2015

Advanced qPCR training
Life Technologies, 2015

Graphpad Prism training
VIB BITS, 2015

R statistics
Stefan van Dongen, 2015

Career development
Sarah Blackford, 2016

Conferences & Symposiums

2012 Biomonitoring of air quality (Antwerp, BE). *Poster*
National gut day symposium (Leuven, BE)
2013 National symposium of Applied Biological Sciences (Ghent, BE). *Poster*
Knowledge for growth symposium (Ghent, BE). *Poster*
1st OPINNO Module (Leuven, BE)
Belgium Society for Microbiology symposium (Brussels, BE). *Poster*
2014 National symposium of Applied Biological Sciences (Gembloux, BE). *Poster*
StatUa Day (Antwerp, BE)
Applying chemical tools to study biology, VIB (Antwerp, BE)
The 22nd international conference on modelling, monitoring and management of air pollution (Opatija, Croatia)
How to pursue an academic career in life sciences (Brussels, BE)
4th international PhD student symposium: VIBes in biosciences (Antwerp, BE)
Immunology summer school (Leuven, BE). ***Oral presentation***
2015 4th European Congress of Immunology (Vienna, AUT). *Poster*
TOLL2015 (Marbella, Spain). *Poster*
2016 National symposium of Applied Biological Sciences (Antwerp, BE). ***Oral presentation***
EuroScience Open Forum (Manchester, UK)
International Endotoxin and Innate Immunity Society: 14th Biennial Meeting (Hamburg, Germany). ***Oral presentation***
2017 Belgium Society for Microbiology symposium (Brussels, BE). *Poster*
12th International symposium on lactic acid bacteria (Egmond aan Zee, NL)
2018 Janssens Sterility Assurance conference (Antwerp, BE).

References

Albrecht A, Witzenberger R, Bernzen U, Jackel U (2007). Detection of airborne microbes in a composting facility by cultivation based and cultivation-independent methods. *Annals of Agricultural and Environmental Medicine* 14(1): 81-85.

Alexander C, Rietschel ET (2001). Invited review: Bacterial lipopolysaccharides and innate immunity. *Journal of endotoxin research* 7(3): 167-202.

Allen J, Bartlett K, Graham M, Jackson P (2011). Ambient concentrations of airborne endotoxin in two cities in the interior of British Columbia, Canada. *Journal of environmental monitoring* 13(3): 631-640.

Aller JY, Kuznetsova MR, Jahns CJ, Kemp PF (2005). The sea surface microlayer as a source of viral and bacterial enrichment in marine aerosols. *Journal of aerosol science* 36(5-6): 801-812.

Alwis KU, Milton DK (2006). Recombinant factor C assay for measuring endotoxin in house dust: Comparison with LAL, and (1→ 3)-β-D-glucans. *American journal of industrial medicine* 49(4): 296-300.

Amato P, Ménager M, Sancelme M, Laj P, Mailhot G, Delort A-M (2005). Microbial population in cloud water at the Puy de Dôme: implications for the chemistry of clouds. *Atmospheric Environment* 39(22): 4143-4153.

Analitis A, Katsouyanni K, Dimakopoulou K, Samoli E, Nikoloulopoulos AK, Petasakis Y, Touloumi G, Schwartz J, Anderson HR, Cambra K, Forastiere F, Zmirou D, Vonk JM, Clancy L, Kriz B, Bobvos J, Pekkanen J (2006). Short-term effects of ambient particles on cardiovascular and respiratory mortality. *Epidemiology* 17(2): 230-233.

Anderson JO, Thundiyil JG, Stolbach A (2012). Clearing the air: a review of the effects of particulate matter air pollution on human health. *Journal of Medical Toxicology* 8(2): 166-175.

Aranda PS, LaJoie DM, Jorcyk CL (2012). Bleach gel: a simple agarose gel for analyzing RNA quality. *Electrophoresis* 33(2): 366-369.

Aulock SV, Deininger S, Draing C, Gueinzius K, Dehus O, Hermann DC (2006). Gender Difference in Cytokine Secretion on Immune Stimulation with LPS and LTA. *Journal of Interferon & Cytokine Research* 26(12): 887-892.

Baccini M, Biggeri A (2012). Short-term impact of air pollution among Italian cities covered by the EpiAir2 project. *Epidemiol. Prev.* 37(4-5): 252-262.

Becker S, Dailey LA, Soukup JM, Grambow SC, Devlin RB, Huang Y-CT (2005a). Seasonal variations in air pollution particle-induced inflammatory mediator release and oxidative stress. *Environmental Health Perspectives* 113(8): 1032.

Becker S, Mundandhara S, Devlin RB, Madden M (2005b). Regulation of cytokine production in human alveolar macrophages and airway epithelial cells in response to ambient air pollution particles: further mechanistic studies. *Toxicology and applied pharmacology* 207(2): 269-275.

Bertolini V, Gandolfi I, Ambrosini R, Bestetti G, Innocente E, Rampazzo G, Franzetti A (2013). Temporal variability and effect of environmental variables on airborne bacterial communities in an urban area of Northern Italy. *Applied microbiology and biotechnology* 97(14): 6561-6570.

Blanchard DC (1989). The ejection of drops from the sea and their enrichment with bacteria and other materials: a review. *Estuaries* 12(3): 127-137.

Boldo E, Medina S, Le Tertre A, Hurley F, Mücke H-G, Ballester F, Aguilera I (2006). Apheis: Health impact assessment of long-term exposure to PM2. 5 in 23 European cities. *Eur. J Epidemiol.* 21(6): 449-458.

Bowers RM, Clements N, Emerson JB, Wiedinmyer C, Hannigan MP, Fierer N (2013). Seasonal variability in bacterial and fungal diversity of the near-surface atmosphere. *Environmental science & technology* 47(21): 12097-12106.

Bowers RM, McCubbin IB, Hallar AG, Fierer N (2012). Seasonal variability in airborne bacterial communities at a high-elevation site. *Atmospheric Environment* 50: 41-49.

Bowers RM, McLetchie S, Knight R, Fierer N (2011a). Spatial variability in airborne bacterial communities across land-use types and their relationship to the bacterial communities of potential source environments. *The ISME journal* 5(4): 601-612.

Bowers RM, Sullivan AP, Costello EK, Collett JL, Knight R, Fierer N (2011b). Sources of bacteria in outdoor air across cities in the midwestern United States. *Applied and environmental microbiology* 77(18): 6350-6356.

Bowers RM, Sullivan AP, Costello EK, Collett JL, Knight R, Fierer N (2011c). Sources of bacteria in outdoor air across cities in the midwestern United States. *Applied and Environmental Microbiology* 77(18): 6350-6356.

Brandenburg K, Howe J, Gutsman T, Garidel P (2009). The expression of endotoxic activity in the Limulus test as compared to cytokine production in immune cells. *Current medicinal chemistry* 16(21): 2653-2660.

Brodie EL, DeSantis TZ, Parker JPM, Zubietta IX, Piceno YM, Andersen GL (2007). Urban aerosols harbor diverse and dynamic bacterial populations. *Proceedings of the National Academy of Sciences* 104(1): 299-304.

Brüggemann E, Gerwig H, Gnauk T, Müller K, Herrmann H (2009). Influence of seasons, air mass origin and day of the week on size-segregated chemical composition of aerosol particles at a kerbside. *Atmospheric Environment* 43(15): 2456-2463.

Bucevic-Popovic V, Pavela-Vrancic M, Dieckmann R (2004). Metal-ion induced conformational changes in alkaline phosphatase from E. coli assessed by limited proteolysis. *Biochimie* 86(6): 403-409.

Bustin S, Dhillon HS, Kirvell S, Greenwood C, Parker M, Shipley GL, Nolan T (2015). Variability of the reverse transcription step: practical implications. *Clinical chemistry* 61(1): 202-212.

Calabrese V, Cighetti R, Peri F (2015). Molecular simplification of lipid A structure: TLR4-modulating cationic and anionic amphiphiles. *Molecular immunology* 63(2): 153-161.

Cao C, Jiang W, Wang B, Fang J, Lang J, Tian G, Jiang J, Zhu TF (2014). Inhalable Microorganisms in Beijing's PM2. 5 and PM10 Pollutants during a Severe Smog Event. *Environmental science & technology* 48(3): 1499-1507.

Cardoso PG, Macedo GC, Azevedo V, Oliveira SC (2006). Brucella spp noncanonical LPS: structure, biosynthesis, and interaction with host immune system. *Microbial cell factories* 5(1): 13.

Castanheiro A, Samson R, De Wael K (2016). Magnetic-and particle-based techniques to investigate metal deposition on urban green. *Science of the Total Environment* 571: 594-602.

Chen S, Chen S, Zeng Y, Lin L, Wu C, Ke Y, Liu G (2018). Size-dependent superparamagnetic iron oxide nanoparticles dictate interleukin-1β release from mouse bone marrow-derived macrophages. *Journal of Applied Toxicology*.

Cheng JYW, Hui ELC, Lau APS (2012). Bioactive and total endotoxins in atmospheric aerosols in the Pearl River Delta region, China. *Atmospheric Environment* 47: 3-11.

Chung K (2006). Cytokines as targets in chronic obstructive pulmonary disease. *Current drug targets* 7(6): 675-681.

Coats SR, Berezow AB, To TT, Jain S, Bainbridge BW, Banani KP, Darveau RP (2011). The lipid A phosphate position determines differential host Toll-like receptor 4 responses to phylogenetically related symbiotic and pathogenic bacteria. *Infect Immun* 79(1): 203-210.

Costa DL, Dreher KL (1997). Bioavailable transition metals in particulate matter mediate cardiopulmonary injury in healthy and compromised animal models. *Environmental Health Perspectives* 105(Suppl 5): 1053.

Das A, Kumar P, Swain S (2014). Recent advances in biosensor based endotoxin detection. *Biosensors and Bioelectronics* 51: 62-75.

De Kok TM, Driece HA, Hogervorst JG, Briedé JJ (2006). Toxicological assessment of ambient and traffic-related particulate matter: a review of recent studies. *Mutation Research/Reviews in Mutation Research* 613(2): 103-122.

De Leeuw G, Andreas EL, Anguelova MD, Fairall C, Lewis ER, O'Dowd C, Schulz M, Schwartz SE (2011). Production flux of sea spray aerosol. *Reviews of Geophysics* 49(2).

DECOS (2010). Endotoxins: health-based recommended occupational limit. Publication No. 2010/04OSH. The Hague: The Health Council of the Netherlands.

Degobbi C, Saldiva PHN, Rogers C (2011). Endotoxin as modifier of particulate matter toxicity: a review of the literature. *Aerobiologia* 27(2): 97-105.

Dehus O, Hartung T, Hermann C (2006). Endotoxin evaluation of eleven lipopolysaccharides by whole blood assay does not always correlate with Limulus amebocyte lysate assay. *Journal of endotoxin research* 12(3): 171-180.

Delfino RJ (2009). Do endotoxin and air pollution have a synergistic relationship to asthma onset or exacerbation? Am Thoracic Soc.

Derveaux S, Vandesompele J, Hellemans J (2010). How to do successful gene expression analysis using real-time PCR. *Methods* 50(4): 227-230.

Di Giorgio C, Krempff A, Guiraud H, Binder P, Tiret C, Dumenil G (1996). Atmospheric pollution by airborne microorganisms in the city of Marseilles. *Atmospheric Environment* 30(1): 155-160.

Ding JL, Ho B (2001). A new era in pyrogen testing. *TRENDS in Biotechnology* 19(8): 277-281.

Ding JL, Ho B (2010). Endotoxin detection–from limulus amebocyte lysate to recombinant factor C, Endotoxins: Structure, Function and Recognition. Springer, pp. 187-208.

Dominici F, McDermott A, Zeger SL, Samet JM (2003). National maps of the effects of particulate matter on mortality: exploring geographical variation. *Environ. Health Perspect.* 111(1): 39.

Duchaine C, Thorne PS, Mériaux A, Grimard Y, Whitten P, Cormier Y (2001). Comparison of endotoxin exposure assessment by bioaerosol impinger and filter-sampling methods. *Applied and environmental microbiology* 67(6): 2775-2780.

Duquenne P, Marchand G, Duchaine C (2013). Measurement of endotoxins in bioaerosols at workplace: a critical review of literature and a standardization issue. *The Annals of occupational hygiene* 57(2): 137-172.

Dybwad M, Skogan G, Blatny JM (2014). Comparative testing and evaluation of nine different air samplers: end-to-end sampling efficiencies as specific performance measurements for bioaerosol applications. *Aerosol Science and Technology* 48(3): 282-295.

EEA (2017). Air quality in Europe- 2017 report. (https://www.eea.europa.eu/publications/air-quality-in-europe-2017) Accessed 20 March 2018.

Erridge C, Bennett-Guerrero E, Poxton IR (2002). Structure and function of lipopolysaccharides. *Microbes and infection* 4(8): 837-851.

EU (2008). Directive 2008/50/EC of the European Parliament and of the Council of 21 May 2008 on ambient air quality and cleaner air for Europe (OJ L 152, 11.6.2008, p. 1-44) (http://eur-lex.europa.eu/LexUriServ/LexUriServ.do?uri=OJ:L:2008:152:0001: 0044:EN:PDF) accessed 29 March 2018.

EU (2016). Directive 2016/2284/EC of the European Parliament and of the Council of 14 December 2016 on the reduction of national emissions of certain atmospheric pollutants, amending Directive 2003/35/EC and repealing Directive 2001/81/ EC (OJ L 344, 17.12.2016, p. 1-31) (http://eur-lex. europa.eu/legal-content/EN/TXT/?uri=uriserv%3AOJ .L_.2016.344.01.0001.01.ENG) accessed 29 March 2018.

Fang Z, Ouyang Z, Zheng H, Wang X, Hu L (2007). Culturable airborne bacteria in outdoor environments in Beijing, China. *Microbial Ecology* 54(3): 487-496.

Frampton MW, Ghio AJ, Samet JM, Carson JL, Carter JD, Devlin RB (1999). Effects of aqueous extracts of PM10 filters from the Utah Valley on human airway epithelial cells. *American Journal of Physiology-Lung Cellular and Molecular Physiology* 277(5): L960-L967.

Franzetti A, Gandolfi I, Gaspari E, Ambrosini R, Bestetti G (2011). Seasonal variability of bacteria in fine and coarse urban air particulate matter. *Applied microbiology and biotechnology* 90(2): 745-753.

Fujimura KE, Johnson CC, Ownby DR, Cox MJ, Brodie EL, Havstad SL, Zoratti EM, Woodcroft KJ, Bobbitt KR, Wegienka G (2010). Man's best friend? The effect of pet ownership on house dust microbial communities. *The Journal of allergy and clinical immunology* 126(2): 410.

Garidel P, Rappolt M, Schromm AB, Howe J, Lohner K, Andra J, Koch MH, Brandenburg K (2005). Divalent cations affect chain mobility and aggregate structure of lipopolysaccharide from Salmonella minnesota reflected in a decrease of its biological activity. *Biochim Biophys Acta* 1715(2): 122-131.

Gehrig R, Hill M, Lienemann P, Zwicky CN, Bukowiecki N, Weingartner E, Baltensperger U, Buchmann B (2007). Contribution of railway traffic to local PM10 concentrations in Switzerland. *Atmospheric Environment* 41(5): 923-933.

Geiser M, Rothen-Rutishauser B, Kapp N, Schürch S, Kreyling W, Schulz H, Semmler M, Hof VI, Heyder J, Gehr P (2005). Ultrafine Particles Cross Cellular Membranes by Nonphagocytic Mechanisms in Lungs and in Cultured Cells. *Environmental Health Perspectives* 113(11): 1555-1560.

Gioannini TL, Teghanemt A, Zhang D, Coussens NP, Dockstader W, Ramaswamy S, Weiss JP (2004). Isolation of an endotoxin–MD-2 complex that produces Toll-like receptor 4-dependent cell activation at picomolar concentrations. *Proceedings of the National Academy of Sciences* 101(12): 4186-4191.

Gordon T, Galdanes K, Brosseau L (1992). Comparison of sampling media for endotoxin-contaminated aerosols. *Applied Occupational and Environmental Hygiene* 7(7): 472-477.

Griffin DW, Gonzalez C, Teigell N, Petrosky T, Northup DE, Lyles M (2011). Observations on the use of membrane filtration and liquid impingement to collect airborne microorganisms in various atmospheric environments. *Aerobiologia* 27(1): 25-35.

Grosse S, Stenvik J, Nilsen AM (2016). Iron oxide nanoparticles modulate lipopolysaccharide-induced inflammatory responses in primary human monocytes. *International journal of nanomedicine* 11: 4625.

Gutsmann T, Howe J, Zähringer U, Garidel P, Schromm A, Koch M, Fujimoto Y, Fukase K, Moriyon I, Martínez-de-Tejada G, Brandenburg K (2010). Structural prerequisites for endotoxic activity in the Limulus test as compared to cytokine production in mononuclear cells. *Innate immunity* 16(1): 39-47.

Han Y, Li L, Liu J, Zhang M (2012). Microbial structure and chemical components of aerosols caused by rotating brushes in a wastewater treatment plant. *Environmental Science and Pollution Research* 19(9): 4097-4108.

Happo M, Hirvonen M-R, Hälinen A, Jalava P, Pennanen A, Sillanpää M, Hillamo R, Salonen R (2010). Seasonal variation in chemical composition of size-segregated urban air particles and the inflammatory activity in the mouse lung. *Inhalation toxicology* 22(1): 17-32.

Heinrich J, Pitz M, Bischof W, Krug N, Borm PJA (2003). Endotoxin in fine (PM2.5) and coarse (PM2.5–10) particle mass of ambient aerosols. A temporo-spatial analysis. *Atmospheric Environment* 37(26): 3659-3667.

Hellemans J, Mortier G, De Paepe A, Speleman F, Vandesompele J (2007). qBase relative quantification framework and software for management and automated analysis of real-time quantitative PCR data. *Genome biology* 8(2): R19.

Hetland RB, Cassee FR, Låg M, Refsnes M, Dybing E, Schwarze PE (2005). Cytokine release from alveolar macrophages exposed to ambient particulate matter: heterogeneity in relation to size, city and season. *Particle and fibre toxicology* 2(1): 4.

Hofman J, Maher BA, Muxworthy AR, Wuyts K, Castanheiro A, Samson R (2017). Biomagnetic monitoring of atmospheric pollution: a review of magnetic signatures from biological sensors. *Environmental science & technology* 51(12): 6648-6664.

Hruz T, Wyss M, Docquier M, Pfaffl MW, Masanetz S, Borghi L, Verbrugghe P, Kalaydjieva L, Bleuler S, Laule O (2011). RefGenes: identification of reliable and condition specific reference genes for RT-qPCR data normalization. *BMC genomics* 12(1): 156.

Huang S-L, Cheng W-L, Lee C-T, Huang H-C, Chan C-C (2002). Contribution of endotoxin in macrophage cytokine response to ambient particles in vitro. *Journal of Toxicology and Environmental Health Part A* 65(17): 1261-1272.

Huffman JA, Pöhlker C, Prenni A, DeMott P, Mason R, Robinson N, Fröhlich-Nowoisky J, Tobo Y, Després V, Garcia E (2013). High concentrations of biological aerosol particles and ice nuclei during and after rain. *Atmospheric Chemistry and Physics Discussions* 13(1): 1767-1793.

Hyvärinen A, Martikainen P, Nevalainen A (1991). Suitability of poor medium in counting total viable airborne bacteria. *Grana* 30(2): 414-417.

Ianaro A, Tersigni M, D'Acquisto F (2009). New insight in LPS antagonist. *Mini reviews in medicinal chemistry* 9(3): 306-317.

Imrich A, Ning YY, Koziel H, Coull B, Kobzik L (1999). Lipopolysaccharide priming amplifies lung macrophage tumor necrosis factor production in response to air particles. *Toxicology and applied pharmacology* 159(2): 117-124.

Iwami K-i, Matsuguchi T, Masuda A, Kikuchi T, Musikacharoen T, Yoshikai Y (2000). Cutting edge: naturally occurring soluble form of mouse Toll-like receptor 4 inhibits lipopolysaccharide signaling. *The Journal of Immunology* 165(12): 6682-6686.

Jarešová I, Rožková D, Špíšek R, Janda A, Brázová J, Šedivá A (2007). Kinetics of Toll-like receptor-4 splice variants expression in lipopolysaccharide-stimulated antigen presenting cells of healthy donors and patients with cystic fibrosis. *Microbes and infection* 9(11): 1359-1367.

Johansson C, Norman M, Gidhagen L (2007). Spatial & temporal variations of PM10 and particle number concentrations in urban air. *Environmental Monitoring and Assessment* 127(1-3): 477-487.

Jones AM, Harrison RM (2004). The effects of meteorological factors on atmospheric bioaerosol concentrations—a review. *Science of The Total Environment* 326(1-3): 151-180.

Jorgensen JH, Smith RF (1974). Measurement of bound and free endotoxin by the Limulus assay. *Proceedings of the Society for Experimental Biology and Medicine* 146(4): 1024-1031.

Jung H-J, Kim B, Malek MA, Koo YS, Jung JH, Son Y-S, Kim J-C, Kim H, Ro C-U (2012). Chemical speciation of size-segregated floor dusts and airborne magnetic particles collected at underground subway stations in Seoul, Korea. *Journal of Hazardous Materials* 213-214: 331-340.

Katsouyanni K, Touloumi G, Samoli E, Gryparis A, Le Tertre A, Monopolis Y, Rossi G, Zmirou D, Ballester F, Boumghar A (2001). Confounding and effect modification in the short-term effects of ambient particles on total mortality: results from 29 European cities within the APHEA2 project. *Epidemiology* 12(5): 521-531.

Kawai T, Adachi O, Ogawa T, Takeda K, Akira S (1999). Unresponsiveness of MyD88-deficient mice to endotoxin. *Immunity* 11(1): 115-122.

Kelly B, O'Neill LA (2015). Metabolic reprogramming in macrophages and dendritic cells in innate immunity. *Cell research* 25(7): 771.

Kelly FJ (2003). Oxidative stress: its role in air pollution and adverse health effects. *Occupational and environmental medicine* 60(8): 612-616.

Kelly FJ, Mudway IS, Donaldson E, Borm P (2007). Particle-mediated extracellular oxidative stress in the lung. *Particle Toxicology*: 89-117.

Klironomos JN, Rillig MC, Allen MF, Zak DR, Pregitzer KS, Kubiske ME (1997). Increased levels of airborne fungal spores in response to Populus tremuloides grown under elevated atmospheric CO2. *Canadian journal of botany* 75(10): 1670-1673.

Krug HF, Wick P (2011). Nanotoxicology: an interdisciplinary challenge. *Angew Chem Int Ed Engl* 50(6): 1260-1278.

Lamkanfi M, Dixit VM (2014). Mechanisms and functions of inflammasomes. *Cell* 157(5): 1013-1022.

Lane DJ (1991). 16S/23S rRNA sequencing. Wiley, New York.

Li K, Dong S, Wu Y, Yao M (2010). Comparison of the biological content of air samples collected at ground level and at higher elevation. *Aerobiologia* 26(3): 233-244.

Li N, Sioutas C, Cho A, Schmitz D, Misra C, Sempf J, Wang M, Oberley T, Froines J, Nel A (2003). Ultrafine particulate pollutants induce oxidative stress and mitochondrial damage. *Environmental Health Perspectives* 111(4): 455.

Li N, Wang M, Oberley TD, Sempf JM, Nel AE (2002). Comparison of the pro-oxidative and proinflammatory effects of organic diesel exhaust particle chemicals in bronchial epithelial cells and macrophages. *The Journal of Immunology* 169(8): 4531-4541.

Li N, Xia T, Nel AE (2008). The role of oxidative stress in ambient particulate matter-induced lung diseases and its implications in the toxicity of engineered nanoparticles. *Free Radical Biology and Medicine* 44(9): 1689-1699.

Liebers V, Raulf-Heimsoth M, Brüning T (2008). Health effects due to endotoxin inhalation (review). *Archives of toxicology* 82(4): 203-210.

Liu AH (2002). Endotoxin exposure in allergy and asthma: reconciling a paradox. *Journal of Allergy and Clinical Immunology* 109(3): 379-392.

Long CM, Suh HH, Kobzik L, Catalano PJ, Ning YY, Koutrakis P (2001). A pilot investigation of the relative toxicity of indoor and outdoor fine particles: in vitro effects of endotoxin and other particulate properties. *Environmental Health Perspectives* 109(10): 1019.

Lu Y-C, Yeh W-C, Ohashi PS (2008). LPS/TLR4 signal transduction pathway. *Cytokine* 42(2): 145-151.

Maris N, Dessing M, De Vos A, Bresser P, Van der Zee J, Jansen H, Spek C, Van der Poll T (2006). Toll-like receptor mRNA levels in alveolar macrophages after inhalation of endotoxin. *European Respiratory Journal* 28(3): 622-626.

Maron PA, Mougel C, Lejon DPH, Carvalho E, Bizet K, Marck G, Cubito N, Lemanceau P, Ranjard L (2006). Temporal variability of airborne bacterial community structure in an urban area. *Atmospheric Environment* 40(40): 8074-8080.

Mattsby-Baltzer I, Lindgren K, Lindholm B, Edebo L (1991). Endotoxin shedding by enterobacteria: free and cell-bound endotoxin differ in Limulus activity. *Infection and immunity* 59(2): 689-695.

Mayall R, Renaud-Young M, Chan N, Birss V (2017). An electrochemical lipopolysaccharide sensor based on an immobilized Toll-Like Receptor-4. *Biosensors and Bioelectronics* 87: 794-801.

Michael S, Montag M, Dott W (2013). Pro-inflammatory effects and oxidative stress in lung macrophages and epithelial cells induced by ambient particulate matter. *Environmental pollution* 183: 19-29.

Monn C, Becker S (1999). Cytotoxicity and induction of proinflammatory cytokines from human monocytes exposed to fine (PM 2.5) and coarse particles (PM 10–2.5) in outdoor and indoor air. *Toxicology and applied pharmacology* 155(3): 245-252.

Morgenstern V, Carty CL, Gehring U, Cyrys J, Bischof W, Heinrich J (2005). Lack of spatial variation of endotoxin in ambient particulate matter across a German metropolitan area. *Atmospheric Environment* 39(36): 6931-6941.

Morris C, Sands D, Bardin M, Jaenicke R, Vogel B, Leyronas C, Ariya P, Psenner R (2011). Microbiology and atmospheric processes: research challenges concerning the impact of airborne micro-organisms on the atmosphere and climate. *Biogeosciences* 8(1): 17-25.

Mueller-Anneling L, Avol E, Peters JM, Thorne PS (2004). Ambient endotoxin concentrations in PM10 from Southern California. *Environmental Health Perspectives* 112(5): 583-588.

Mukhopadhyay S, Hoidal JR, Mukherjee TK (2006). Role of TNFα in pulmonary pathophysiology. *Respiratory research* 7(1): 125.

Mutius V (2000). Exposure to endotoxin or other bacterial components might protect against the development of atopy. *Clinical & Experimental Allergy* 30(9): 1230-1234.

Nemmar A, Hoet PM, Vanquickenborne B, Dinsdale D, Thomeer M, Hoylaerts M, Vanbilloen H, Mortelmans L, Nemery B (2002). Passage of inhaled particles into the blood circulation in humans. *Circulation* 105(4): 411-414.

Nilsson S, Merritt A, Bellander T (2011). Endotoxins in urban air in Stockholm, Sweden. *Atmospheric Environment* 45(1): 266-270.

Novitsky TJ, Schmidt-Gengenbach J, Remillard JF (1986). Factors Affecting Recovery of Endotoxin Adsorbed to Container Surfaces. *PDA Journal of Pharmaceutical Science and Technology* 40(6): 284-286.

Oblak A, Pohar J, Jerala R (2015). MD-2 determinants of nickel and cobalt-mediated activation of human TLR4. *PloS one* 10(3): e0120583.

Oshikawa K, Sugiyama Y (2003). Gene expression of Toll-like receptors and associated molecules induced by inflammatory stimuli in the primary alveolar macrophage. *Biochemical and biophysical research communications* 305(3): 649-655.

Pan YL, Pinnick RG, Hill SC, Rosen JM, Chang RK (2007). Single-particle laser-induced-fluorescence spectra of biological and other organic-carbon aerosols in the atmosphere: Measurements at New Haven, Connecticut, and Las Cruces, New Mexico. *Journal of Geophysical Research: Atmospheres* 112(D24).

Parham P (2014). The immune system, fourth edition ed. Garland Science.

Perrone MG, Gualtieri M, Ferrero L, Porto CL, Udisti R, Bolzacchini E, Camatini M (2010). Seasonal variations in chemical composition and in vitro biological effects of fine PM from Milan. *Chemosphere* 78(11): 1368-1377.

Peters M, Fritz P, Bufe A (2012). A bioassay for determination of lipopolysaccharide in environmental samples. *Innate immunity* 18(5): 694-699.

Polymenakou PN (2012). Atmosphere: a source of pathogenic or beneficial microbes? *Atmosphere* 3(1): 87-102.

Rachmawati D, Bontkes HJ, Verstege MI, Muris J, von Blomberg BME, Scheper RJ, van Hoogstraten IM (2013). Transition metal sensing by Toll-like receptor-4: next to nickel, cobalt and palladium are potent human dendritic cell stimulators. *Contact Dermatitis* 68(6): 331-338.

Ravva SV, Hernlem BJ, Sarreal CZ, Mandrell RE (2012). Bacterial communities in urban aerosols collected with wetted-wall cyclonic samplers and seasonal fluctuations of live and culturable airborne bacteria. *Journal of Environmental Monitoring* 14(2): 473-481.

Rietschel ET, Kirikae T, Schade FU, Mamat U, Schmidt G, Loppnow H, Ulmer AJ, Zähringer U, Seydel U, Di Padova F (1994). Bacterial endotoxin: molecular relationships of structure to activity and function. *The FASEB Journal* 8(2): 217-225.

Roslansky PF, Dawson ME, Novitsky TJ (1991). Plastics, Endotoxins, and the Limulus Amebocyte Lysate Test. *PDA Journal of Pharmaceutical Science and Technology* 45(2): 83-87.

Roslansky PF, Novitsky TJ (1991). Sensitivity of Limulus amebocyte lysate (LAL) to LAL-reactive glucans. *Journal of clinical microbiology* 29(11): 2477-2483.

Ryan PH, Bernstein DI, Lockey J, Reponen T, Levin L, Grinshpun S, Villareal M, Hershey GK, Burkle J, LeMasters G (2009). Exposure to traffic-related particles and endotoxin during infancy is associated with wheezing at age 3 years. *American journal of respiratory and critical care medicine* 180(11): 1068-1075.

Rylander R (2006). Endotoxin and occupational airway disease. *Current opinion in allergy and clinical immunology* 6(1): 62-66.

Rylander R, BAKE B, Fischer JJ, Helander IM (1989). Pulmonary Function and Symptoms after Inhalation of Endotoxin1, 2. *Am Rev Respir Dis* 140: 981-986.

Samuvel DJ, Sundararaj KP, Nareika A, Lopes-Virella MF, Huang Y (2009). Lactate boosts TLR4 signaling and NF-κB pathway-mediated gene transcription in macrophages via monocarboxylate transporters and MD-2 up-regulation. *The Journal of Immunology* 182(4): 2476-2484.

Santos-Burgoa C, Rosas I, Yela A (1994). Occurrence of airborne enteric bacteria in Mexico City. *Aerobiologia* 10(1): 39-45.

Schins RP, Knaapen AM, Weishaupt C, Winzer A, Borm PJ (2002). Cytotoxic and inflammatory effects of coarse and fine particulate matter in macrophages and epithelial cells. *Annals of Occupational Hygiene* 46(suppl 1): 203-206.

Schins RPF, Lightbody JH, Borm PJA, Shi T, Donaldson K, Stone V (2004). Inflammatory effects of coarse and fine particulate matter in relation to chemical and biological constituents. *Toxicol Appl Pharmacol* 195(1): 1-11.

Schmidt M, Raghavan B, Müller V, Vogl T, Fejer G, Tchaptchet S, Keck S, Kalis C, Nielsen PJ, Galanos C (2010). Crucial role for human Toll-like receptor 4 in the development of contact allergy to nickel. *Nature immunology* 11(9): 814-819.

Schromm AB, Brandenburg K, Loppnow H, Moran AP, Koch MH, Rietschel ET, Seydel U (2000). Biological activities of lipopolysaccharides are determined by the shape of their lipid A portion. *Eur J Biochem* 267(7): 2008-2013.

Schuijs MJ, Willart MA, Vergote K, Gras D, Deswarte K, Ege MJ, Madeira FB, Beyaert R, van Loo G, Bracher F (2015). Farm dust and endotoxin protect against allergy through A20 induction in lung epithelial cells. *Science* 349(6252): 1106-1110.

Sciple G, Riemensnider D, Schleyer C (1967). Recovery of microorganisms shed by humans into a sterilized environment. *Applied microbiology* 15(6): 1388-1392.

Seagrave J, Knall C, McDonald JD, Mauderly JL (2004). Diesel particulate material binds and concentrates a proinflammatory cytokine that causes neutrophil migration. *Inhalation toxicology* 16(sup1): 93-98.

Shaffer BT, Lighthart B (1997). Survey of culturable airborne bacteria at four diverse locations in Oregon: urban, rural, forest, and coastal. *Microbial Ecology* 34(3): 167-177.

Smets W (2018). PhD thesis: Interactions between phyllosphere bacteria and urban air pollution, Bioscience Engineering. University of Antwerp.

Smets W, Moretti S, Denys S, Lebeer S (2016). Airborne bacteria in the atmosphere: presence, purpose, and potential. *Atmospheric Environment* 139: 214-221.

Soukup JM, Becker S (2001). Human alveolar macrophage responses to air pollution particulates are associated with insoluble components of coarse material, including particulate endotoxin. *Toxicology and applied pharmacology* 171(1): 20-26.

Spaan S, Doekes G, Heederik D, Thorne PS, Wouters IM (2008a). Effect of extraction and assay media on analysis of airborne endotoxin. *Applied and environmental microbiology* 74(12): 3804-3811.

Spaan S, Heederik DJ, Thorne PS, Wouters IM (2007). Optimization of airborne endotoxin exposure assessment: effects of filter type, transport conditions, extraction solutions, and storage of samples and extracts. *Applied and environmental microbiology* 73(19): 6134-6143.

Spaan S, Schinkel J, Wouters IM, Preller L, Tielemans E, Nij ET, Heederik D (2008b). Variability in endotoxin exposure levels and consequences for exposure assessment. *Annals of Occupational Hygiene* 52(5): 303-316.

Srimuruganandam B, Shiva Nagendra SM (2012). Source characterization of PM10 and PM2.5 mass using a chemical mass balance model at urban roadside. *Science of The Total Environment* 433: 8-19.

Stafoggia M, Zauli-Sajani S, Pey J, Samoli E, Alessandrini E, Basagaña X, Cernigliaro A, Chiusolo M, Demaria M, Díaz J (2016). Desert dust outbreaks in Southern Europe: contribution to daily PM10 concentrations and short-term associations with mortality and hospital admissions. *Environ. Health Perspect.* 124(4): 413.

Steerenberg P, Withagen C, Van Dalen W, Dormans J, Cassee F, Heisterkamp S, Van Loveren H (2004). Adjuvant activity of ambient particulate matter of different sites, sizes, and seasons in a respiratory allergy mouse model. *Toxicology and applied pharmacology* 200(3): 186-200.

Steimle A, Autenrieth IB, Frick J-S (2016). Structure and function: Lipid A modifications in commensals and pathogens. *International Journal of Medical Microbiology* 306(5): 290-301.

Stromberg LR, Mendez HM, Mukundan H (2017). Detection Methods for Lipopolysaccharides: Past and Present, Escherichia coli-Recent Advances on Physiology, Pathogenesis and Biotechnological Applications. InTech.

Tager IB, Lurmann FW, Haight T, Alcorn S, Penfold B, Hammond SK (2010). Temporal and spatial patterns of ambient endotoxin concentrations in Fresno, California. *Environmental Health Perspectives* 118(10): 1491-1496.

Thorne PS, Bartlett KH, Phipps J, Kulhankova K (2003). Evaluation of five extraction protocols for quantification of endotoxin in metalworking fluid aerosol. *Annals of Occupational Hygiene* 47(1): 31-36.

Thorne PS, Perry SS, Saito R, O'Shaughnessy PT, Mehaffy J, Metwali N, Keefe T, Donham KJ, Reynolds SJ (2010). Evaluation of the Limulus amebocyte lysate and recombinant factor C assays for assessment of airborne endotoxin. *Applied and environmental microbiology* 76(15): 4988-4995.

Thorpe A, Harrison RM (2008). Sources and properties of non-exhaust particulate matter from road traffic: a review. *Science of The Total Environment* 400(1-3): 270-282.

Traversi D, Alessandria L, Schilirò T, Gilli G (2011). Size-fractionated PM10 monitoring in relation to the contribution of endotoxins in different polluted areas. *Atmospheric Environment* 45(21): 3515-3521.

Traversi D, Alessandria L, Schilirò T, Piat SC, Gilli G (2010). Meteo-climatic conditions influence the contribution of endotoxins to PM10 in an urban polluted environment. *Journal of Environmental Monitoring* 12(2): 484-490.

Tsujimoto H, Ono S, Efron PA, Scumpia PO, Moldawer LL, Mochizuki H (2008). Role of Toll-like receptors in the development of sepsis. *Shock* 29(3): 315-321.

Turner S, Pryer KM, Miao VP, Palmer JD (1999). Investigating deep phylogenetic relationships among cyanobacteria and plastids by small subunit rRNA sequence analysis. *Journal of Eukaryotic Microbiology* 46(4): 327-338.

Vaïtilingom M, Amato P, Sancelme M, Laj P, Leriche M, Delort A-M (2010). Contribution of microbial activity to carbon chemistry in clouds. *Applied and environmental microbiology* 76(1): 23-29.

Valavanidis A, Fiotakis K, Vlachogianni T (2008). Airborne particulate matter and human health: toxicological assessment and importance of size and composition of particles for oxidative damage and carcinogenic mechanisms. *Journal of Environmental Science and Health, Part C* 26(4): 339-362.

Valavanidis A, Fiotakis K, Vlahogianni T, Bakeas EB, Triantafillaki S, Paraskevopoulou V, Dassenakis M (2006). Characterization of atmospheric particulates, particle-bound transition metals and polycyclic aromatic hydrocarbons of urban air in the centre of Athens (Greece). *Chemosphere* 65(5): 760-768.

Valko M, Morris H, Cronin M (2005). Metals, toxicity and oxidative stress. *Current medicinal chemistry* 12(10): 1161-1208.

Vandesompele J, De Preter K, Pattyn F, Poppe B, Van Roy N, De Paepe A, Speleman F (2002). Accurate normalization of real-time quantitative RT-PCR data by geometric averaging of multiple internal control genes. *Genome biology* 3(7): research0034. 0031.

Vassallo R, Limper AH (1999). Fungal β-glucan can yield false-positive results with the limulus amebocyte lysate endotoxin assay. *Chest* 116(2): 583-584.

Vercauteren J, Matheeussen C, Wauters E, Roekens E, Van Grieken R, Krata A, Makarovska Y, Maenhaut W, Chi X, Geypens B (2011). Chemkar PM10: An extensive look at the local differences in chemical composition of PM10 in Flanders, Belgium. *Atmospheric Environment* 45(1): 108-116.

VMM (2016). Luchtkwaliteit in het Vlaamse Gewest. Jaarverslag Immissiemeetnetten – 2015 D/2016/6871/052 ed.

Wheeler AJ, Dobbin NA, Lyrette N, Wallace L, Foto M, Mallick R, Kearney J, Van Ryswyk K, Gilbert NL, Harrison I (2011). Residential indoor and outdoor coarse particles and associated endotoxin exposures. *Atmospheric Environment* 45(39): 7064-7071.

WHO (2006). Air Quality Guidelines: Global update 2005 — Particulate matter, ozone, nitrogen dioxide and sulphur dioxide. (http://apps.who.int/iris/bitstream/handle/10665/69477/WHO_SDE_PHE_OEH_06.02_eng.pdf;jsessionid=312FCC12CEDC460886FAFE14A9182D98?sequence=1) Accessed 29 March 2018.

WHO (2016). Health risk assessment of air pollution — General principles, WHO Regional Office for Europe, Copenhagen.

Williams KL (2007). Endotoxins: pyrogens, LAL testing and depyrogenation. CRC Press.

Womack AM, Bohannan BJ, Green JL (2010). Biodiversity and biogeography of the atmosphere. *Philosophical Transactions of the Royal Society B: Biological Sciences* 365(1558): 3645-3653.

Zaffaroni L, Peri F (2018). Recent advances on Toll-like receptor 4 modulation: new therapeutic perspectives. *Future medicinal chemistry* 10(4): 461-476.

Zhao Y, Aarnink AJ, De Jong MC, Groot Koerkamp PW (2014). Airborne microorganisms from livestock production systems and their relation to dust. *Critical Reviews in Environmental Science and Technology* 44(10): 1071-1128.

“Leave it better than you found it”

-- Robert Baden-Powell